universität wien

MASTERARBEIT / MASTER'S THESIS

Titel der Masterarbeit / Title of the Master's Thesis

„Molecular mechanisms of intestinal inflammation.

A role for the Calcium-Sensing Receptor."

verfasst von / submitted by

Nadja Kupper, B.Sc.

angestrebter akademischer Grad / in partial fulfilment of the requirements for the degree of

Master of Science (MSc)

Wien, 2021 / Vienna, 2021

Studienkennzahl lt. Studienblatt / degree programme code as it appears on the student record sheet:	UA 066 877
Studienrichtung lt. Studienblatt / degree programme as it appears on the student record sheet:	Masterstudium Genetik und Entwicklungsbiologie
Betreut von / Supervisor:	Assoc. Prof. Univ.-Doz. Mag. Dr. Enikö Kállay (Medizinische Universität Wien)

“In my heart I believe that biology is the beginning and the end of everything. It's the biggest source of ideas, the biggest source of invention. Nobody can invent better than nature and so if you like nature is my biggest source of inspiration.”

Ken Yeang (2017)

Declaration of authorship

I, Nadja Kupper, B.Sc., declare that this master thesis was written by me. I have not used any other than the listed sources, nor have I received any unauthorized help.

Date Signature

Danksagung

Ich danke von ganzem Herzen meinen Betreuern **Professor Enikö Kallay** und **Dr. Martin Schepelmann**. Ihr wart immer hilfsbereit an meiner Seite. Ich durfte von eurer unglaublichen Expertise profitieren, aber auch von eurer Geduld und eurem Verständnis. Ich glaube, ich habe keinen Fehler, den man auf dem Weg zu seiner Masterarbeit machen kann, ausgelassen, aber ihr wart immer da, um mich aufzufangen. Aber am allerwichtigsten ist, dass ihr mir nicht nur das Handwerk gelehrt habt, sondern dass ihr es geschafft habt die Leidenschaft für die Forschung zu vermitteln. Ich denke, das ist das Wertvollste, das ihr mir mitgegeben habt. Es war mein 6er im Lotto, bei euch meine Masterarbeit machen zu dürfen.

Dann ist natürlich unsere wunderbare **Teresa Manhardt** zu nennen, du bist wirklich der Sonnenschein unseres Instituts. Vielen Dank für all deine Hilfe und Unterstützung Teresa und für die wundervollen Mittagessen in der Mensa!

Bardzo dziękuję **Karina Piątek** za bycie moją koleżanką i przyjaciółką w laboratorium. Znikim innym nie chcę myć 100 razy ręcznie płytek ELISA! Oby bylo jeszcze wiele więcej okazji do wypicia Matcha od Starbucks.

A big thank you to my aunt **Dr. Geralde Eikenaar**, who became an expert on calcium and prostaglandins on her own! Thank you for proofreading!

Und dann wären da noch die Sponsoren der ganzen Studiererei zu nennen – vielen lieben Dank an meine Eltern **Claudia und Ulrich Kupper**, dass ihr mich immer unterstützt habt, euch all das Gejammer angehört habt und mir diese Jahre ermöglicht habt.

Und zu guter Letzt, möchte ich **Ava Kleinwächter** danken. Vom Bachelor bis über die Ziellinie des Masters - mit niemand anderen hätte ich diese Reise unternehmen wollen. Danke für alles meine liebe Ava.

Abstract

The Calcium-Sensing Receptor (CaSR) is a multifunctional G-protein coupled receptor. It can be activated by various ligands, leading to different cellular responses (ligand-biased signaling). The role of the CaSR in intestinal inflammation is still unclear. Recent studies in our group suggested a pro-inflammatory effect of CaSR agonists (calcimimetics). In my master thesis, I wanted to prove the CaSR as point of origin for this inflammatory response and to elucidate whether the pro-inflammatory prostaglandin E2 (PGE2) pathway is affected through the CaSR.

I treated colon cancer cells with CaSR-specific and -unspecific enantiomers of a calcimimetic and a calcilytic (negative CaSR-modulator). Only the CaSR-selective binding enantiomer of the calcimimetic increased expression of inflammatory markers and of certain PGE2 pathway member genes, confirming the CaSR as the point of origin for this inflammatory response. Cyclooxygenase 2 (COX-2) was found to be a major target of the CaSR induced pro-inflammatory response.

Further, I found that among all tested ligands only spermine increased the inflammatory gene expression, underlining the ligand-biased characteristic of the CaSR.

Finally, I transfected CaSR mutants in HT29 cells, an *in vitro* model which can be used to study the influence of CaSR-mutants on the gene response in the future.

In summary, I found that the pro-inflammatory effect induced by calcimimetics in colon cancer cells is mediated *via* the CaSR and influences the PGE2 pathway. The findings of my master thesis thus provide further important clues for our understanding of the pro-inflammatory role of the CaSR in colon cancer cells and beyond.

Zusammenfassung

Der Calcium-Sensing Receptor (CaSR) ist ein multifunktionaler G-Protein gekoppelter Rezeptor. Er kann durch viele verschiedene Liganden aktiviert werden und zu pleiotropen zellulären Antworten führen (Liganden-abhängige Signaltransduktion). Die Rolle des CaSR in intestinalen Entzündungen ist immer noch unklar. Ergebnisse einer kürzlich publizierten Studie unserer Arbeitsgruppe postulieren einen pro-inflammatorischen Effekt von CaSR Agonisten (Calcimimetics). Im Rahmen meiner Masterarbeit wollte ich nun nachweisen, dass diese Entzündungsreaktion tatsächlich über den CaSR vermittelt wird und zudem testen, ob der pro-inflammatorische Prostaglandin E2 (PGE2) Signalweg von der CaSR-Aktivierung beeinflusst ist.

Ich behandelte die Kolonkrebszellen mit spezifischen- und unspezifischen Enantiomeren eines Calcimimetic und Calcilytic (negativer CaSR-Modulator). Nur das CaSR-spezifisch bindende Enantiomer des Calcimimetics erhöhte die Expression von inflammatorischen Markern und von gewissen Genen des PGE2-Signalwegs. Dies bestätigt, dass der CaSR an der Entzündungsmediation ursächlich beteiligt ist. Cyclooxygenase 2 (COX-2 scheint hauptsächlich an der CaSR-induzierte inflammatorischen Antwort beeinflusst zu sein.

Des Weiteren wollte ich untersuchen, ob unterschiedliche Liganden des CaSR die inflammatorische Genexpression in HT29 Zellen unterschiedlich beeinflussen. Nur Spermin erhöhte die inflammatorische Genexpression – ein Ergebnis, das die Liganden-abhängige Signalweiterleitung des CaSR weiter bekräftigt.

Zudem habe ich HT29 Zellen erfolgreich mit CaSR-Mutanten transfiziert. Damit wurde ein *in vitro* Modell für weitere Untersuchungen von CaSR-Mutanten auf die Genexpression etabliert.

In meiner Arbeit konnte ich also bestätigen, dass die pro-inflammatorischen Effekte von Calcimimetics auf Kolonkrebszellen durch den CaSR mediiert sind und dass diese den PGE2 Signalweg beeinflussen. Die Ergebnisse meiner Masterarbeit liefern weitere wichtige Erkenntnisse für das Verständnis der pro-inflammatorischen Rolle in Kolonkrebszellen und darüber hinaus.

List of abbreviations

1,25-dihydroxyvitamin D_3	$1,25(OH)_2D_3$
1,4,5-triphosphate	IP_3
15-hydroxy PG dehydrogenase	15-PGDH
4-(2-hydroxyethyl)-1-piperazineethanesulfonicacid	HEPES
Adenomatous-polyposis-coli-protein	APC
Agonist-driven insertional signaling	ADIS
Airway hyperresponsiveness	AHR
Arachidonic acid	AA
Autosomal dominant hypocalcemia	ADH1
Bone mineral density	BMD
Calcium-Sensing Receptor	CaSR
CC-chemokine ligand 20	CCL20
Colitis-associated CRC	CA-CRC
Colorectal cancer	CRC
Crohn´s disease	CD
Cycle Threshold	CT
Cyclic adenosine monophosphate	cAMP
Cyclooxygenase 1/2	COX-1/2
Cystein-rich domain	CRD
Dextran sulfate sodium	DSS
Diacylglycerol	DAG
Dulbecco´s Modified Eagle Medium	DMEM
Enzyme-linked immunosorbent assay	ELISA
Escherichia Coli	*E.Coli*
Ethylendiamintetraacetate	EDTA
Extracellular domain	ECD
Familial hypocalciuric hypercalcemia	FHH1
Fetal calf serum	FCS
Gastrointestinal	GI
G-protein coupled receptor	GPCR
Green fluorescent protein	GFP
Guanine nucleotide-binding protein	G-protein

Heptahelical domain	HD
Housekeeping gene	HK gene
Inflammatory bowel disease	IBD
Interleukin	IL
Ionized calcium	Ca^{2+}
IP_3 receptor	IP_3R
Luria Bertani agar power	LB agar powder
Lysogeny Broth medium	LB-medium
Messenger-RNA	mRNA
Mitogen-activated protein kinase	MAPK
Neonatal severe hyperparathyroidism	NHSPT
Non-steroidal anti-inflammatory drugs	NSAIDs
Parathyroid hormone	PTH
Phosphate-buffered saline	PBS
Phospholipase A2	PLA2
Phospholipase C	PLC
Primary hyperparathyroidism	PHPT
Prostaglandin E2	PGE2
Prostaglandin G2	PGG2
Prostaglandin H2	PGH2
Prostaglandin synthase	PGES
Ras homology family member A	RhoA
Reverse transcription	RT
Rho guanine nucleotide exchange factor	RhoGEF
TRIS-borate-EDTA	TBE
Ulcerative colitis	UC
Vascular smooth muscle cell	VSMC
Venus flytrap domain	VFTD
Volume of distribution	V_D

List of figures

Table of Contents

1 Introduction

1.1 Calcium

Calcium is one of the most versatile and universal signaling agents in the human body and critical for human health [1]. Most of the body's calcium is stored in the skeleton in bound form as hydroxyapatite, making up the bone structure but there is also free and hydrated calcium ("ionized calcium", Ca^{2+}) which is a mediator of metabolic and regulatory processes [2]. Ca^{2+} in the plasma has a key function in cellular metabolism, vascular activities, wound healing, nerve impulse transmission, and muscle contraction [1]. Ionized calcium is abundant in the extracellular fluid [2]. The normal range for Ca^{2+} in the blood of adults is 2.1-2.6 mmol/l total Ca^{2+}, of which around half (1.1-1.3 mmol/l) is free or "unbound", while the other half is bound to plasma proteins. Levels greater than 2.6 mmol/l are defined as hypercalcemia and levels lower than 2.1 mmol/l as hypocalcemia [3, 4].

1.2 The Calcium-Sensing Receptor

The Calcium-Sensing Receptor (CaSR) was first discovered by Brown *et al.* in 1993 [5]. It is a class C guanine nucleotide-binding protein (G protein)-coupled receptor (GPRC). Class C GPCR are composed of a seven-transmembrane spanning protein and a large extracellular domain (ECD), with a Venus Flytrap domain (VTFD). The VFTD is connected *via* a cysteine-rich region (CRD) to a heptahelical domain (HD) (**Figure 1**) [6].

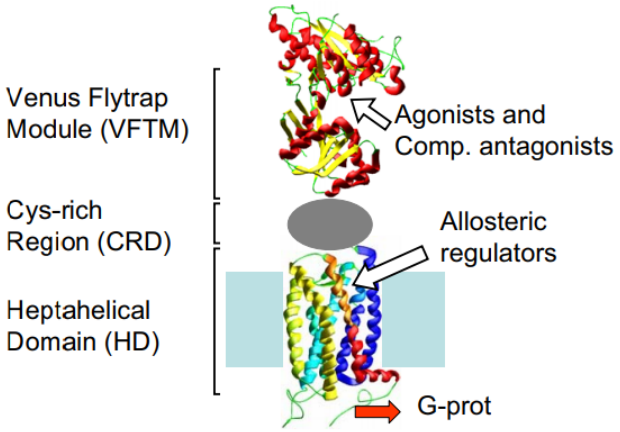

Figure 1: Schematic general structure of a class C G-protein coupled receptors.
A class C G-protein coupled receptor with venus flytrap module, cys-rich region and heptahelical domain [6]. Image used under the license from John Wiley and Sons.

The human CaSR is encoded by a single copy gene located on the long arm of chromosome 3 (3q21-q24) [7], it spans ~130 kb and has eight exons [8]. The human CaSR protein consists of 1078 amino acids. The CaSR, as a bona fide C GPCR, has a bilobed, large extracellular domain of 612 amino acids consisting of the VFTD and a CRD [9, 10] (**Figure 2**). It also has a hydrophobic 7-transmembrane spanning domain (250 amino acids), and finally a long carboxyl terminal intracellular tail, formed of 216 amino acids [11]. After translation, the CaSR is glycosylated on multiple sites with high mannose carbohydrates in the endoplasmic reticulum. In the Golgi apparatus, the CaSR is further modified with complex carbohydrates. The core-glycosylated CaSR is retained intracellularly in the endoplasmic reticulum or in pre-plasma membrane compartments [12]. If required, the CaSR is transported to the plasma membrane where it can function either as homo- or heterodimer and it signals *via* G-proteins (see chapter CaSR signaling) [13, 14].

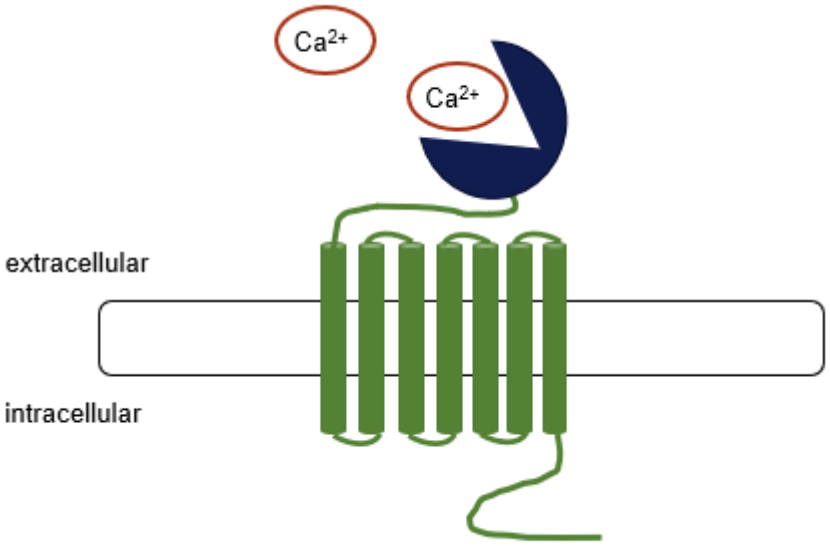

Figure 2: Scheme of the Calcium-Sensing Receptor (CaSR) expressed in the cell membrane.
The venus flytrap domain is depicted in blue, "catching" extracellular Ca^{2+}.The seven transmembrane domain is indicated in green.

The main and best characterized function of the CaSR is regulating calcium homeostasis in the body, by modulating the secretion of parathyroid hormone (PTH). The CaSR is expressed in tissues regulating Ca^{2+} homeostasis, so called “calcitropic”, tissues, such as parathyroid glands, kidneys, and bones. For many physiological processes, like nerve impulse transmission and muscle contraction, a steady calcium serum concentration is of great importance. Therefore, the CaSR regulates extracellular Ca^{2+} within a tight range of 1.1-1.3 mmol/l free ionized Ca^{2+} in the blood *via* modulating intracellular pathways that alter PTH and calcitonin secretion or renal cation handling, as described below [15]. Other GPCRs (*e.g.* β-adrenergic receptors) are rapidly deactivated after ligand binding [16], but as the CaSR is exposed to a constant level of extracellular Ca^{2+} it needs a resistance to desensitization. A unique feature, termed agonist-driven insertional signaling (ADIS), allows the CaSR to regulate its own trafficking to the plasma membrane upon activation [17]. In the Golgi apparatus, a pool of maturate, glycosylated CaSRs is stored that is poised for rapid insertion into the plasma membrane [17].

In addition to its pivotal role in maintaining serum Ca^{2+} homeostasis, the CaSR is also expressed in non-calcitropic tissues where it regulates various other fundamental processes including smooth muscle contraction, gene expression, ion channel activity, and cell fate [18]. In blood vessels, the CaSR affects cardiovascular function. It is expressed in human vascular smooth muscle cells (VSMCs) and endothelial cells [19, 20]. The CaSR was shown to have an effect on VSMC proliferation and apoptosis [21]. Studies in a mouse model with a VSMC-specific ablation of the CaSR showed a decrease in in the contractility of the aorta and mesenteric arteries, leading to a decrease of diastolic and mean arterial blood pressure [22].

The CaSR is further expressed in human and mouse airway smooth muscle and bronchial epithelium [23]. CaSR expression is increased in the airways of patients with asthma and allergen-sensitized mice [23] (refer to chapter “CaSR in inflammation”).

In epidermal cells the activation of the CaSR triggers keratinocyte differentiation, survival and adhesion [24] and has a key function for maintaining an intact

epidermal barrier [25]. In epidermis-specific CaSR-null mice, the barrier function of the skin has been shown to be defective due to impaired keratinocyte differentiation [26].

Altered CaSR expression or mutations in the *CaSR* gene that lead to a dysfunctional receptor have also been associated with several pathological conditions including inflammation in the lung and adipose tissue, vascular calcification and certain cancers [18]. Further mutations in the CaSR gene lead to calcitropic-disorders such as hyper-/hypocalcemia and hyper-/hypoparathyroidism (refer to chapter “mutations of the CaSR”).

1.3 **Regulation of calcium homeostasis *via* parathyroid hormone**

As Ca^{2+} plays a crucial role in the human body, its concentration has to be tightly controlled. For short-term control, the serum proteins (albumin) can help to maintain calcium homeostasis. Any transient drop of free ionized calcium can be compensated by the release of bound calcium from the binding sites on an albumin molecule. The albumin-calcium complex works as a calcium buffer system [2].

Long-term calcium homeostasis is mainly maintained by PTH and by 1,25-dihydroxyvitamin D_3 ($1,25(OH)_2D_3$) [27, 28]. The interaction of PTH and $1,25(OH)_2D_3$ is displayed in **Figure 3**. PTH is secreted by the chief cells of the parathyroid glands and is suppressed in response to high blood Ca^{2+} levels. The secretion of PTH is suppressed by the CaSR, which is expressed on the surface of parathyroid cells and constantly senses the extracellular Ca^{2+} levels. If the free Ca^{2+} levels drop, the CaSR-mediated PTH suppression is released, leading to higher PTH levels. PTH then directly stimulates osteoclast activity leading to resorption of Ca^{2+} of the bones. In the kidney, PTH stimulates the Ca^{2+} reabsorption from renal tubular fluid while increasing the excretion of phosphate in the urine. PTH further activates 25-hydroxyvitamin D_3 1α-hydroxylase in the kidney which converts 25-hydroxyvitamin D_3 ($25(OH)D_3$) to its most active metabolite $1,25(OH)_2D_3$. $1,25(OH)_2D_3$ facilitates the absorption of Ca^{2+} and phosphorus from the intestine. Rising Ca^{2+} concentrations lead to a negative feedback loop, activating the CaSR and inhibiting PTH excretion [28]. A short

peak production of PTH, where the Ca^{2+}-needs of the body can be immediately satisfied *via* Ca^{2+} resorption from the intestine, leads to a short time increased Ca^{2+} concentration in the blood serum and the surplus Ca^{2+} is stored in the bones. If there is a Ca^{2+} deficiency in the intestine due to malnutrition, the activation of the CaSR increases PTH but no Ca^{2+} can be absorbed from the intestine. The PTH levels stay elevated and lead to bone resorption to balance the Ca^{2+} and in the long term to bone demineralization, *i.e.* osteopenia, or in case of kidney failure, the clinical symptoms of chronic kidney disease mineral bone disorder due to insufficient renal production of $1,25(OH)_2D_3$ in response to PTH [29].

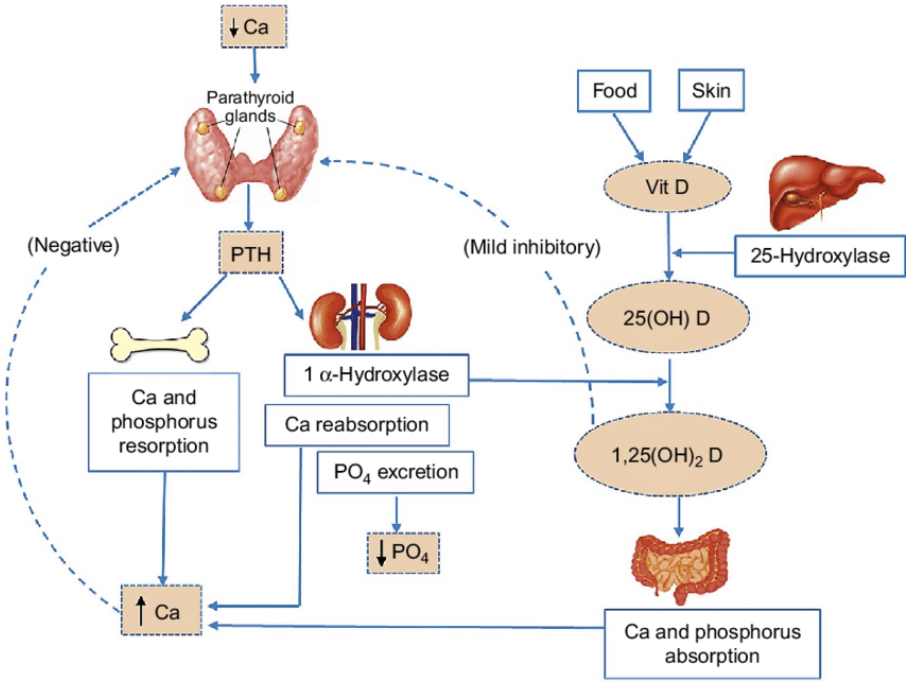

Figure 3: Schematic diagram of calcium homeostasis signaling.
Dropping Ca^{2+} levels are sensed by the calcium-sensing receptor (CaSR; not shown here) in the parathyroid glands which leads to a reduced suppression of parathyroid hormone (PTH) production and thus an increase in PTH levels. PTH leads to Ca^{2+} reabsorption in the bones and in the kidney. Vitamin D3 (Vit D) is converted via 25-hydroxlyase to 25-hydroxyvitamin D3 (25(OH)D) and then, catalyzed by PTH, converted into 1,25-dihydroxyvitamin D3 ($1,25(OH)_2D$). $1,25(OH)_2D$ leads to Ca^{2+} absorption in the intestine. Solid lines indicate stimulatory interaction, dashes line negative feedback [28]. Image used under the license from Elsevier.

1.4 **Calcium-Sensing Receptor ligands**

Ca^{2+} is the main physiological ligand of the CaSR, but there is a plethora of other agonists. Calcimimetics are agonists / positive modulators of the CaSR and are classified as either type 1 or type 2 calcimimetics. Type 1 calcimimetics are the naturally occurring ligands and bind orthosterically to the VFTD of the receptor and activate the receptor directly [30]. These can be di- and trivalent cations, polyamines, polypeptides, or aminoglycoside antibiotics [31], like neomycin [32]. An example for such a polyamine is spermine, which is found in eukaryotic cells and involved in many cellular processes such as cellular metabolism, transcription and translation [33]. Due to their positive charge at physiological pH, polyamines are known to support nucleic acid structure and stability [34]. In 1977, the polyamines spermine and spermidine were already reported as immune-regulators [35], as spermine downregulates macrophage activation [36]. Aromatic amino acids, such as L-phenylalanine and L-tryptophan can act either as type-1 or as type-2 ligands and have a higher affinity for the receptor than aliphatic and polar L-amino acids [37]. Structures of these compounds are shown in (**Figure 4**).

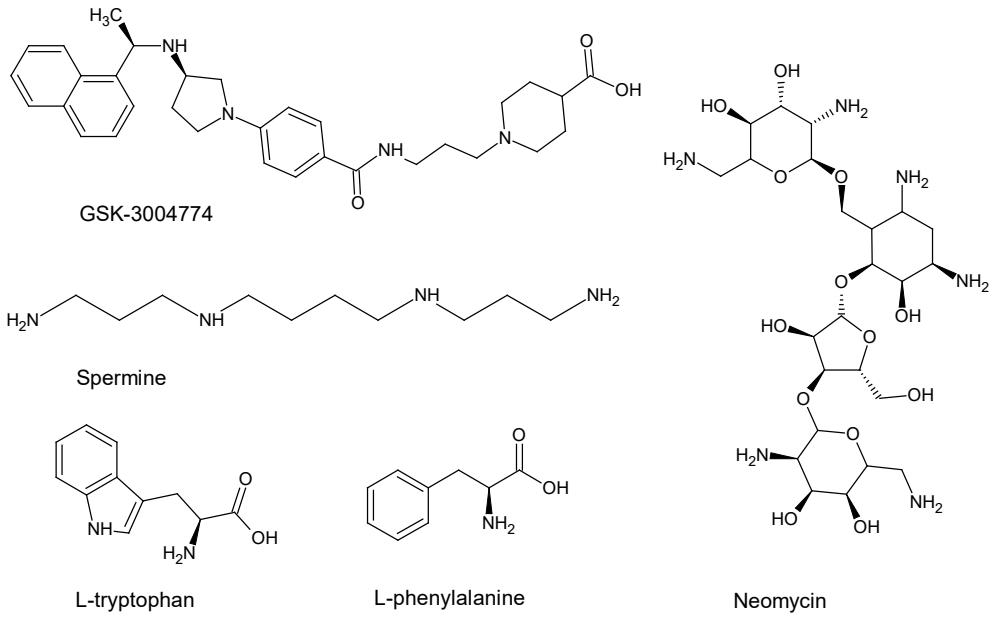

Figure 4: Chemical structures of CaSR ligands.
GSK-3004744, spermine, the aromatic acids L-tryptophan and L-phenylalanine, and the antibiotic neomycin.

Pure type 2 calcimimetics bind allosterically within the seven-transmembrane region of the CaSR [30]. Type 2 calcimimetics can occur naturally, such as L-amino acids, or they can also be synthetic compounds which increase the sensitivity of the CaSR to extracellular Ca^{2+} [43]. They increase the sensitivity of the CaSR for its type 1 agonists which can be seen *e.g.* as shift of the half maximal effective concentration (EC_{50}) for Ca^{2+} to lower concentrations. As a result, the CaSR already inhibits PTH release at lower Ca^{2+} concentrations [38]. This leads to a decrease in PTH plasma levels that is followed by a decrease of plasma Ca^{2+} levels [39].

Synthetic type-2 calcimimetics are used as targeted therapies for parathyroid disorders but also for treating symptomatic hypercalcemia [40]. In a drug discovery program in the 1990s, NPS R-568, one of the first calcimimetics, was synthesized and entered the clinic in 1994 [41] but failed in clinical trials and is since used as the main research calcimimetic. NPS R-568 is a phenylalkylamine (**Figure 5**) derived from Ca^{2+}-channel blockers like verapamil and acts like a type 2 calcimimetic [42]. NPS R-568 selectively activates the CaSR on parathyroid cells, resulting in inhibition of PTH secretion in parathyroid cells both *in vitro* and *in vivo* [38]. Based on NPS R-568, cinacalcet (Figure 5) was the first calcimimetic approved in the clinic as a therapy for secondary hyperparathyroidism in chronic kidney disease and it is also used for “off-label” applications to treat hypercalcemia in some forms of primary hyperparathyroidism [39]. Besides cinacalcet there is now another calcimimetic, etelcalcetide, which is an approved drug for the treatment of secondary hyperparathyroidism administered intravenously in combination with hemodialysis [43]. The calcimimetic velcalcetide (AMG 416) is currently under regulatory reviews and could be also a potential drug for the treatment of secondary hyperparathyroidism [43]. In 2017, GSK-3004774, a small molecule compound, was published [44]. It is a chemical non-absorbable, gastrointestinally-restricted calcimimetic [44].

Calcilytics act as negative allosteric modulators of the CaSR, binding in the transmembrane domain. They decrease the sensitivity of the CaSR to extracellular Ca^{2+} and increase the EC_{50} of the CaSR for extracellular Ca^{2+}. Calcilytics cause an increase in plasma levels of PTH, followed by an increase

in plasma levels of Ca^{2+} [45]. Calcilytics are used as targeted therapies for parathyroid disorders but also for treating symptomatic hypocalcemia [40] The calcilytic NPS 2143 is an amino-alcohol compound (**Figure 5**) and negatively modulates the CaSR, which leads to an increased secretion of PTH [46].

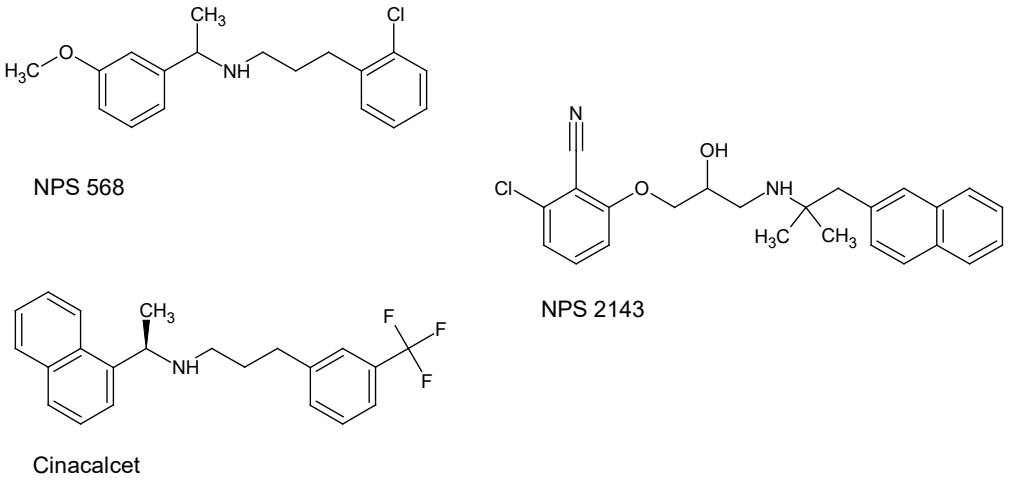

Figure 5: Chemical structure of NPS 568, Cinacalcet and NPS 2143.
The structures are displayed in a non-stereo defined way.

Because of this rise in PTH secretion, NPS 2143 was developed for the treatment of osteoporosis, taking advantage of the induced anabolic effects on bone mass [46]. As already described above, only short-term peaks of PTH leads to an increase in blood serum Ca^{2+} and to the storage of surplus Ca^{2+} in the bones. As a results, the peak expression counteracts the symptoms of osteoporosis [29]. In rat *in vivo* experiments, a rapid and sustained increase of plasma PTH was observed after injection of NPS 2143 [47] but no alteration in bone mineral density (BMD) [47]. This lack of bone anabolic effect is probably due to a large volume of distribution (V_D) of NPS 2143 [48]. The V_D represents the degree to which a drug is distributed in body tissue rather than the plasma. The large V_D leading to long-term systemic exposure and sustained elevations of PTH plasma concentrations [48] and thus, rather to bone resorption. In phase 2 clinical trials, also other calcilytics with improved pharmacokinetics compared to NPS 2143 and a lower V_D, such as ronacaleret and JTT-305/MK-5442 have proven to be ineffective for treating osteoporosis [49, 50].

1.5 **Calcium-Sensing Receptor-mediated signaling**

Ca^{2+} signaling functions over a varied time range. Starting from signals in microseconds, for example at synaptic junctions during Ca^{2+}-triggered exocytosis, to minutes and hours, when events such as gene transcription and cell proliferation are mediated [51]. As a GPCR, the CaSR regulates various downstream signaling pathways by the activation of the heterotrimeric G protein subunits. The CaSR-mediated signaling pathway is illustrated in **Figure 6**. Extracellular Ca^{2+} binds on the VFTD, which initiates a conformational change and allows the CRDs to interact [10]. The conformational changes reorientate the seven-transmembrane domain, leading to the activation of the G-proteins, which in turn leads to signal transduction [10]. A recent study of Gao *et al.* showed by cryo-electron microscopy that the activated configuration of the CaSR is stabilized by calcimimetics, whereas the binding of calcilytics lock the CaSR in its inactive configuration [52]. The CaSR signals through three main groups of G proteins, $G_{q/11}$, $G_{i/o}$ and $G_{12/13}$. In certain cell contexts, it may also activate G_s. The predominant signaling occurs *via* the $G_{q/11}$ pathway. Activation leads to the suppression of cyclic adenosine monophosphate (cAMP) and activation of mitogen-activated protein kinase (MAPK) cascades [53]. Through activation of $G_{q/11}$, the phospholipase C (PLC) pathway is activated [54]. PLC hydrolyses the membrane phospholipid PIP2 to 1,4,5-triphosphate (IP_3) and diacylglycerol (DAG). IP_3 binds to the IP_3 receptor (IP3R), located on the endoplasmic reticulum (ER) or, as shown in **Figure 6**, on the sarcoplasmic reticulum (SR). Activation of the IP3R leads to Ca^{2+} release from the lumen of the ER/SR and intracellular Ca^{2+} signaling *via* a variety of effector molecules like protein kinase C (PKC) [55].

The G protein subunit $G_{\alpha 12/12}$ activates the Rho guanine nucleotide exchange factor (RhoGEFs). RhoGEFs converts the inactive protein Ras homolog family member A (RhoA) to the active form [56]. The RhoA/RhoA-activated kinase pathway amplifies the Ca^{2+}-induced contractile force of smooth muscle cells, a process called Ca^{2+} sensitization [57]. Regulating the contraction of smooth muscles is of importance for critical physiological functions, such as the maintenance of proper blood pressure within the vasculature [57]. In other cell types the RhoA/RhoA-activated kinase pathway is involved in actin organization

[58] and tissue polarity [59], cell development [60], transcription control [61], and in cell cycle maintenance [58].

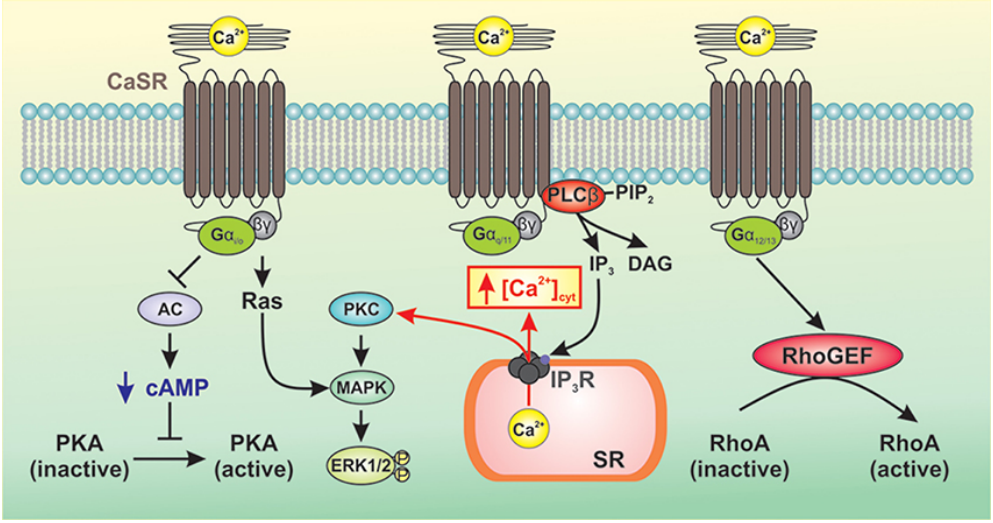

Figure 6: CaSR mediated signaling via the three main groups of G-proteins.
Extracellular Ca^{2+} binds to the venus flytrap domain (VFTD) and leads to conformational changes of the receptor. The seven-transmembrane is reorientated and the different G-proteins can be activated. The $G_{i/o}$ pathway leads to the suppression of adenylyl cyclase (AC) and with that to a downregulation of cyclic adenosine monophosphate (cAMP). cAMP suppresses the activation of cAMP-dependent protein kinase (PKA). Furthermore, the mitogen-activated protein kinase (MAPK) cascades are enhanced. The $G_{q/11}$ subunit activates phospholipase C (PLC), which generates inositol 1,4,5-triphosphate (IP3) and diacylglycerol (DAG). IP3 binds to the IP3 receptor (IP3R) on the sarcoplasmic reticulum (SR) which leads to an increase of the cytosolic Ca^{2+} concentration ($[Ca^{2+}]$cyt) via influx from the SR stores. $G_{12/13}$ activates Rho guanine nucleotide exchange factor (RhoGEFs) leading to an activation of protein Ras homolog family member A (RhoA) [62]., CC-BY 4.0.

1.6 Biased signaling of the Calcium-Sensing Receptor

Seven-transmembrane GPCRs can have various physiological conformations, depending on the binding ligand. Different ligands lead to different forms of cell signaling, a phenomenon termed ligand bias. The different ligands might stabilize these unique receptor conformations [63]. Biased signaling raises the possibility of cell- or tissue-specific signaling profiles that vary in a ligand-specific manner. As described previously, the CaSR has various ligands, resulting in different cellular responses, depending on the tissue where the CaSR is expressed, and which ligand is activating the receptor [64].

1.7 **Enantio-selective receptor activation**

Enantiomers are stereoisomers that are mirror images of each other. A single chiral atom leads to the non-superposable characteristic. For example, an asymmetric carbon is bound to four different atoms or groups. Depending on their order, the molecule has the prefix S (lat. *sinister*) or R (lat. *recte*) (**Figure 7**) [65]. Enantiomers can be distinguished by their ability to rotate plane-polarized light in opposite directions. This characteristic is termed optically active. The prefix (+) indicates that the molecule rotates light in a clockwise direction, and (-) in a counter-clockwise direction. Importantly, an S-enantiomer does not have to be a (-)-enantiomer or *vice versa*, as these properties are independent.

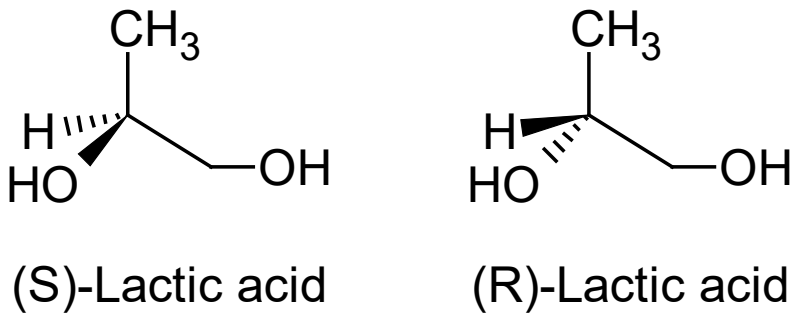

Figure 7: Representative example for enantiomers.
On the left side, the R-enantiomer of lactic acid is shown, the hydroxy group is drawn out of the plane. On the right side, the S-enantiomer of lactic acid, the hydroxy group is drawn into the plane.

Enantiomers of a pharmacological compound can be used to test whether the compound binds selectively to a target. The differently configured side chain of the chiral atom prevents the “inactive” or non-selective enantiomer from binding. This dependence of the ligand / target interaction on the stereo-configuration of the ligand is called “enantioselectivity”.

Many chiral compounds display enantioselectivity in their biological effects. Enantioselectivity is an important aspect of receptor-mediated biological activity. A very prominent and tragic example is thalidomide (trade name Contergan), known through the thalidomide scandal in the late 1950s and early 1960s. Being traded as a medication for anxiety and morning sickness, thalidomide became quite popular as a sedative for pregnant women, but without proper clinical trials [66]. While the (+)-(*R)*-enantiomer has the sedative effect, the (-)-(*S)*-enantiomer

is teratogenic [67]. The individual enantiomers can racemize (*i.e.* be metabolized into each other *in vivo*) [67, 68]. Thalidomide can nowadays be used for different cancer treatments by exploiting its anti-angiogenic effect.

For the calcimimetic cinacalcet, only the R-enantiomer is used in the clinic, as the S-enantiomer does not bind specifically to the CaSR and therefore has no therapeutic effect. The R-enantiomer of NPS 568 was shown to be 10-fold more potent at the CaSR than the S-enantiomer [69].

The CaSR shows this enantioselectivity also for the calcilytic NPS 2143. The R-enantiomer is many times more potent since the stereochemistry of the hydroxy group is critical for the binding to the receptor [70].

1.8 **Mutations of the Calcium-Sensing Receptor**

Mutations in the *CaSR* gene are linked with altered signaling output by the receptor and reduced cell surface expression, leading to Ca^{2+} homeostasis-related diseases. Heterozygous inactivating mutations lead to familial hypocalciuric hypercalcemia (FHH1), usually transmitted as an autosomal dominant trait and leading to a moderate hypercalcemia and a normal or high plasma PTH value. Homozygous inactivating mutations lead to neonatal severe hyperparathyroidism (NSHPT), with a clinical presentation of a marked hypercalcemia and increased PTH serum levels and resulting in a severe life-threatening disorder. Autosomal dominant hypocalcemia (ADH1) is caused by heterozygous activating mutations of the CaSR and causes hypocalcemia with normal or low PTH levels (reviewed in [71]).

There are also several known polymorphisms of the CaSR, which might have an impact on receptor function and Ca^{2+}-regulated PTH secretion. The definition of genetic polymorphisms by Cavalli and Bodmer from 1971 is still used: “Genetic polymorphism is the occurrence in the same population of two or more alleles at one locus, each with appreciable frequency" [72]. Genetic variants that occur with an allele frequency below 1% are termed mutations rather than polymorphisms, a widely accepted concept to differentiate between mutations and polymorphisms.

Missense polymorphisms are leading to amino acid changes [73]. The heterozygous variant of the missense polymorphism Q1001E leads to higher serum calcium and PTH levels compared to the WT-variant [74]. The effect of the polymorphism A986S is controversial. On the one hand, A986S has been associated with higher serum Ca^{2+} levels and an increased risk of developing primary hyperparathyroidism (PHPT) [75, 76]. On the other hand, studies have shown that A986S does not correlate with serum Ca^{2+} levels and does not play a relevant role in the pathogenesis of PHPT [74, 77].

R185Q leads to a dominant negative loss-of-function of the CaSR [78, 79]. Amino acid 185 is located within a subdomain of the extracellular VFTD, containing putative Ca^{2+}-binding sites [80]. The R185Q mutant retains normal maturation and membrane trafficking in human embryonic kidney cells (HEK-293). However, it is known that the R185Q mutant leads to defective cell signaling and clinically to a higher risk of hypercalcemia and hyperparathyroidism [79, 81]. F612S is a gain of function mutation of the CaSR, causing hypocalcemia and hypoparathyroidism by increasing receptor sensitivity to extracellular Ca^{2+} and maximal signal transduction capacity [82].

1.9 **The Calcium-Sensing Receptor in inflammatory processes**

Hypocalcemia is a known issue in critically ill patients with a history of sepsis and major burn injury. One crucial factor leading to hypocalcemia was identified to be decreased secretion of PTH and/or kidney and bone resistance to PTH [83]. There is evidence that increased circulating levels of proinflammatory cytokines could be the reason for systemic calcium dyshomeostasis [84, 85]. Increasing levels of interleukin (IL)-1β and IL-6 are inversely related to serum calcium concentration [86]. Neilsen *et al.* demonstrated that IL-1β suppresses PTH secretion. In addition, they observed an upregulation of CaSR messenger-(m)RNA levels in bovine parathyroid tissue slices [87]. Neilsen *et al.* proposed a model in which inflammatory processes lead to a higher abundance of cytokines, which suppress PTH secretion but enhance CaSR mRNA expression. Both, decreasing PTH secretion and increasing CaSR expression, led to reduced Ca^{2+} levels and with that to hypocalcemia.

The CaSR is not only activated by divalent cations but also by polycations, known to play a role in inflammatory processes, such as spermine, spermidine, and eosinophil-derived cationic proteins [23, 88]. In the lung, the CaSR, expressed in airway smooth muscle cells and epithelial cells, was shown to be activated by inflammatory cationic proteins known to correlate with asthma severity [23]. As asthma-relevant cytokines can further increase CaSR expression in airway smooth muscle cells, this would generate a positive feedback loop. Calcilytics can prevent this effect and may be effective asthma therapeutics [23]. These findings suggest that the CaSR is directly involved in mechanisms in inflammatory cell recruitment and activation [23].

In a follow-up study from 2021, various calcilytics were tested for the treatment of airway hyperresponsiveness (AHR) and for the inhibition of airway inflammation [89]. Inhaled calcilytics had no side effects, but reduced airway inflammation and abolished AHR [89]. These findings are giving evidence that calcilytics are indeed a potential therapy for asthma control and prophylaxis.

The CaSR is expressed also in human adipose cells. Activation with the calcimimetic cinacalcet in adipose tissue and in *in vitro* cultured adipose cells led to an elevation in the expression of the proinflammatory cytokines IL6, IL1-β and CC-chemokine ligand 20 (CCL20). This suggests a role of the CaSR in the pathophysiology of obesity-induced adipose tissue dysfunction [90] and further strengthens the link of the CaSR to inflammatory processes in general.

The dextran sulfate sodium (DSS)-induced inflammation is a well-established model for chemically induced acute colitis. Amino acids and glutamyl dipeptides are known agonists of the CaSR and were linked to a CaSR-dependent inhibition of pro-inflammatory cytokines release [91, 92]. γ-glutamyl dipeptides reduced the production of inflammatory cytokines and chemokines including IL-8, IL-6 and IL1-β in colon cancer cells [92]. *In vivo*, γ-glutamyl dipeptides ameliorated clinical signs in a mouse DSS-model [92]. The anti-inflammatory effects of amino acids and glutamyl dipeptides were also shown in other *in* vivo DSS-studies, where the ameliorating effect was reduced by the intravenous administration of NPS 2143 [91, 92].

In a study from 2014, Cheng *et al* used an intestinal epithelial cell-specific CaSR knockout mouse model to examine the role of the CaSR in the intestine [93]. Deletion of the CaSR induced inflammatory responses and increased expression of inflammatory cytokines. CaSR-knockout mice were more prone to DSS-induced intestinal inflammation. These results link the CaSR to intestinal inflammation. However, in contrast to the previously mentioned findings in the lung and adipose tissue, the research suggested an anti-inflammatory effect of the CaSR in the intestine.

As these findings suggest that the CaSR could function as potential target for treatments in intestinal inflammation, our group tested the effect of highly selective pharmacological CaSR ligands in a DSS mouse model. Furthermore, they administered orally the calcimimetic to activate the CaSR. Contrary to the expectations, the treatment with cinacalcet had a pro-inflammatory effect in this DSS-mouse model. Inhibiting the CaSR with NPS 2143 improved the clinical symptoms of colitis. These findings suggested a pro-inflammatory effect of the CaSR also in the intestines [94].

To examine further these contradictory results, our group wanted to study the impact of the CaSR in an *in vitro* experiment. As described previously, during carcinogenesis the CaSR is downregulated. Because of this, the colon cancer cell line HT29 was stably transfected with the CaSR, using the lentiviral system [95]. The cells were transfected with a plasmid vector containing the CaSR labelled with green fluorescence protein (GFP) ($HT29^{GFP\text{-}CaSR}$). As control cells, HT29 cells were transfected with a vector lacking the CaSR and only coding for GFP ($HT29^{GFP}$). This study has shown that NPS R-568 increased the expression of inflammatory markers such as IL-8, CCL20 and COX-2 [95].

To conclude, the CaSR was shown to play a pro-inflammatory role in several tissues, including the lung, adipose tissue and recently also the colon. It seems to be directly involved in promoting inflammatory mechanisms.

1.10 **Chronic intestinal inflammation**

Inflammatory bowel diseases (IBD) include Crohn´s disease (CD) and ulcerative colitis (UC), and are characterized by chronic inflammation of the gastrointestinal (GI) tract. CD can affect any part of the GI tract, even though it most often affects the small intestine. In UC, mucosal inflammation is limited to the large intestine and the rectum. The molecular mechanisms of the development of CD and UC are not completely understood. Studies suggest that CD and UC result from an inappropriate inflammatory response to intestinal microbes and that the host-microbe interactions lead to the pathogenesis of these diseases. Further causes can also be autoimmune reactions of the body [96]. IBD is a polygenic, complex disorder with different genetic risk factors [97].Pathogenesis is highly linked with genetics. Familial clustering of cases and twin studies have underlined the role for genetic factors. The inheritable component seems to be stronger in CD [98] than in UC. Several environmental factors such as age, lifestyle and especially the gut microbiota seem to play a role in IBD pathogenesis [99]. One of the main inflammatory pathways in the intestine is the prostaglandin pathway and is explained in the following paragraph.

1.11 **Prostaglandin pathway**

Prostaglandins are a subfamily of the eicosanoids, a group of physiologically active lipid compounds. They are synthesized from arachidonic acid (AA), which is found in the lipid bilayer of the cell-membrane. AA is released from the plasma membrane by the enzyme phospholipase A2 (PLA2) and then processed in the prostaglandin pathway. The prostaglandin E2 (PGE2) pathway is shown in **Figure 8**. In the first step, COX-1/-2 catalyzes the conversion of AA to prostaglandin G2 (PGG2) *via* its cyclooxygenase activity. In the second step, PGG2 is reduced to the intermediate product prostaglandin H2 (PGH2) *via* the peroxidase activity of prostaglandin synthase (PGES). PGH2 is further processed into PGE2 [100]. The AA release by PLA2 and the cyclooxygenases are the key rate-limiting steps for prostaglandin biosynthesis. Nonsteroidal anti-inflammatory drugs (NSAIDs) inhibit cyclooxygenase activity by blocking the AA binding to COX-binding sites [101].

PGH2 can now be further processed by specialized prostaglandin synthases to several structurally related prostaglandins [102]. In the PGE2 pathway, PGH2 is converted to PGE2 *via* the prostaglandin synthases [103]. The synthesized PGE2 is immediately transported outside the cell after its synthesis where it interacts with specific cell-surface G-protein-coupled receptors termed EP1-4 and induces autocrine or paracrine signaling [104]. Alternatively, PGE2 can be degraded by 15-hydroxy PG dehydrogenase (15-PGDH) (not indicated in **Figure 8**) [105]. 15-PGDH catalyzes the NAD^+-dependent oxidation of the 15(S)-hydroxyl-group of prostaglandins, which results in a greatly reduced biological activity of the prostaglandins [105]

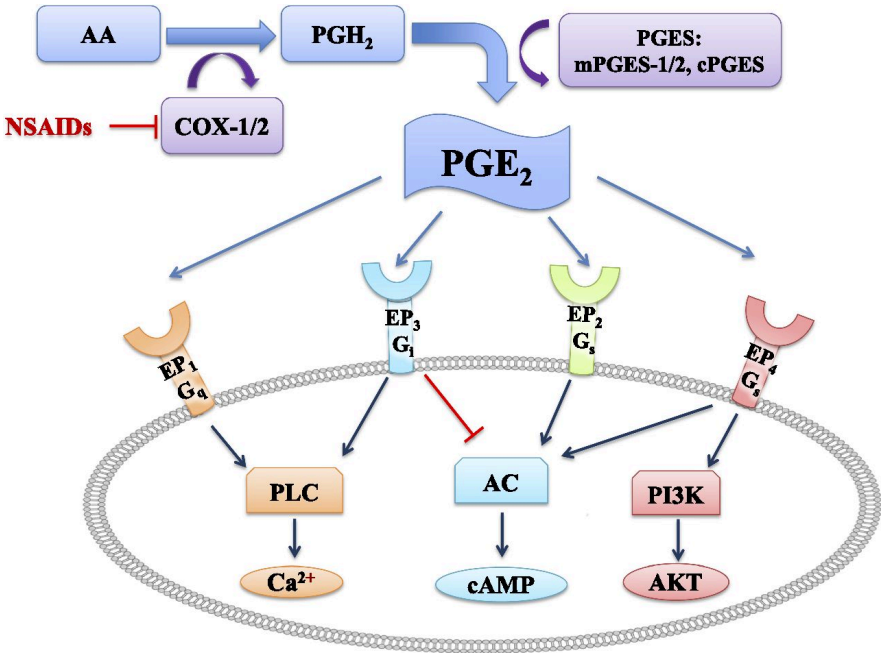

Figure 8: The Prostaglandin synthase pathway.

Arachidonic acid (AA) is metabolized into prostaglandin H2 (PGH2), catalyzed by cyclooxygenase 1/2 (COX-1/2). COX-1/-2 can be inhibited by nonsteroidal anti-inflammatory drugs (NSAIDs). PGH2 is an intermediate product and is further processed by prostaglandin synthase (PGES) to prostaglandin E2 (PGE2). PGE2 bind to the receptors EP1-4 and leads to different cellular responses. PLC: phospholipase C, AC: adenylate cyclase, cAMP: cyclic adenosine monophosphate, PI3K: phosphoinositide 3-kinase; AKT: protein kinase B [103]. Image was modified and used under the license of the American Society of Nephrology.

Prostaglandins are found in almost every tissue in humans and play a key role in the generation of the inflammatory response. COX-1 and COX-2 are the two main isoforms of COX, they are 60% homologous but are encoded by separate genes [106]. COX-1 is found in almost every tissue and is termed as “housekeeping

enzyme", maintaining basal prostaglandin levels important for tissue homeostasis [102]. It is especially important for the production of natural mucus lining, which protects the inner stomach [107].

In contrast, COX-2 expression is normally not detectable in tissues, but it is inducible and is expressed in most inflammatory states. Indeed, COX-2 is the primary isoform involved in inflammation. The pro-inflammatory role of specific prostaglandins is well established and the aberrant expression of COX-2 in the majority of colorectal tumors is thought to play a crucial role in CRC carcinogenesis [108, 109]. Both COX-2 and PGE2 seem to affect most hallmarks of cancer [102]. Several studies have revealed that pharmacological inhibition of COX-2 leads to a decrease in adenoma size and number in murine models of intestinal tumorigenesis [110].

PGE2 is the most important member of the PGE2 pathway, and it is generated in high levels by colon tumor cells. Increased expression of COX-2 in colorectal cancer cells [111-114], and the production of PGE2, leads to the promotion of growth and development of the tumor as well as invasion, metastasis and angiogenesis [115]. Furthermore, high PGE2-levels increased the resistance to apoptosis [115]. Research suggests a positive feedback loop in colon cancer cells between COX-2 and PGE2, in which COX-2 induces the generation of PGE2 while the upregulation of PGE2 increases the expression of COX-2 [115].

Targeting the COX-2/PGE2/EP-receptors is therefore a promising treatment especially for the prevention of CRC and inflammation-associated CRC.

1.12 **The prostaglandin pathway in the intestine**

PGE2 is responsible for normal physiological functions of the GI tract including gastric mucosal protection, wound healing and motility. But it is also considered to be one of the main inflammatory mediators in the intestine and implicated in the genesis of IBD [116] and CRC [111]. This diversity in cellular responses can be explained through the four different subtypes of EP receptors (EP1-4) that lead to different signals with alternating intracellular Ca^{2+} or cAMP levels [117].

As mentioned earlier, NSAIDs inhibit cyclooxygenase activity by preventing AA from binding to COX-binding sites [101] and thus inhibiting PGE2 synthesis. Early studies from 1980 [118] and 1981 [119] suggested that NSAIDs like acetylsalicylic acid (aspirin) have a chemopreventive effect against intestinal cancer in animal models. Studies by Thun *et al* in 1991 and 1993 further investigated the relationship between aspirin use and colon cancers in humans. They showed not only a protective effect from aspirin tablets for the relative risk of colon cancer but also that aspirin use reduced deaths from esophageal, gastric and rectal cancer [120, 121].

1.13 **Colorectal cancer**

Colorectal cancer (CRC) is one of the most common cancers in industrialized societies. It is the second most common cause of cancer in both men and women, in 2018 1.8 million new cases were reported worldwide [122]. The incidence of CRC increases significantly from the age of 50 and is often considered as elderly people´s disease [123]. There are some genetic risk factors for CRC, but it is presumed that most CRCs are caused by lifestyle factors, such as unhealthy nutrition, smoking, obesity, and lack of physical activity [124]. About 65 % of all new cases occur in high-income countries [123]. The most common genetic cause for colorectal cancer is hereditary nonpolyposis CRC (Lynch syndrome), which still represents only 3 % of patients with CRC [125]. Lynch syndrome is an autosomal dominant genetic condition. Other genetic causes can be Gardner syndrome and familial adenomatous polyposis. Both of these syndromes are inherited in an autosomal dominant way as well [126]. The classical model of sporadic CRC pathogenesis is the adenoma to

cancer progression sequence (**Figure 9**). An adenoma is the abnormal growth of tissue leading over benign tumors to the transition into CRC over many years [127].

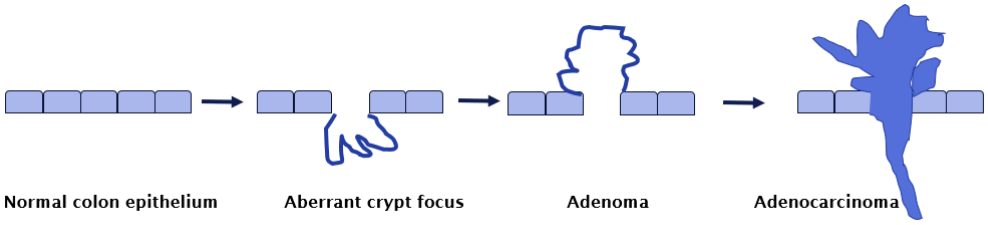

Figure 9: Polyp to cancer progression sequence.
The crypt develops into an adenoma and further into an adenocarcinoma.

1.14 Colitis-associated colorectal cancer

One of the most severe consequences of IBD is the development of colitis associated CRC (CA-CRC). Studies have shown that patients with a history of IBD have a higher risk in developing CRC compared to patients with no history of IBD (sporadic development of CRC) [128-130]. The risk for colon cancer increases with the duration and anatomic extent of colitis. Meta-analyses have been shown that patients with UC have a cumulative risk for CRC from 2% after 10 years of disease to 18% after 30 years of disease [130]. This is also seen in patients with CD, where the risk for CRC increases from 2.9% at 10 years to 8.3% after 30 years of disease [131].

CA-CRC differs from the normal “mucosa-adenoma-dysplasia-carcinoma” sequence. CA-CRC arises in the inflamed mucosa and develops through an “inflammation-dysplasia-carcinoma” sequence, with the characteristic clinicopathological features of CRC [132].

In the genetic profile of CA-CRC mutations, microsatellite instability and DNA hypermethylation are found. The genetic characteristics of CA-CRC are quite different compared with those found in sporadic CRC. In CA-CRC, mutations in the cell cycle control gene *p53* occur early in the adenoma-carcinoma sequence and adenomatous-polyposis-coli-protein (APC) mutations in the late phase. In contrast, in sporadic CRC APC aberrations occur early in their pathogenesis and p53 mutations occur in the late phase [133, 134].

There is accumulating evidence that control of long-term background inflammation and mucosal damage is vital and that chronic ulcerative colitis therapies could be an important strategy for reducing CRC risk in UC patients [135].

1.15 **The role of the Calcium Sensing Receptor in cancer**

The CaSR influences cell fate-regulating processes including proliferation, differentiation, and apoptosis, suggesting a substantial impact in cancer development [31, 136]. The CaSR seems to play a paradoxical role in the development of cancer. Depending on the tissue involved. It can prevent or promote tumor growth. In prostate and breast tumors, the CaSR functions as an oncogene and its expression in the tumor is increased, promoting proliferation, and inhibiting apoptosis.

In contrast, studies have shown that in parathyroid or colon, the increased expression of the CaSR inhibits proliferation and induces differentiation of cells, acting as a tumor suppressor [137]. The CaSR is expressed in normal colonic mucosa and in early adenomas, but it becomes lost in late-stage undifferentiated adenomas, due to promoter hypermethylation and histone deacetylation [138]. This tumor suppressing action was postulated in several studies *in vivo* and *in vitro* [139-141].

1.16 **Aims and research questions**

The CaSR is still subject to intensive research. The cellular response mediated by the CaSR is both tissue and ligand dependent. This promiscuity makes the CaSR a challenging research target. As it was shown to have a “Ying Yang” role in tumorigenesis [31], also its role in inflammation is controversial. While previous studies have shown a rather anti-inflammatory effect of the CaSR in the intestine, recent results of our group provided evidence that the CaSR has a rather pro-inflammatory effect in the intestine, similar to the effects seen in the lung or adipose tissue.

After stably transfecting the CaSR in HT29 cancer cells, an increase in inflammatory genes, such as IL-8, COX-2 and CCL-20 has been observed by our group. This effect was further enhanced through the activation of the CaSR with calcimimetics (explained in detail in the introduction) [95]. However, it was still not clear whether the observed effects were indeed mediated *via* the CaSR. And even if it is confirmed, it is still unknown over which pathway the inflammatory response is mediated.

In my research of my master thesis, my first aim was to confirm *via* enantio-selective activation whether the inflammatory response is really mediated *via* the CaSR and if genes of the inflammatory PGE2 pathway are affected by CaSR activation.

For my second aim I wanted to see whether different ligands of the CaSR lead to a different inflammatory cellular response in $HT29^{CaSR\text{-}GFP}$ and $HT29^{GFP}$ cells.

For the first two experiments, preliminary experiments were performed by two bachelor students in our group, Gitta Frisch and Marta Sladczyk.

As mutations in the *CaSR* gene are known to lead to clinical symptoms, such as hyper- and hypocalcemia, another aim of my master thesis was to test the effect of different CaSR mutations on colorectal cancer cells and if they affect the CaSR-mediated inflammatory gene response.

My study is thus guided by the following research questions:

1) Is the inflammatory response in transfected $HT29^{CaSR\text{-}GFP}$ mediated by the CaSR? (To be confirmed using enantioselective activation of the CaSR).
2) Do different ligands of the CaSR have different effects on the inflammatory gene expression in HT29 colon cancer cells?
3) Do mutations or polymorphisms of the CaSR have an effect on the general gene expression and the inflammatory gene response in HT29 colon cancer cells?

2 Methods

2.1 Cell culture

HT29 cells were stored at in liquid N_2. For thawing, I quickly placed the cells in a 37°C water bath and then added slowly cell medium, to a final volume of 10 ml. The suspension was then centrifuged for 10 minutes at 1.000 x *g*, afterwards I removed the medium and resuspended the cells in 1 ml new medium. I transferred the cell suspension in a 25 cm^2 flask. The cells were cultured in Dulbecco´s Modified Eagle Medium (DMEM) supplemented with 10 % fetal calf serum (FCS), 1 % 4-(2-hydroxyethyl)-1-piperazineethanesulfonic acid (HEPES) buffer, 1 % L-glutamine (**Table 1**) at 37 °C in a humid atmosphere containing 5 % CO_2. $HT29^{CaSR\text{-}GFP}$ and $HT29^{GFP}$ were cultured in the same supplemented medium with the addition of puromycin (5 µg/ml) to select for stably transfected cells. I used the cells until passage 18.

Table 1: *Components used for cell medium.*

Component	Amount	Concentration	Catalog number	Company
DMEM	500 ml	4.5 g/l D-Glucose	41965-039	Gibco™ USA
HEPES Buffer	5 ml	1 M	15140-122	
L-Glutamine	5 ml	200 mM	25030-024	
PenStrep	5 ml	10.000 Units/ml penicillin + streptomycin	15630-056	
Heat-inactivated FCS	50 ml	100 % serum	10270-106	

Medium was changed three times per week. Cells were passaged every 7 days, when they reached at least 80% confluence. For cell dissociation from flasks, the cells were first washed with 1x phosphate-buffered saline (PBS), and then treated with Trypsin (Trypsin-EDTA 0.05 % phenol red, Gibco™, USA). Cells were kept in the incubator until all the cells were detached from the bottom. 4 ml of cell medium were added to the detached cells to inhibit the Trypsin. The supernatant was centrifuged for 5 minutes at 1.000 x *g* and subsequently

removed. The cells were resuspended in 1 ml medium and counted with an automated cell counter (TC20 Automated Cell Counter, BioRad™, Hercules, USA) and the appropriate number of cells (**Table 2**) was transferred into a new culture flask or to cell plates for upcoming treatments.

Table 2: *Number of $HT29^{GFP\text{-}CaSR}$ and $HT29^{GFP}$ cells, which were seeded for cell culture flask or 6-well plate.*

	$HT29^{GFP\text{-}CaSR}$	**$HT29^{GFP}$**
25 cm^2 cell culture flask	200.000	100.000
6-well plate (per well)	90.000	40.000

2.2 Cell treatment

$HT29^{CaSR\text{-}GFP}$ and $HT29^{GFP}$ cells were used for the treatments with the different compounds. I seeded cells on 6-well plates with medium containing puromycin for selection. Cells were treated at a confluency of around 80 %. The day before treatment, the medium was changed to a medium without puromycin. I treated the cells with different compounds for 4 hours. The rationale for the different treatments with the enantiomers of NPS 2143 and NPS 568, as well as with the different ligands are explained in the introduction. The stock solutions and the final concentration in the treatments are listed in **Table 3**. For the enantiomer-treatment, 0.1 % DMSO was used as a control, as NPS 2143 and NPS 568 were dissolved in DMSO. The concentrations for the treatments with the modulators and ligands were taken from the literature.

The enantiomers of NPS 2143 and NPS 568 [64] were used at 1 µM. 5 mM Ca^{2+} were used as positive control GSK-3004774 was used at 10 µM [44]. 0.1 % DMSO was used as vehicle control for the calcimimetics. Spermine was used at 5 mM [142]), neomycin at 300 µM [143], and the amino acids at 1 mM [144]). For these compounds, 100 µl H_2O was used as vehicle control (**Table 4**, **Table 5**). After 4 hours, the medium was removed, cells were washed with ice-cold PBS, and Trizol (TRIzol™, Invitrogen™, Carlsbad, USA) was added for RNA isolation (1 ml per well). The plates were either stored at -80 °C or RNA isolation was performed right away.

Table 3: *Stock solutions and the final concentration used for the treatments of the different compounds.*

Compound	Stock solution	Concentration for the treatment
DMSO	100 % solution	0.1 %
NPS R-568	100 mM	1 µM
NPS R-2143	100 mM	1 µM
NPS S-2143	4.45 mg/100 µl	1 µM
NPS S-568	3.4 mg//100 µl	1 µM
Spermine	100 mM	5 mM
Neomycin	300 mM	300 µM
L-phenylalanine	100 mM	1 mM
L-tryptophan	20 mM	1 mM
GSK-3004774	100 mM	10 µM
Ca^{2+}	250 mM	5 mM

Table 4: *Plate scheme for the treatment conditions with R- / S- enantiomers of NPS 568 and NPS 2143. 6-well plates were used, and the treatment was performed for 4 hours. DMSO 0.1% was used as control, Ca^{2+} as a positive control.*

DMSO 0.1 %	NPS R-568 1 µM	NPS S-568 1 µM
NPS R-2143 1 µM	NPS S-2143 1 µM	NPS S-568 1 µM + NSP S-2143 1 µM

NPS R-568 1 µM + NPS R-2143 1 µM	NPS R-568 1 µM + NPS S-2143 1 µM	Ca^{2+} 5 mM

Table 5: *Plate scheme for the treatment conditions for experiment 2 (test of different ligands). 6-well plates were used, and the treatment was performed for 4 hours. DMSO 0.1% and H_2O were used as a control.*

DMSO 0.1 %	100 µl H_2O	NPS R-2143 1 µM + Spermine 5 mM
Spermine 5 mM	Neomycin 300 µM	L-phenylalanine 1 mM

L-tryptophan 1 mM	GSK- 3004774 10 µM	NPS R-568 1 µM

2.3 **RNA isolation**

After Trizol was added, cells were lysed by vigorously pipetting up and down. Cell lysates were transferred into new tubes, containing 20 µl chloroform, mixed by vortexing and incubated for 2-3 minutes. The samples were centrifuged for 15 minutes at 12.000 x *g* at 4 °C. The mixture separated into three different phases; the upper, aqueous phase contained the RNA. This upper phase was transferred into a new tube containing 500 µl isopropanol. The samples were incubated at -20 °C over-night. The next day, samples were centrifuged for 10 minutes at 12.000 x *g* at 4 °C to precipitate the RNA. The supernatant was discarded, and the pellet was resuspended in 1 ml 75 % ethanol to wash the RNA. Samples were centrifuged at 7.500 x *g* at 4 °C and the washing step was repeated. After completely removing the ethanol, the pellet was dried on a heat-block for 2-3 minutes at 55 °C. The open tubes were left on room temperature for another 10 minutes to ensure complete ethanol evaporation. In the next step, the pellet was resuspended in 20-40 µl RNase-free water (depending on the size of the pellet) and incubated for another 12 minutes on 55 °C after which the samples were immediately put on ice. To test the integrity of the isolated RNA, 1 µl of each sample, + 4 µl RNAse free water + 1 µl loading buffer (DNA Gel Loading Dye (6X), Thermo Scientific, Waltham, USA) were loaded on a 1% agarose-gel to see if the specific RNA bands (ribosomal 28S, 18S und 5S RNAs) were present. The absence of these distinct bands would indicate degraded RNA.

2.4 **Agarose gel electrophoresis**

1 g agarose powder (Biozym LE Agarose, Biozym™, Oldendorf, Germany) was added to 100 ml 1x tris(hydroxymethyl)aminomethane-borat- ethylenediamine-tetraacetic acid buffer (TBE) and boiled in a microwave to prepare a 1 % agarose gel. TBE was prepared as a 10x stock (**Table 6**) and then further diluted 1:10 with distilled water to receive a 1x TBE solution.

***Table 6**: Preparation of 1-liter 10x TBE stock solution.*

Component	**Amount**	**Catalog number**	**Company**
Tris base	108 g	T 1503-1KG	Merck, Darmstadt, Germany
Boric acid	55 g	AM0932865616	
Double-distilled water	900 ml		
0.5 M EDTA solution (pH 8.0)	40 ml	K13468718	
Adjust volume to 1-liter			

The solution was cooled down to 50-60 °C and 5 µl gel staining (pegGreen DNA/RNA Dye, Peglab™, Hong Kong, China) were added for subsequent visualization of RNA/DNA bands and mixed. I poured the gel to a thickness of ~10 mm and left to it to set at room temperature. Then, I transferred the gel to the electrophoresis chamber filled up with 1x TBE until the marked line. Samples were mixed with 6x DNA loading dye (6x MassRuler DNA loading Dye, Fermentas™, Waltham, USA). All gels were run at 100 V (PowerPac Basic Power Supply, BioRad™, Hercules, USA).

2.5 **Reverse transcription**

Reverse transcription (RT) was performed using the High-Capacity cDNA Reverse Transcription Kit (Applied Biosystems™, Waltham, USA). I measured the RNA concentration from each sample with a spectrophotometer (DS-11 FX+, DeNovix™, Wilmington, USA). The 260/230 and 260/280 ratio of the wavelength were used as a measure of purity of the RNA samples. A ratio of ~2.0 is considered “pure” RNA. Abnormally low 260/230 ratios can be caused by a problem with the sample, or with the extraction procedure, or ethanol

contamination [145]. Low 260/280 values indicate that the sample is contaminated by protein or a reagent like phenol [145]. For all my extracted RNA samples, the 260/230 and 260/280 ratios were in the acceptable range of 1.6-2.0.

For each reaction, I used 1 µg RNA, and the amount of ingredients were used as described in the manufacturer´s protocol (**Table 7**). The reaction was performed in a thermo cycler (MyCycler, BioRad™, Hercules, USA) with the program shown in **Table 8**.

***Table 7**: Composition of ingredients for the reverse transcription reaction.*

	For 1 sample [µl]
Master Mix	
RT buffer	2
dNTPs	0.8
Random primers	2
Reverse transcriptase	1
RNase free water	4.2
Total master mix volume	**10**
RNA	As needed for 1000 ng
RNase free water	Fill up to 10 µl
Total reaction volume	**20 µl**

***Table 8**: Temperature and the duration of reverse transcription cycles.*

	Temperature [°C]	**Time [min]**
Primer annealing	25	10:00
DNA polymerization	37	120:00
Enzyme deactivation	85	05:00
	4	∞

2.6 **Quantitative real-time PCR**

Using qPCR, the amount of template was measured. The qPCR machine measures in real-time the amplification of the PCR-product. For that it combines the function of a thermal cycler and a fluorimeter. The thermal cycler changes and holds the temperature suitable for efficient DNA-amplification and the fluorimeter measures intensity and wavelength of the PCR product bound to the reporter dye SYBR green [146]. SYBR Green is a fluorophore, which binds the newly synthesized double stranded PCR products. Thus, with increasing amounts of the PCR product the fluorescence is increasing too, and this is detected by the fluorimeter. The cycle threshold (CT) value is the number of cycles of a given sample that is required for the fluorescent signal to cross a predefined fluorescence signal threshold [146]. The lower the CT-value, the more cDNA of the target (and thus mRNA) was initially present in the sample, as fewer cycles are required to reach the threshold.

Biogen 96-well plates and SYBR Green Master Mix (Power SYBR Green PCR Master Mix, Applied Biosystems™, Foster City, USA) were used. 5 mM stocks of mixed forward and reverse primer were made and then used for preparing the PCR solution. PCR master mix solution was prepared in about 10 % excess depending on the number of samples. The samples were processed in a clean environment and pipetted as shown in **Table 9**.

***Table 9**: Pipetting scheme for quantitative real-time PCR for one sample in µl.*

	For 1 sample [µl]
SYBR Green MasterMix	6.5
Primer (5M stock)	0.5
water	4
cDNA (1:10 diluted in H_2O)	2
Total volume	**13**

The PCR was performed in the QuantStudio™ 12K Flex Real-Time PCR System (Applied Biosystems™, Foster City, USA) and QuantStudio™ 5 Real-Time PCR System (Applied Biosystems™, Foster City, USA) using the default program (**Table 10**).

***Table 10**: The q-PCR program, used for the experiments.*

	Temperature [°C]	Time [min]
Primer annealing	25	10:00
DNA polymerization	37	120:00
Enzyme deactivation	85	05:00
	4	∞

I used the primers listed in **Table 11**. As a reference for the total amount of cDNA in the reaction, "housekeeping genes" were used and measured in technical triplicates. I used as housekeeping (HK) genes *RPLP0* and *hB2m*. Technical duplicates were used for the other genes. To standardize the results between individual PCR experiments, a human total RNA calibrator (qPCR Human Reference Total RNA, Takara, Kusatsu, Japan) was used. The measured results are given in CT values. First, the mean value of the CTs for all technical triplicates and duplicates was calculated. Then, the mean value of both individual CT mean values for the two housekeeping genes was calculated. Relative gene expression (fold change of gene expression *vs.* calibrator) was then calculated according to the ΔΔCT method as shown below.

For calibrator and samples *vs.* housekeeping genes (HK):

$$\Delta CT\ vs. HK = mean\ CT\ (target\ gene) - mean\ CT\ (HK)$$

Then, for samples vs. calibrator:

$$\Delta\Delta CT\ vs. calibrator = \Delta CT\ vs. HK\ (sample) - \Delta CT\ vs. HK\ (calibrator)$$

$$fold\ change\ vs. calibrator = 2^{-\Delta\Delta CT}$$

***Table 11**: List of primers that were used. All primers were received from Sigma Aldrich, St. Louis, USA, if not stated otherwise.*

hRPLP0 forward	5´-TGGTCATCCAGCAGGTGTTCGA-3´
hRPLP0 reverse	5´-GCAGCAGCTGGCACCTTATTG-3´
hIL8 forward	5´-CTTGGCAGCCTTCCTGATTT-3´
hIL8 reverse	5´-TTCTTTAGCACTCCTTGGCAAAA-3´
hCaSR Ex 5-6 forward	5´-GCCAAGAAGGGAGAAAGAC-3´
hCaSR Ex 5-6 reverse	5´-CACACTCAAAGCAGCAGG-3´
hPTGES forward	5´-GCTGGTCATCAAGATGTACG-3´
hPTGES reverse	5´-GTCGCTCCTGCAATACTG-3´
hCox2 forward	5´-CAAGACAGATCATAAGCGAGGG-3´
hCox2 reverse	5´-GTCTAGCCAGAGTTTCACCG-3´
hCox1 forward	5´-TTGAATGAGTACCGCAAGAGG-3´
hCox1 reverse	5´-GAAGCAGTCCAGGGTAGAAC-3´
hEP1 forward	5´-GGCCAGCTTGTCGGT-3´
hEP1 reverse	5´-GCCACCAACACCAGC-3´
hEP4 forward	5´-TGCTCATCTGCTCCATGG-3´
hEP4 reverse	5´-TTACTGACTTCTCGCTCCA-3´
hB2m Ex 2-4 forward	5´-GATGAGTATGCCTGCCGTGTG-3´
hB2m EX 2-4 reverse	5´-CAATCCAAATGCGGCATCT-3´
hPGDH forward	5´-TGCTTCAAAGCATGGCATG-3´
hPGDH reverse	5´-AACAAGCCTGGACAAATGG-3´

As a quality control, I checked the melting curves for the targets in each RT-qPCR experiment. The melting curve is shown as the first derivative of the fluorescence intensity when heating the finished PCR products (after 40 cycles of amplification) slowly from 60 to 95 °C. When the DNA double-strands are denaturing (according to their denaturing temperature which is determined by the PCR product's size), the fluorescence intensity decreases. The temperature at the steepest drop is the melting temperature where most amplicons denature at the same time and thus lose their bound SYBR-green. The melting curve confirms that the reaction was specific and that the same target was amplified in all samples if only one steep peak is visible for all samples.

The melting curves for all RT-qPCR experiments were correct; three examples are shown below (**Figure 10-12**).

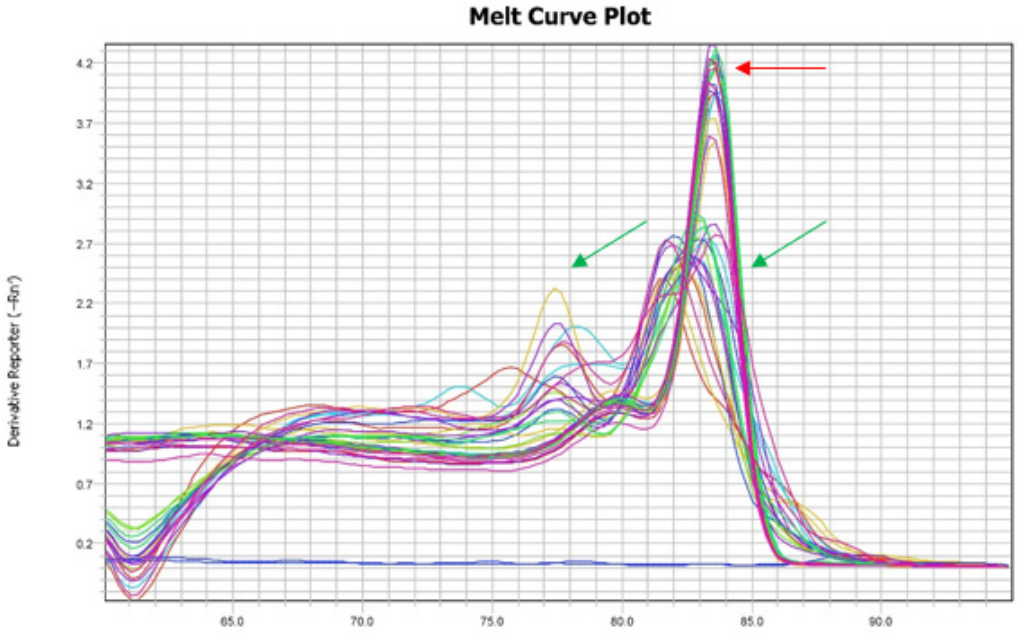

***Figure 10**: Melting curve of a representative RT-qPCR experiment with the target gene CaSR.*
Melt curve was created by the QuantStudio™ 12K Flex Real-Time PCR Software, Applied Biosystems (Waltham, USA). The specific melting curve for the CaSR gene is shown in (red arrow, meting temperature ~ 84.5 °C), the unspecific curves (green arrows, curves with multiple peaks) are from the HT29^{GFP} cells, which have undetectable levels of CaSR. The blue line on the bottom is the negative control.

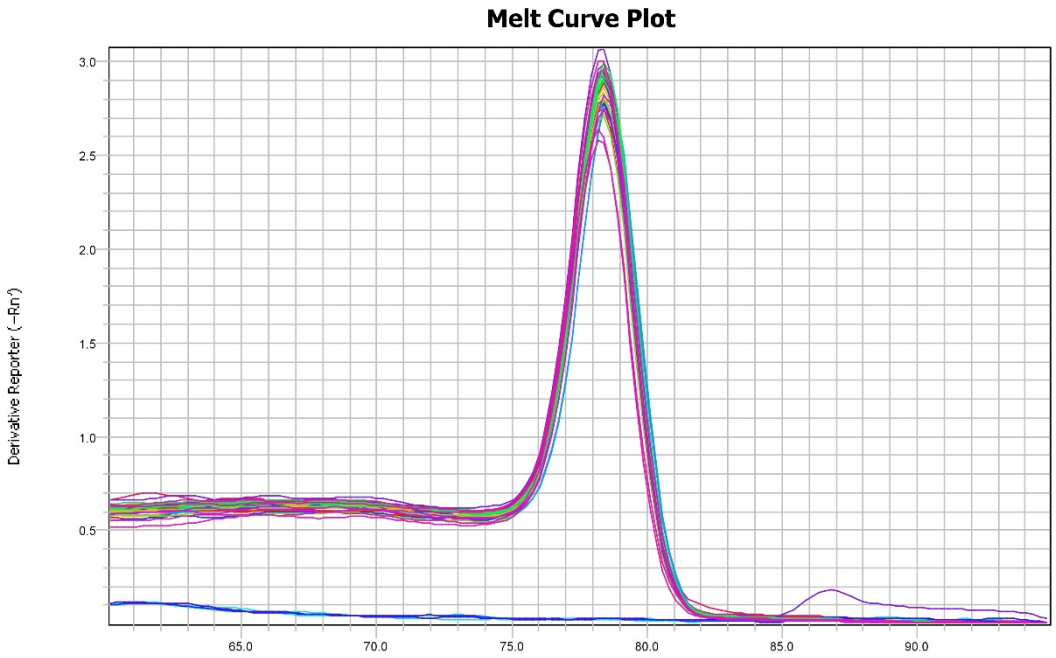

Figure 11: Melting curve of a representative RT-qPCR experiment with the target gene IL-8.
Melt curve was created by the QuantStudio™ 12K Flex Real-Time PCR Software, Applied Biosystems (Waltham, USA). The blue line on the bottom is the negative control.

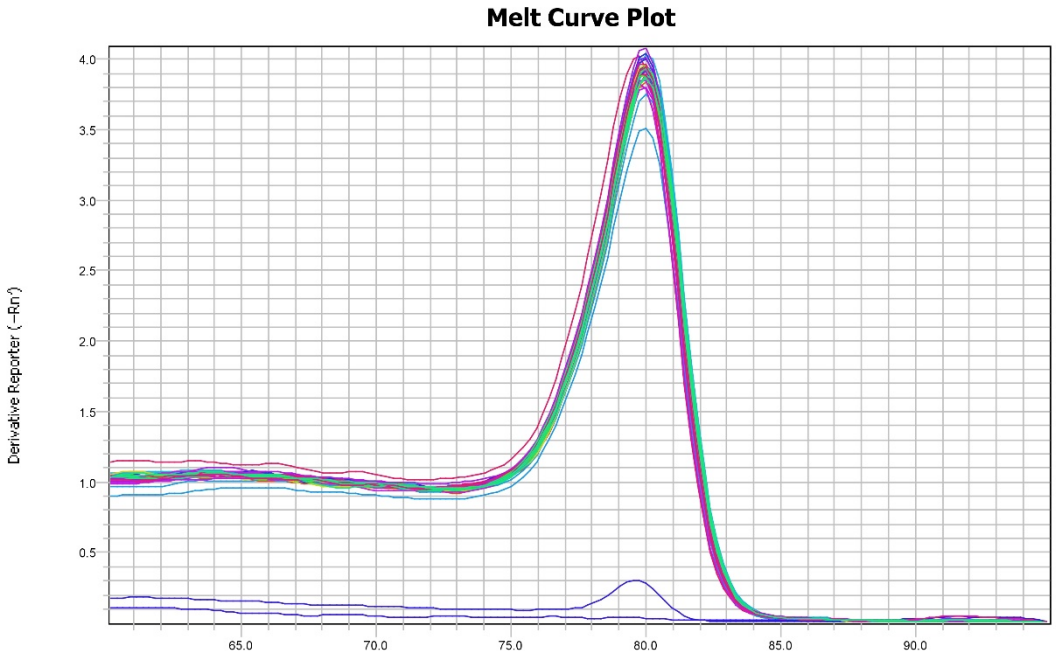

Figure 12: Melting curve of a representative RT-qPCR experiment with the target gene COX-2.
Melt curve was created by the QuantStudio™ 12K Flex Real-Time PCR Software, Applied Biosystems (Waltham, USA). The blue line on the bottom is the negative control.

2.7 **ELISA experiments**

I performed two enzyme-linked immunosorbent assay (ELISA) experiments with the supernatants of the treated cells.

The bottom of the microplate for the IL-8 ELISA (Human IL-8 Uncoated ELISA, Invitrogen, Waltham, USA) was coated with the target-specific "capture" antibody. The samples are added and bound to this "capture" antibody. In the next step, a detector antibody was added, which binds to IL-8 on a different epitope, forming a so called "sandwich" (**Figure 13**). The second antibody is bound to an Avidin-horseradish peroxidase detection-enzyme that catalyzes the conversion of tetramethylbenzidine to a colored product. The resulting color signal is thus directly proportional to the concentration of the target present in the samples.

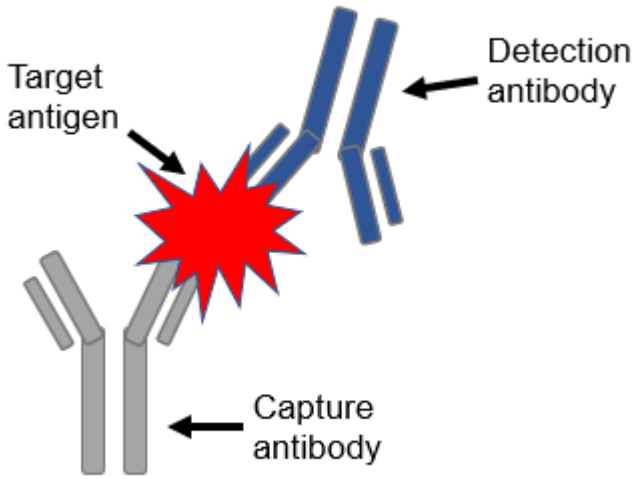

Figure 13: Scheme of an ELISA-"Sandwich".
The capture antibody binds the target antigen. The detection antibody binds in the next step, forming a sandwich.

I used a forward sequential competitive binding ELISA (Parameter PGE2 ELISA, R&D systems, Minneapolis, USA) for PGE2 detection. The PGE2 that is present in the sample competes with horseradish peroxidase (HRP)-labeled PGE2 for a limited number of binding sites on a mouse monoclonal antibody. In the first incubation step, the sample was added and the PGE2 found in the sample binds

to the antibody. In the second incubation step, HRP-labeled PGE2 is added and binds to the remaining antibody sites. HRP then catalyzes again a color reaction. The intensity of the measured color is inversely proportional to the concentration of PGE2 in the sample.

2.8 **Preparation of LB-Medium**

For the preparation of 1 liter of liquid Lysogeny Broth (LB) Medium, 10 g peptone, 5 g yeast extract (Sigma Aldrich, St. Louis, USA) and 5 g sodium chloride (Merck, Darmstadt, Germany) were dissolved in double distilled water. When the medium had cooled down after autoclaving to around 60 °C, ampicillin (Invitrogen™, Carlsbad, USA) was added for an end concentration of 50 µg/ml.

2.9 **Preparation of LB-Agar plates**

LB agar plates with ampicillin were prepared for the antibiotic selection of *Escherichia Coli (E.Coli)* after the heat-shock transformation.

For 15-20 plates, I dissolved 8.14 g premixed Luria Bertani (LB) agar powder (Sigma Life Science, St. Louis, USA) in 220 ml sterile water. The solution was autoclaved at 121 °C and 20 psi for 30 minutes. After the bottle had cooled down to 40-60 °C, ampicillin (Invitrogen™, Carlsbad, USA) was added for an end concentration of 50 µg/ml. I poured the agar on the plates under sterile conditions and left to set for around 30 minutes. The plates were stored at 4°C and covered with parafilm to avoid contamination.

2.10 **Plasmid elution from filter**

Plasmids were received on a filter paper (kindly provided by Prof. A. Conigrave, University of Sydney, Australia). Different substitution mutations of the CaSR were cloned in a pcDNA3.1(+) vector (**Table 12**), possessing an ampicillin resistance.

Table 12: *Variants of substitution-mutations which were cloned into pcDNA3.1(+) vector.*

Mutation	**Effect on the CaSR**
R185Q	Dominant negative loss-of-function
F612S	Gain of function
A986S	Common polymorphism
Q1011E	Common polymorphism

All cell and bacterial work were performed in a clean environment; scissor and tweezer were sterilized in advance under UV light for 30 minutes. The marked regions, containing the plasmid DNA, were cut out, placed in a tube, and incubated with 10 µl Tris(hydroxymethyl)aminomethane-ethylenediamine-tetraacetic acid (TE) buffer (Invitrogen^{TM}, Carlsbad, USA) for 10 minutes at room temperature and for another 10-15 minutes on 37 °C. The tubes were centrifuged for 1 minute, the plasmid DNA was eluted in TE buffer and placed on the bottom of the tube. To ensure an accurate elution from the filter paper, I cut the thin end of a 200 µl pipette tip and placed it between tube bottom and filter paper. After centrifugation, the filter paper was removed. In the next step the concentration of eluted plasmid DNA was measured *via* spectrophotometry (see below).

2.11 **Bacterial transformation**

Bacterial transformation is used to multiply the eluted plasmids. For this, competent *E.Coli* (One Shot™ TOP10 Chemically Competent E. coli, Invitrogen™, Carlsbad, USA) were used. 50 µl aliquots of *E.Coli* were thawed on ice, then 20 ng/µl plasmid DNA was added and incubated for 30 minutes on ice. The mixture was heat-shocked at 42 °C for 45 seconds and immediately put back on ice afterwards. For recovery, 200 µl of Super-Optimal-Broth medium (Invitrogen™, Carlsbad, USA), which had room temperature was added and incubated for 60 minutes at 37 °C on a shaker set to 500 rpm. After this incubation time, I spread 100 µl of the liquid with a Drigalski-spatula on agar-plates containing ampicillin (see above) and incubated upside down, overnight at 37 °C. A single colony was then picked and transferred into a sterile tube with 5 ml LB-medium (see above) and was incubated over-night at 37 °C, vigorously shaking with 170 rpm. After the colony has multiplied, plasmids were extracted the next day

2.12 **Plasmid extraction (miniprep)**

The PureLink™ Quick Plasmid Miniprep Kit (Invitrogen™, Carlsbad, USA) was used for the extraction of the plasmid from the bacteria. The manufacturer's instructions were followed but modified as followed: Instead of eluting with 75 µl TE buffer at once, it was first eluted with 35 µl and a second time with 40 µl.

2.13 **Enzymatic digestion**

To control that only the preferred plasmid construct was extracted, an enzymatic digestion was performed and later the sample was run on an agarose gel to compare the bands. For my plasmid of interest, the restriction enzyme Sal1 (Sal1, 10 U/µl), Thermo Scientific™, Waltham, USA) was used. The restriction sites of Sal1 are shown in **Figure 14**. Depending on the efficiency of the extraction, an amount between 0.5-1 µg DNA was used and digested with 1 µl Sal1. To DNA and restriction enzyme, I added 7 µl of water as well as 2 µl buffer O, provided with the restriction enzyme (Sal1, 10 U/µl), Thermo

Scientific™, Waltham, USA). The samples were incubated for 45 minutes at 37 °C. 1 µl digested DNA were mixed with 1 µl loading dye (Orange DNA, R0631, Thermo Scientific™, Waltham, USA) and 4 µl H_2O. The total amount of 6 µl was added on the gel and run as described above for 30 minutes.

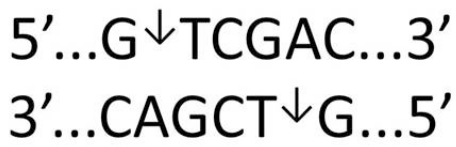

Figure 14: Restriction site of Sal1.
The restriction enzyme Sal1 is used for the enzymatic digestion of the isolated plasmids.

2.14 **Transfection with Lipofectamine**

For transfections, Lipofectamine (Lipofectamine™ LTX Reagent with PLUS™ Reagent, Invitrogen™, Carlsbad, USA) was used. I seeded HT29 cells in a 24-well plate, 2.0 x10^5 cells per well in 1 ml medium. After 24 hours a confluence of 70-80 % was reached. 2 µl Lipofectamine were diluted in 50 µl OPTIMEM-Medium (Invitrogen™, Carlsbad, USA) and 5 ng plasmid DNA and 5 µl Lipofectamine-Plus-Reagent were diluted in 250 µl OPTIMEM-Medium. 50 µl of the diluted plasmid DNA and Lipofectamine-Plus-Reagent mix were then added to the diluted lipofectamine. I added 50 µl of this combined mixture to each 24-well plate. Next day, the medium was changed to remove remaining plasmids and lipofectamine. The exact treatment conditions with controls are described in the results section. On the second day, transfected cells were treated for 4 hours with different compounds, then washed with ice-cold PBS, afterwards Trizol was added for RNA isolation (see above).

2.15 **Statistical analysis**

Statistical analysis was performed using GraphPad Prism version 7.0 (GraphPad, LaJolla, USA). The applied statistical tests are indicated in the legends of each figure.

3 Results

3.1 Enantioselective activation of the CaSR

To test whether upregulation of inflammatory genes is mediated *via* the CaSR, I treated cultured $HT29^{CaSR\text{-}GFP}$ and $HT29^{GFP}$ cells with NPS 568 and NPS 2143 enantiomers. If only the selective forms modulated the expression of inflammatory cytokines, the CaSR could be confirmed as mediator of these pro-inflammatory processes.

The cells were treated for 4 hours with the different enantiomers (**Table 4**), and the RNA was isolated. The isolated RNA samples were run on a gel electrophoresis to confirm that the RNAs were intact. The representative gel (**Figure 15)** shows the three ribosomal subunits, 28S rRNA, 18S rRNA and 5S rRNA of the isolated RNA.

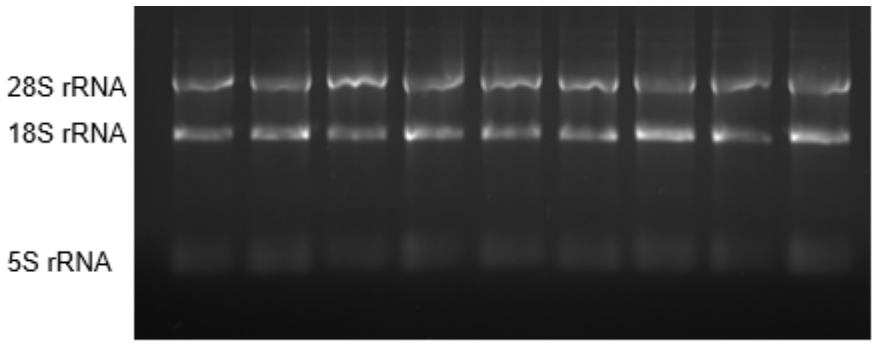

Figure 15: Representative gel picture of the isolated RNA samples.
A gel electrophoresis was run with the extracted RNA samples. The 28S rRNA, 18S rRNA and 5S rRNA subunits are visible. The fluorescence intensity correlates with the amount of RNA in the sample.

After converting the RNA samples into cDNA *via* reverse transcription, I used the samples for RT-qPCR experiments. The primers I used are listed in the methods section (**Table 11**).

First, I looked at the expression of inflammatory genes, IL-8 and CCL-20 being among the most prominent ones according to Iamartino *et al*, 2020 [95]. NPS R-568 significantly increased IL-8 (p<0.001) and CCL-20 (p<0.001) expression, while none of the unspecific enantiomers had any effect (**Figure 16 A+B, left panel**). The combination of the specific calcimimetic NPS R-568 with the unspecific enantiomer of the calcilytic, NPS S-2143, led to significantly higher IL-8 (p<0.001) and CCL-20 (p<0.01) expression than when combining NPS R-568 with the specific enantiomer NPS R-2143 (**Figure 16 A+B, right panel**). This indicates CaSR-specific inhibition of the calcimimetic-induced IL-8 expression.

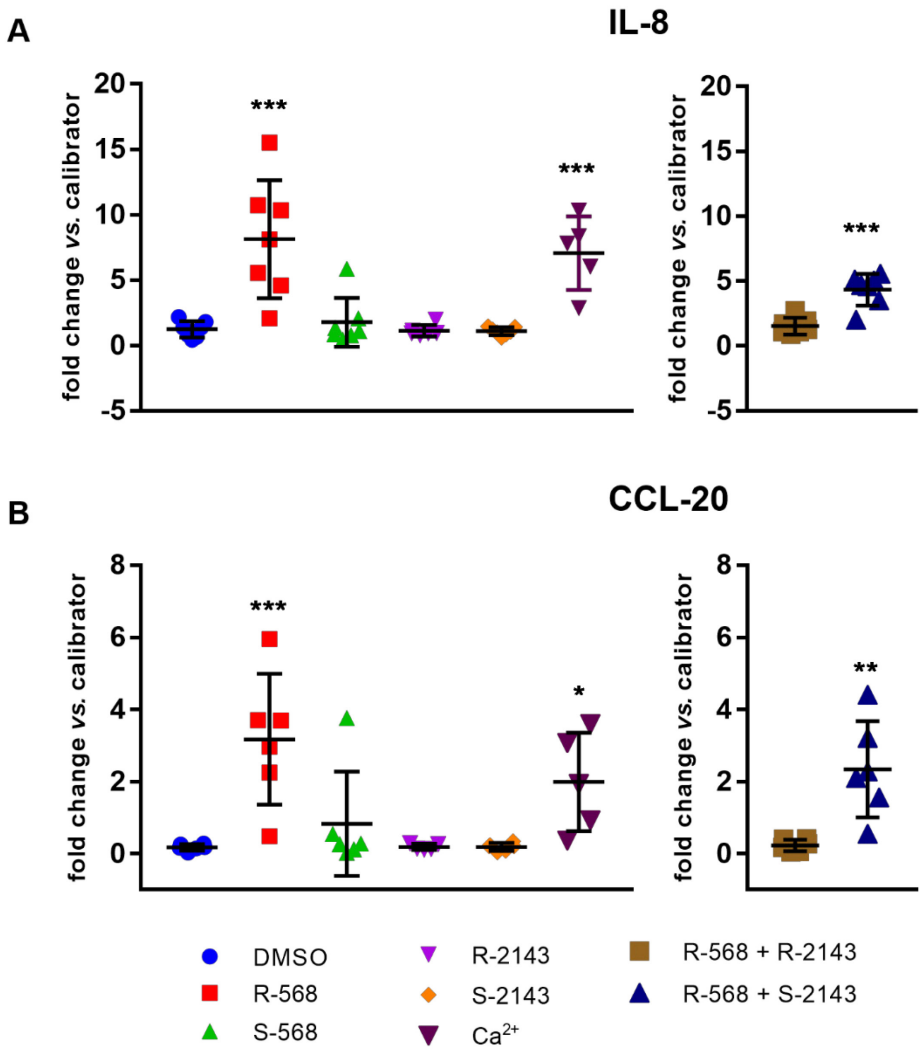

Figure 16: Relative gene expression results from HT29$^{GFP\text{-}CaSR}$ cells treated with CaSR-modulators. *RT-qPCR results from the HT29$^{GFP\text{-}CaSR}$ cells with the targets IL-8 (A) and CCL-20 (B). For the treatments 0.1 % DMSO, 1 µM NPS R-568, 1 µM NPS S-568, 1 µM NPS R-2143, 1 µM NPS S-2143 were used. Control treatment was 5 mM Ca^{2+}. Data are shown as a mean ± SD, N=6-7. Statistical analysis was performed using ordinary one-way ANOVA with multiple comparison to DMSO with Dunnett post-test or unpaired t-test for the two combinations in the right graphs.*

In the next step, I wanted to see if the genes of the prostaglandin E2 pathway were influenced by the enantio-selective activation of the CaSR. NPS R-568 increased COX-2 expression (p<0.01) (**Figure 17, left panel**). The combination of NPS R-568 with NPS S-2143 appeared to increase COX-2 expression, but this did not reach statistical significance (p=0.0612) compared to the combination treatment of NPS R-568 + NPS R-2143 (**Figure 17, right panel**).

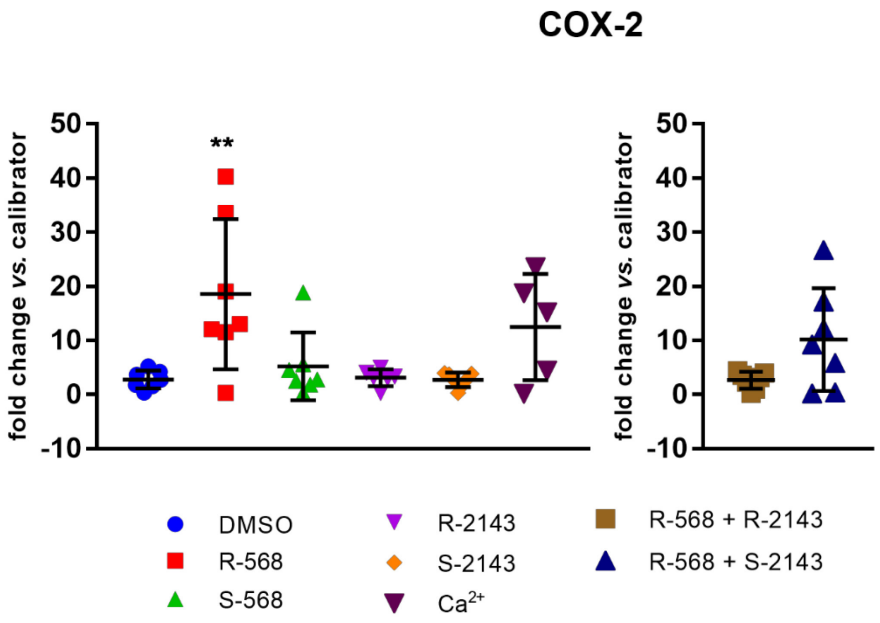

Figure 17: Relative gene expression results from HT29$^{GFP\text{-}CaSR}$ cells treated with CaSR-modulators.
RT-qPCR results from the HT29$^{GFP\text{-}CaSR}$ cells with the targets COX-2. For the treatments 0.1 % DMSO, 1 µM NPS R-568, 1 µM NPS S-568, 1 µM NPS R-2143, 1 µM NPS S-2143 were used. Control treatment was 5 mM Ca^{2+}. Data are shown as a mean ± SD, N=6-7. Statistical analysis was performed using ordinary one-way ANOVA with multiple comparison to DMSO with Dunnett post-test or unpaired t-test for the two combinations in the right graphs.

The results of the treatments on the expression of other genes of the PGE2 pathway are shown in **Figure 18** (COX-1 (A), PTGES (B), 15-PGDH (C)) and **Figure 19** (EP-1 (A), EP-4 (B)). None of the treatments affected any of them.

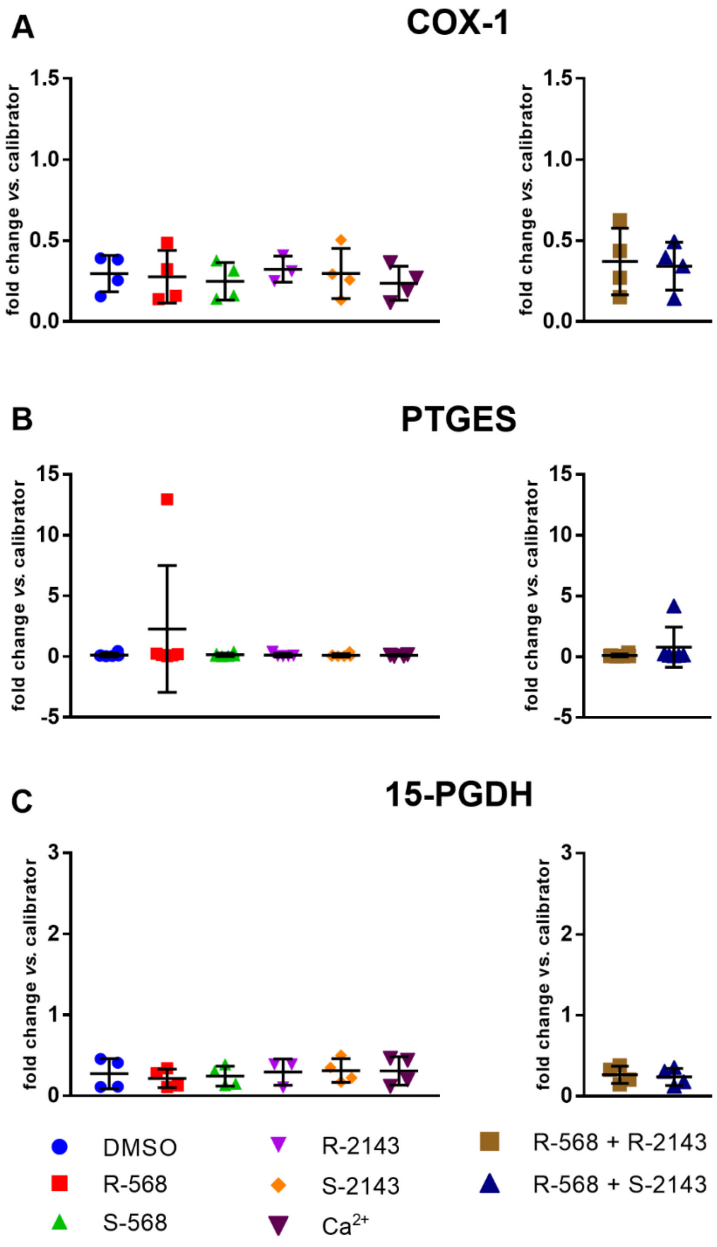

Figure 18: Relative gene expression results from HT29$^{GFP\text{-}CaSR}$ cells treated with CaSR-modulators.
RT-qPCR results from the HT29$^{GFP\text{-}CaSR}$ cells with the targets COX-1 (A), PTGES (B), 15-PGDH (C). For the treatments 0.1 % DMSO, 1 µM NPS R-568, 1 µM NPS S-568, 1 µM NPS R-2143, 1 µM NPS S-2143 were used. Control treatment was 5 mM Ca^{2+}. Data are shown as a mean ± SD, N=6-7. Statistical analysis was performed using ordinary one-way ANOVA with multiple comparison to DMSO with Dunnett post-test or unpaired t-test for the two combinations in the right graphs.

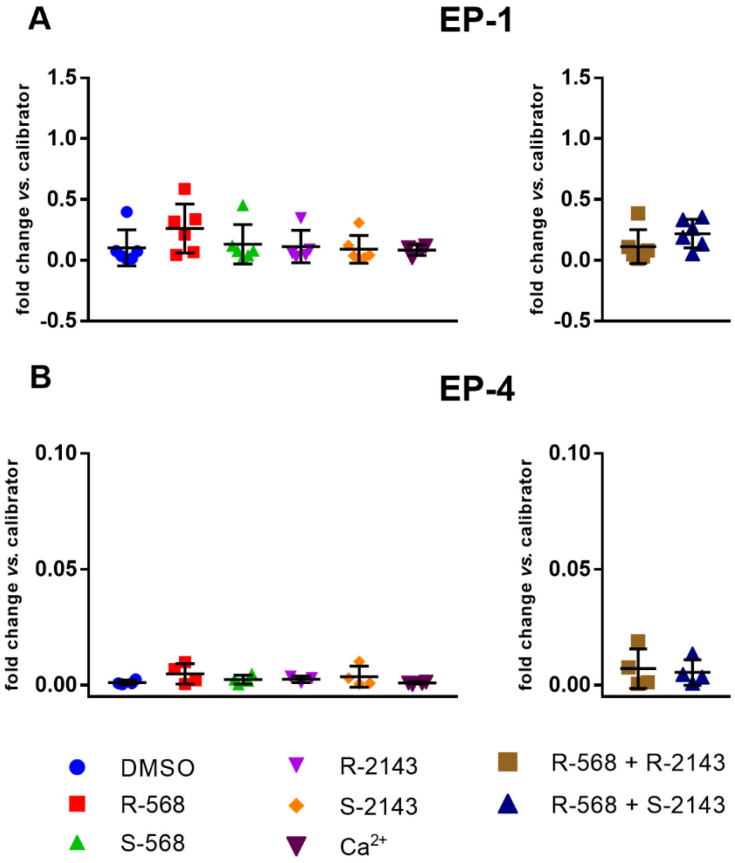

Figure 19: Relative gene expression results from HT29$^{GFP\text{-}CaSR}$ cells treated with CaSR-modulators.
RT-qPCR results from the HT29$^{GFP\text{-}CaSR}$ cells with the targets EP-1 (A) and EP-4 (B). For the treatments 0.1 % DMSO, 1 µM NPS R-568, 1 µM NPS S-568, 1 µM NPS R-2143, 1 µM NPS S-2143 were used. Control treatment was 5 mM Ca^{2+}. Data are shown as a mean ± SD, N=4-7. Statistical analysis was performed using ordinary one-way ANOVA with multiple comparison to DMSO with Dunnett post-test or unpaired t-test for the two combinations in the right graphs.

As described in the introduction, the CaSR has the feature of agonist-driven insertional signaling (ADIS). I was interested whether the expression of the *CaSR* gene itself would be enhanced by the enantio-selective receptor activation. Indeed, NPS R-568 increased CaSR expression (p<0.001), none of the other enantiomers had an effect. Ca^{2+}, the main Type 1 agonist, which was used in my experiments as the positive control of receptor activation, also increased CaSR expression (p<0.01) (**Figure 20**). The treatment with NPS R-568 + NPS R-2143 increased the expression of CaSR (p<0.01) compared with the treatment where NPS R-568 is combined with NPS R-2143.

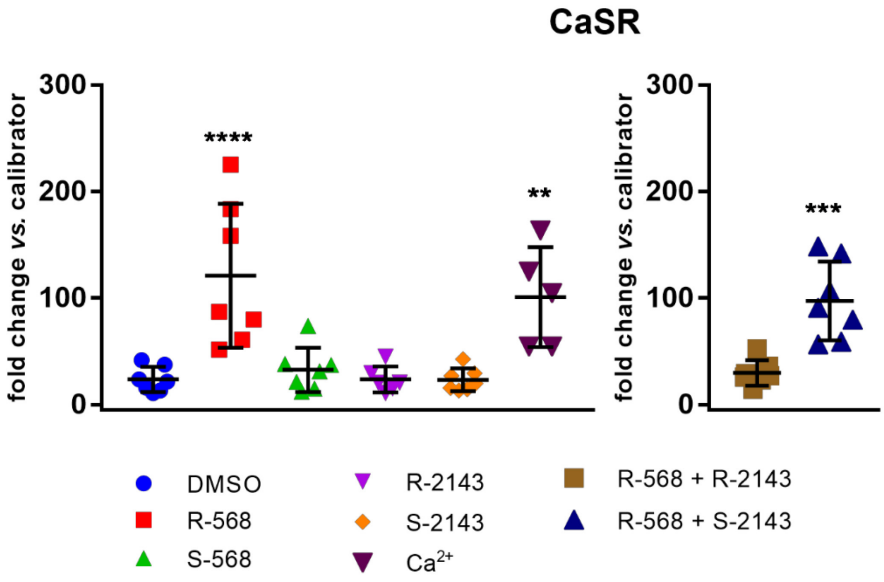

Figure 20: Relative gene expression results from HT29$^{GFP\text{-}CaSR}$ cells treated with CaSR-modulators. *RT-qPCR results from the HT29$^{GFP\text{-}CaSR}$ cells with the targets CaSR. For the treatments 0.1 % DMSO, 1 µM NPS R-568, 1 µM NPS S-568, 1 µM NPS R-2143, 1 µM NPS S-2143 were used. Control treatment was 5 mM Ca^{2+}. Data are shown as a mean ± SD, N=6-7. Statistical analysis was performed using ordinary one-way ANOVA with multiple comparison to DMSO with Dunnett post-test or unpaired t-test for the two combinations in the right graphs.*

None of the treatments affected the expression of the analyzed genes in the HT29^{GFP} cells, lacking the CaSR (**Figure 21**).

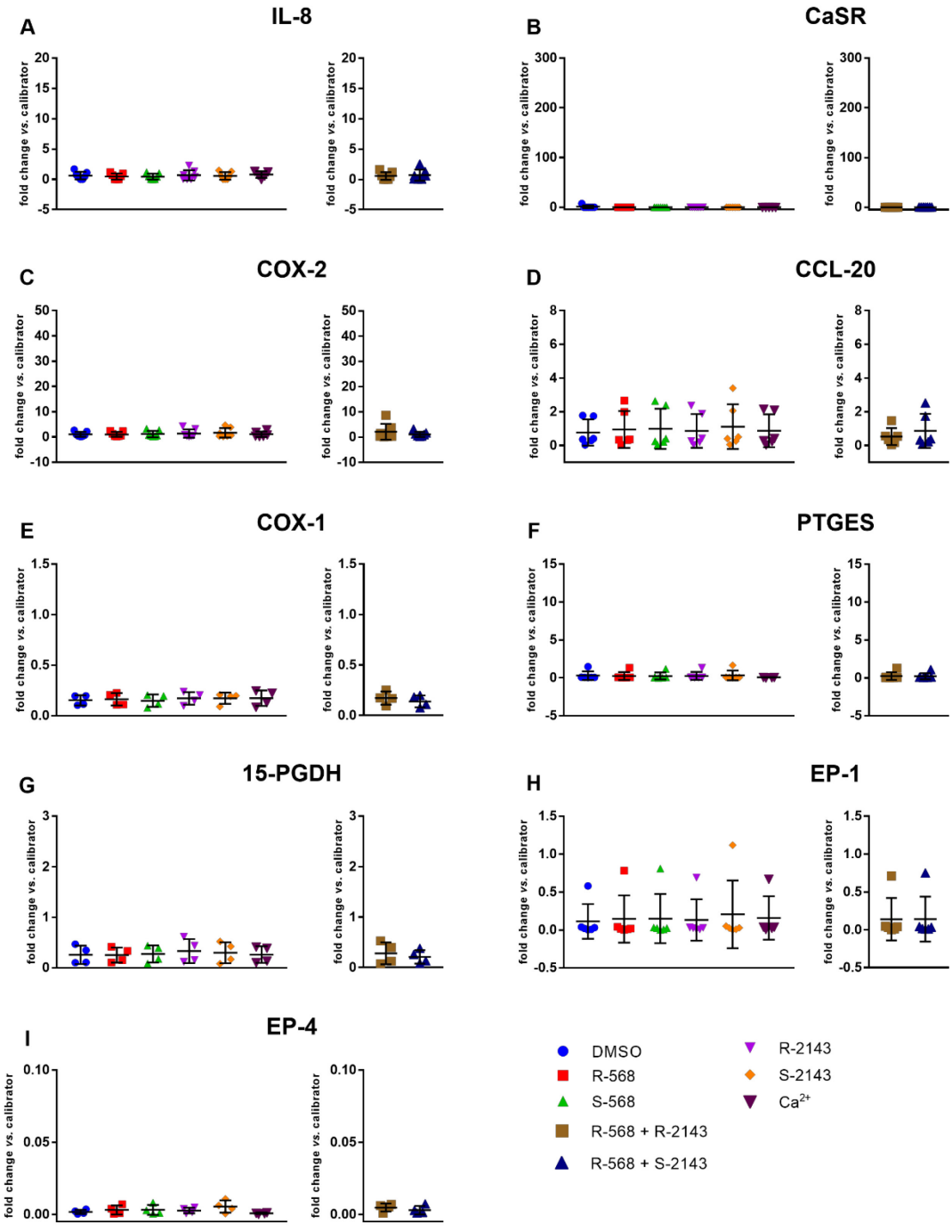

Figure 21: Relative gene expression results from HT29^{GFP} cells treated with CaSR modulators.
RT-qPCR results from the HT29^{GFP} cells for the targets IL-8 (A), CaSR (B), COX-2 (C), CCL-20 (D), COX-1 (E), PTGES (F), 15-PGDH (G), EP-1 (H), and EP-4 (I). For the treatments 0.1 % DMSO, 1 µM NPS R-568, 1 µM NPS S-568, 1 µM NPS R-2143, 1 µM NPS S-2143 were used. Control treatment was 5 mM Ca^{2+}. Data are shown as a mean ± SD, N=6-7. Statistical analysis was performed using ordinary one-way ANOVA with multiple comparison to DMSO with Dunnett post-test or unpaired t-test for the two combinations in the right graphs.

To see whether the treatments with the enantiomers affected protein/product expression in a similar fashion as gene expression, I measured secreted IL-8 and PGE2 levels from the culture medium using ELISA. For the analysis I used the standard curve shown in **Figure 22** with an R^2=0.9564.

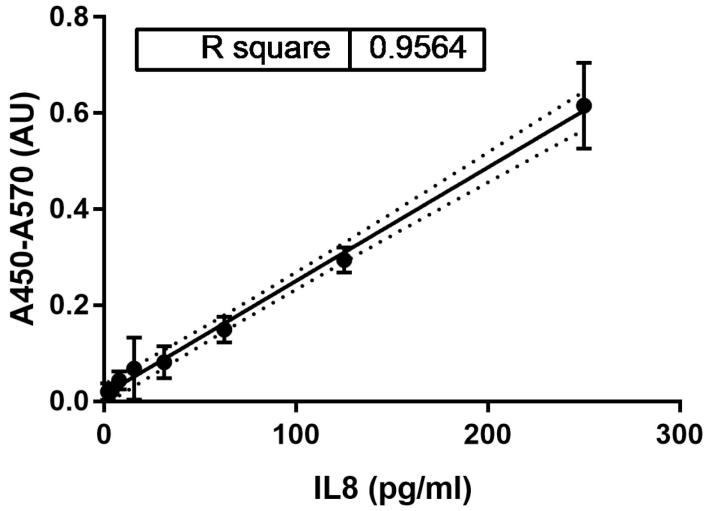

Figure 22: Standard curve of IL-8 ELISA.
The IL-8 protein concentration [pg/ml] is plotted against the optical density measured with A450 from which the correction optical density at 570 nm was subtracted (arbitrary units, AU). Linear regression, as recommended in the manufacturer's instructions. Dotted lines: 95% confidence interval.

NPS R-568 increased IL-8 protein expression (p<0.01) compared to DMSO (**Figure 23 A, left panel**). Similar to the RT-qPCR results, the combined treatment with NPS R-568 + NPS R-2143 did not increase IL-8 expression, but when cells were treated with NPS R-568 + NPS S-2143, IL-8 expression was significantly increased (p<0.01) (**Figure 23 A, right panel**). None of the treatments had an effect on the IL-8 protein expression in HT29^{GFP} cells (**Figure 23 B**).

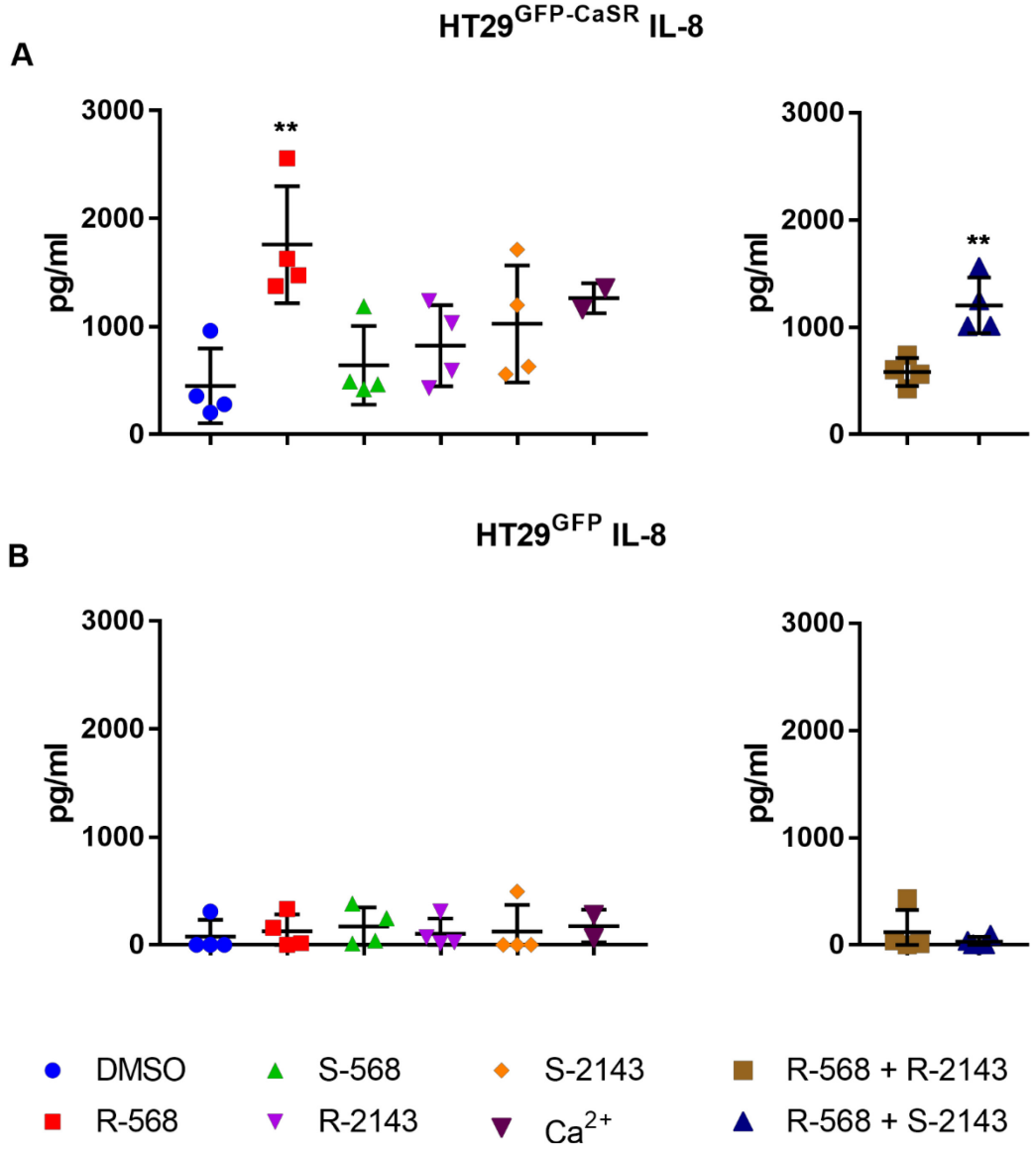

Figure 23: Effect of the treatments with CaSR modulators on IL-8 protein secretion.
HT29$^{GFP-CaSR}$ cells (A) and HT29^{GFP} cells (B) were treated for 4 hours, and the supernatants were used for the ELISA experiment to determine IL-8 protein levels. For the treatments 0.1 % DMSO, 1 µM NPS R-568, 1 µM NPS S-568, 1 µM NPS R-2143, 1 µM NPS S-2143 were used. Control treatment was 5 mM Ca^{2+}. Data are represented as a mean ± SD, N=2-4. Statistical analysis was performed using ordinary one-way ANOVA with multiple comparison to DMSO with Dunnett post-test and to analyze the combined treatments an unpaired t-test. Note that the results for Ca^{2+} were not included in the analysis as only two measurements were available.

To measure the secreted amount of PGE2, I treated HT29$^{GFP\text{-}CaSR}$ and HT29^{GFP} cells for 4 and 48 hours with vehicle, 1 µM NPS R-568 alone, or in combination with 1 µM NPS R-2143 to assess whether the cells respond differently when they are treated for different durations. In this ELISA, I obtained the standard curve shown in **Figure 24** with an R^2=0.9863.

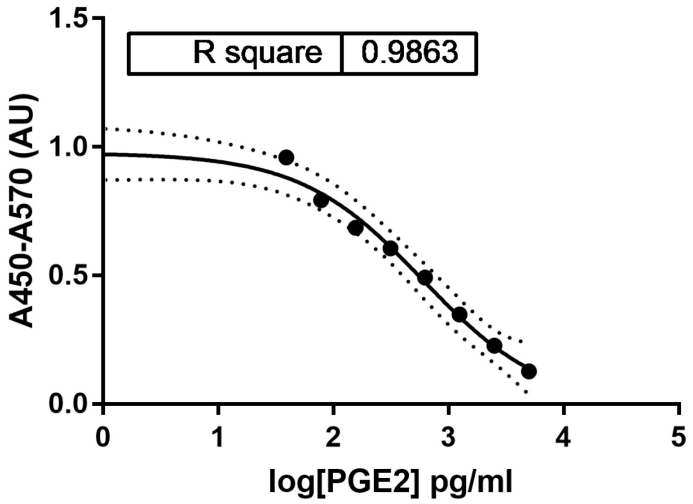

Figure 24: Standard curve of PGE2 ELISA.
PGE2 concentration [pg/ml] is plotted against the optical density measured at 450 nm from which the correction optical density at 570 nm was subtracted (arbitrary units; AU). 4 parameter non-linear fit, as recommended in the manufacturer's instructions. Dotted lines: 95% confidence interval.

NPS R-568 increased PGE2 levels after 4 hours (2,000-fold compared to vehicle control) (**Figure 25 A)** and after 48 hours treatment (2,000-fold compared to vehicle control) (**Figure 25 B**). Combining NPS R-2143 with NPS R-568 effectively inhibited the NPS R-568-induced PGE2 expression, as observed for IL-8 (**Figure 25 A+B**).

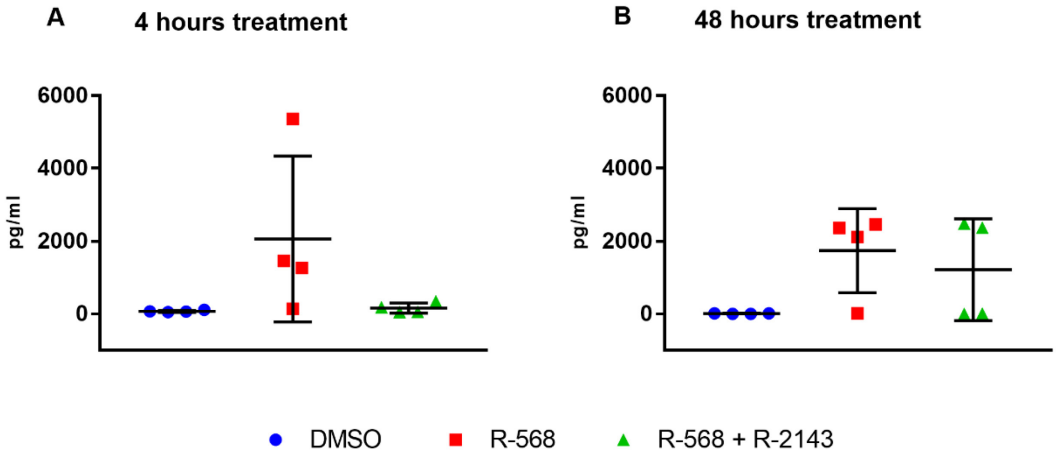

Figure 25: Effect of the treatments with CaSR modulators on PGE2 secretion.
HT29$^{GFP\text{-}CaSR}$ were treated with CaSR-modulators for 4 hours (A) and 48 hours (B). The supernatants were used for the ELISA experiment to determine PGE2 levels. For the treatments 0.1 % DMSO, 1 µM NPS R-568 and 1 µM NPS R-2143 were used. Data are represented as a mean ± SD, N=4. Statistical analysis was performed using ordinary one-way ANOVA with multiple comparison to DMSO with Dunnett post-test.

In the HT29^{GFP} cells, NPS R-568 had no effect on PGE2 (**Figure 26)**.

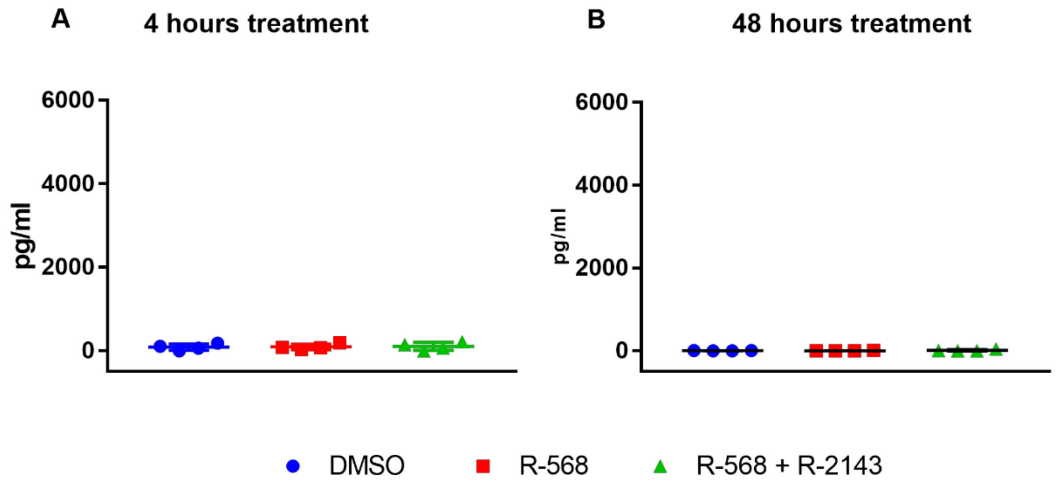

Figure 26: Effect of the treatments with CaSR modulators on PGE2 secretion.
HT29^{GFP} were treated with CaSR-modulators for 4 hours (A) and 48 hours (B). The supernatants were used for the ELISA experiment to determine PGE2 levels. For the treatments 0.1 % DMSO, 1 µM NPS R-568 and 1 µM NPS R-2143 were used. Data are represented as a mean ± SD, N=4. Statistical analysis was performed using ordinary one-way ANOVA with multiple comparison to DMSO with Dunnett post-test.

3.2 **Dose-response-curve for IL-1β on HT29 cells.**

IL-1β is a cytokine produced by activated macrophages. It is an important mediator of inflammatory response. IL-1β triggers the release of other cytokines, such as IL-8 and leads trough the induction of COX-2 to a higher production of PGE2 [147]

To lay the foundation for these upcoming experiments, I prepared a dose-response-curve on $HT29^{GFP\text{-}CaSR}$ and $HT29^{GFP}$ cells to determine the EC50 for IL-1β induced inflammatory responses in these cells. The EC50 could then be used as a starting point for future experiments to assess whether exogenous induction of inflammation *via* IL-1β can be inhibited by blocking the CaSR. For this, I treated the cells with 0.1 ng/µl, 0.3 ng/µl, 1 ng/µl, 10 ng/µl and 25 ng/µl IL-1β for 4 hours and calculated the EC50 from the non-linear sigmoidal regression of the induced IL-8 gene expression. In the $HT29^{GFP\text{-}CaSR}$ cells, I found a strong IL-1β dose-dependent increase of IL-8 gene expression even though there was a rather high variability in the responses as indicated by the medium goodness-of fit of the curve (R^2=0.6452) (**Figure 27 A**). The calculated EC50 for IL-1β was 2.49 ng/µl (±1.268). In the $HT29^{GFP}$ cells, IL-1β had no observable effect on IL-8 expression (**Figure 27 B**).

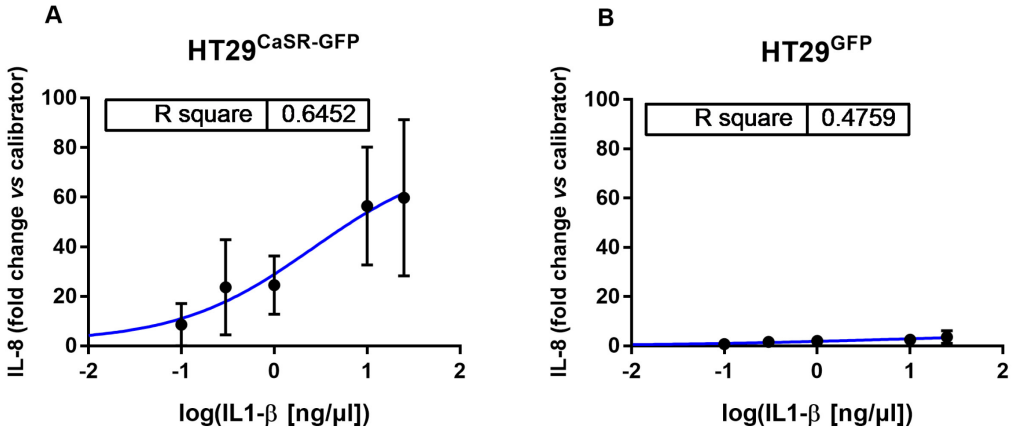

Figure 27: Relative gene expression results for the dose-response-curve with IL1-6.
RT-qPCR results from the $HT29^{GFP\text{-}CaSR}$ cells (A) and $HT29^{GFP}$ cells (B) with the target IL-8. The EC50 for $HT29^{GFP\text{-}CaSR}$ cells is 2.49 (± 1.268). 3 parameter sigmoidal non-linear regression.

On the protein level, the same dose-response-relationship between IL-1β concentration and IL-8 secretion was seen in HT29$^{GFP\text{-}CaSR}$ cells (**Figure 28 A**). There was no alteration in IL-8 protein expression independent of IL-1β concentration in HT29^{GFP} cells (**Figure 28 B**). In further experiments, our group plans to treat HT29$^{GFP\text{-}CaSR}$ and HT29^{GFP} cells with IL-1β and NPS R-2143, to see whether the exogenously induced inflammation can be inhibited *via* the CaSR.

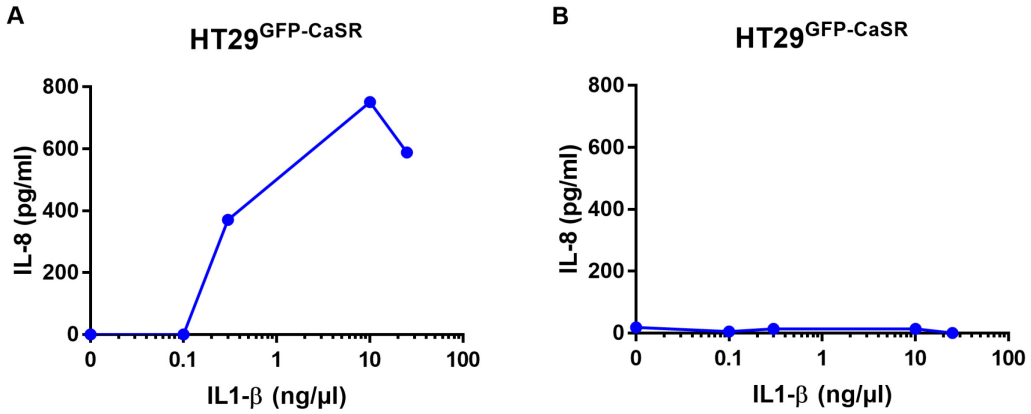

Figure 28: ELISA results for the protein IL-8.
HT29$^{GFP\text{-}CaSR}$ (A) and HT29^{GFP} cells were treated with 0.1 ng/µl, 0.3 ng/µl, 1 ng/µl, 10 ng/µl and 25 ng/µl IL-16. With the supernatants of the cells an IL-8 ELISA was performed. The EC50 for HT29$^{GFP\text{-}CaSR}$ cells is 2.49 (± 1.268). The point 0 on the x-axis is manually inserted for the vehicle control as a true 0 is not possible in a logarithmic scale.

3.3 Testing the effect of different CaSR ligands on the inflammatory gene response

I have shown that the inflammatory response is indeed mediated *via* the CaSR through enantio-selective CaSR activation. Next, I wanted to test whether the CaSR ligands spermine, L-phenylalanine, L-tryptophan, neomycin and the calcimimetic GSk-3004774, would also induce inflammatory gene response.

$HT29^{GFP\text{-}CaSR}$ and $HT29^{GFP}$ cells were cultured and treated with potential ligands of the CaSR, as explained in the methods (**Table 5**). Gel electrophoresis confirmed isolation of intact RNA as exemplified in (**Figure 29)**.

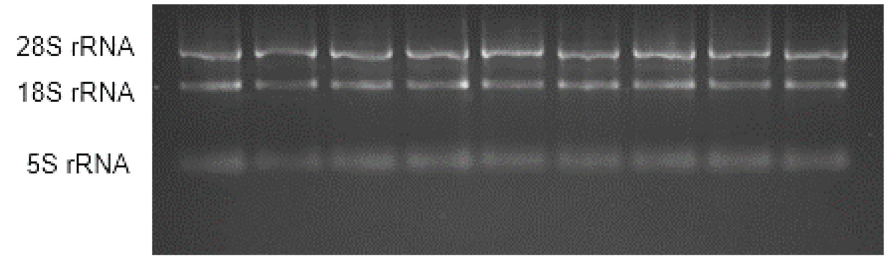

Figure 29: Representative gel picture of the isolated RNA samples.
A gel electrophoresis was run with the extracted RNA samples. The 28S rRNA, 18S rRNA and 5S rRNA subunits are visible.

For the following RT-qPCR experiments, NPS R-568 was used as a positive control, as it was shown to reliably activate the CaSR and lead to an inflammatory response.

I first tested the gene expression of the inflammatory cytokine IL-8. Treatment with spermine increased expression of IL-8 (p<0.001), but neither the treatment with neomycin, L-phenylalanine nor L-tryptophan altered the expression of IL-8 (**Figure 30, left panel**).

NPS R-568 increased the expression of IL-8, but the calcimimetic GSK-3004774 did not alter IL-8 expression. Combining NPS R-2143 with spermine lowered the effect of spermine, indicating that the effect of spermine was probably through activation of the CaSR (**Figure 30, right panel**). Of note, the spermine + NPS R-2143 experiment was deemed a pilot experiment and only performed twice. A statistical analysis was thus not possible.

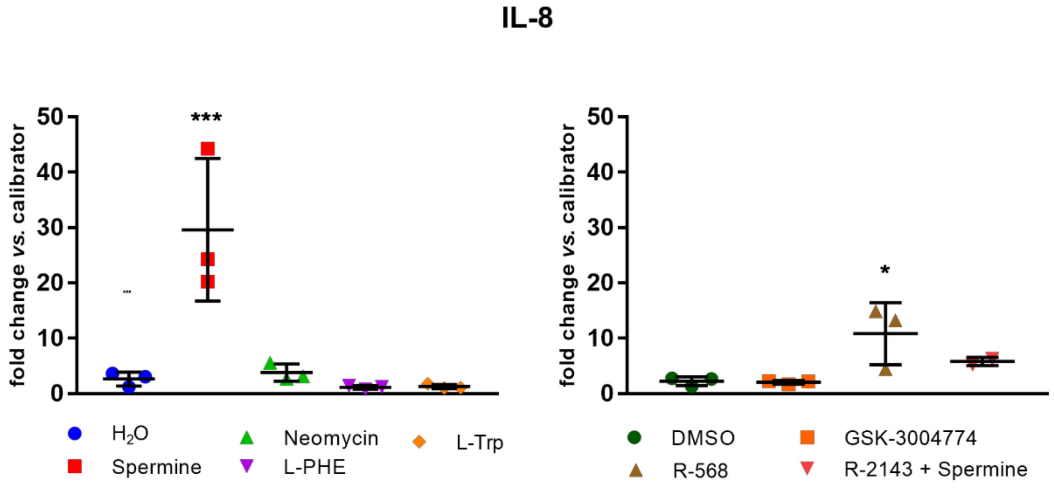

Figure 30: Relative gene expression results of treated HT29$^{GFP\text{-}CaSR}$ cells.

RT-qPCR results for the gene target IL-8. For the treatments 2 µl H_2O, 5 mM spermine, 300 µM neomycin, 1 mM L-phenylalanine and 1 mM L-tryptophan were used. Control treatment was 1 µM NPS R-568. Data are represented as a mean ± SD, N=2-5. Statistical analysis was performed using ordinary one-way ANOVA with multiple comparison to DMSO or H_2O with Dunnett post-test test (Spermine + NPS R-2143 was not included in the analysis, as only two replicates were performed).

Testing for the genes of the PGE2 pathway, spermine significantly increased expression of COX-2 (p<0.001) and PTGES (p<0.001). Neither neomycin nor L-phenylalanine or L-tryptophan influenced the gene expression (**Figure 31 A+B, left panel**). NPS R-568 increased COX-2 (p<0.001) and PTGES (p<0.001) expression but GSK-3004774 had no effect. NPS R-2143 lowered the effect of spermine for these two targets as well (**Figure 31 A + B, right panel**).

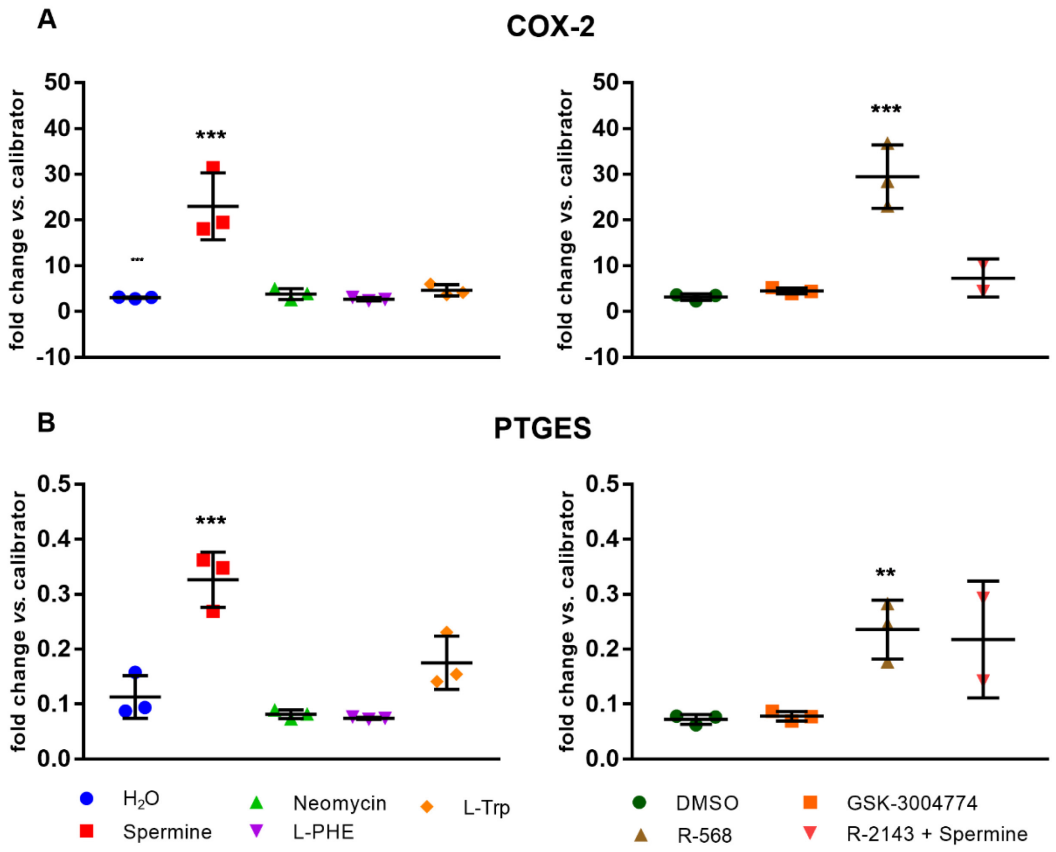

Figure 31: Relative gene expression results of treated HT29$^{GFP\text{-}CaSR}$ cells.

RT-qPCR results for the gene targets COX-2 (A) and PTGES (B). For the treatments 2 µl H_2O, 5 mM spermine, 300 µM neomycin, 1 mM L-phenylalanine and 1 mM L-tryptophan were used. Control treatment was 1 µM NPS R-568. Data are represented as a mean ± SD, N=3. Statistical analysis was performed using ordinary one-way ANOVA with multiple comparison to DMSO or H_2O with Dunnett post-test (Spermine + NPS R-2143 was not included in the analysis, as only two replicates were performed).

For the other tested genes of the PGE2 pathway, NPS R-568 increased EP1 expression (p<0.01) (**Figure 32 B, right panel**). The other tested genes COX-1, 15-PGDH, and EP-4 were not significantly affected by the treatments (**Figure 32**).

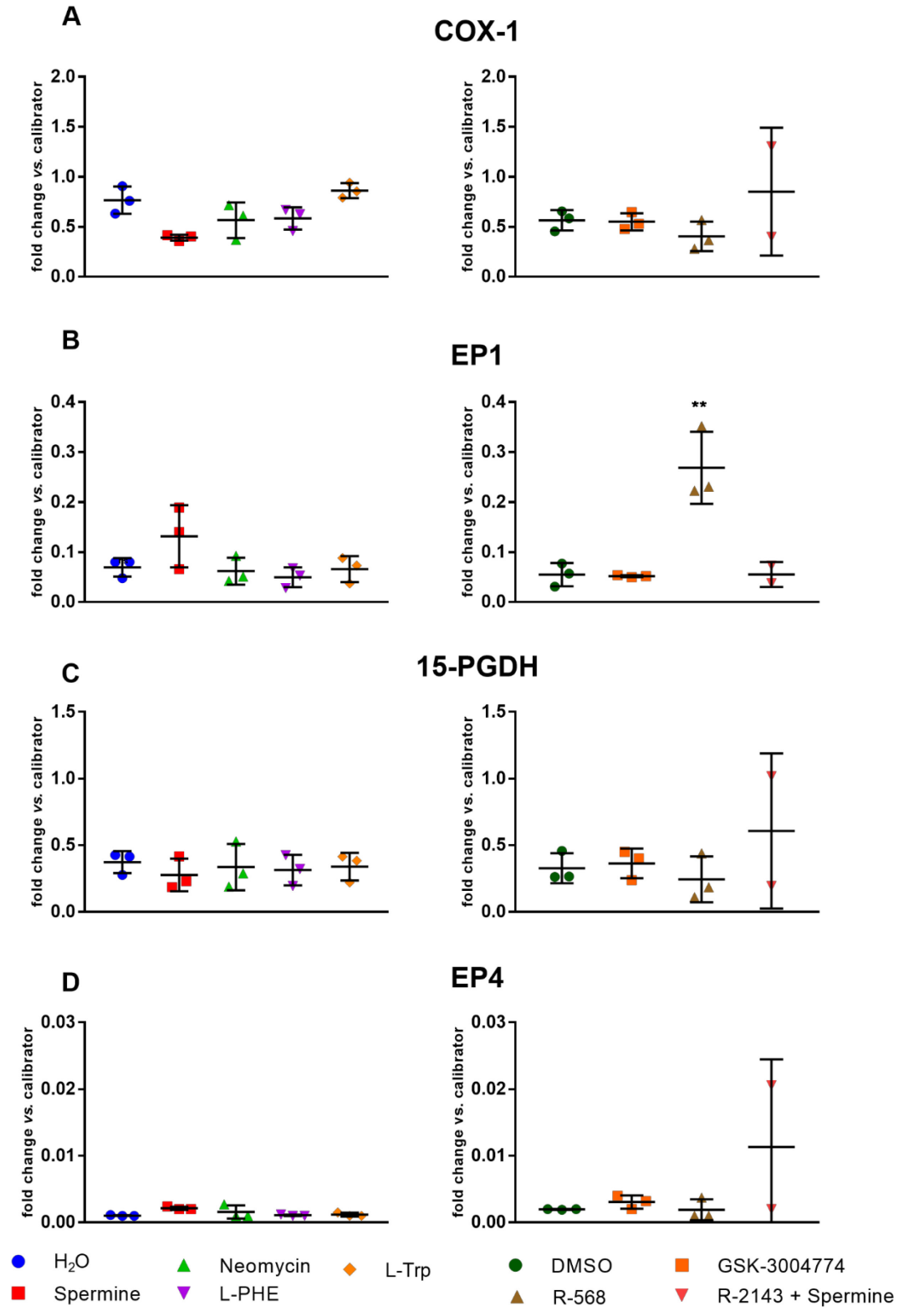

Figure 32: Relative gene expression results of treated HT29$^{GFP\text{-}CaSR}$ cells.

RT-qPCR results for the gene targets COX-1 (A), PTGES (B), 15-PGDH (C), and EP-4 (D). For the treatments 2 µl H_2O, 5 mM spermine, 300 µM neomycin, 1 mM L-phenylalanine and 1 mM L-tryptophan were used. Control treatment was 1 µM NPS R-568. Data are represented as a mean ± SD, N=2-5. Statistical analysis was performed using ordinary one-way ANOVA with multiple comparison to DMSO or H_2O with Dunnett post-test test (Spermine + NPS R-2143 was not included in the analysis, as only two replicates were performed).

Finally, I also investigated whether CaSR expression was affected by the different ligands, as observed in the previous experiment using the allosteric modulators. CaSR gene expression was indeed increased by spermine (p<0.001) and NPS R-568 (p<0.01), following the trend of the previous results.

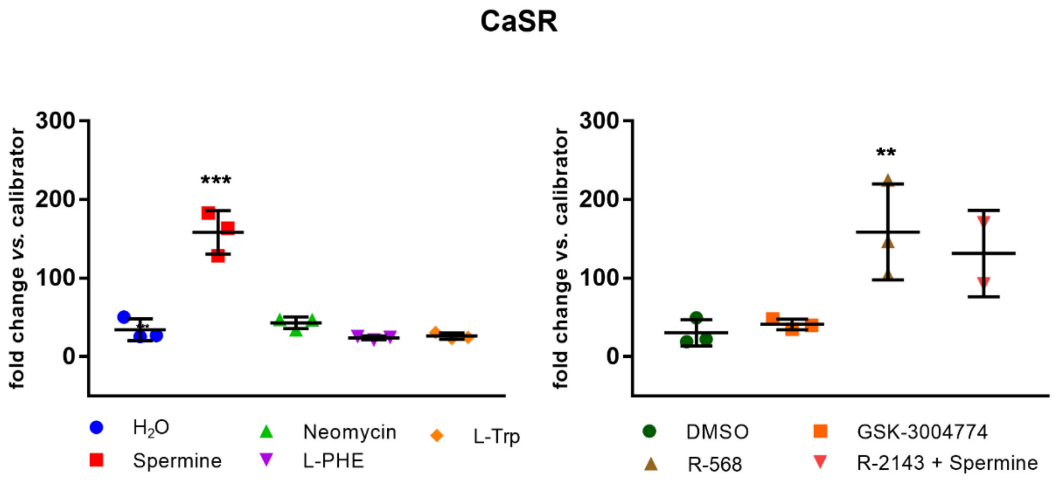

Figure 33: Relative gene expression results of treated HT29$^{GFP\text{-}CaSR}$ cells.
RT-qPCR results for the gene target CaSR. For the treatments 2 µl H_2O, 5 mM spermine, 300 µM neomycin, 1 mM L-phenylalanine and 1 mM L-tryptophan were used. Control treatment was 1 µM NPS R-568. Data are represented as a mean ± SD, N=2-5. Statistical analysis was performed using ordinary one-way ANOVA with multiple comparison to DMSO or H_2O with Dunnett post-test (Spermine + NPS R-2143 was not included in the analysis, as only two replicates were performed).

For HT29^{GFP} cells (lacking the CaSR) none of the treatments had any effect. The RT-qPCR results from the HT29^{GFP} cells are summarized in **Figure 34** (IL-8 (A), CaSR (B), COX-2 (C), COX-1 (D)) and **Figure 35** (PTGES (A), 15-PGDH (B), EP-1 (C) and EP-4 (D)).

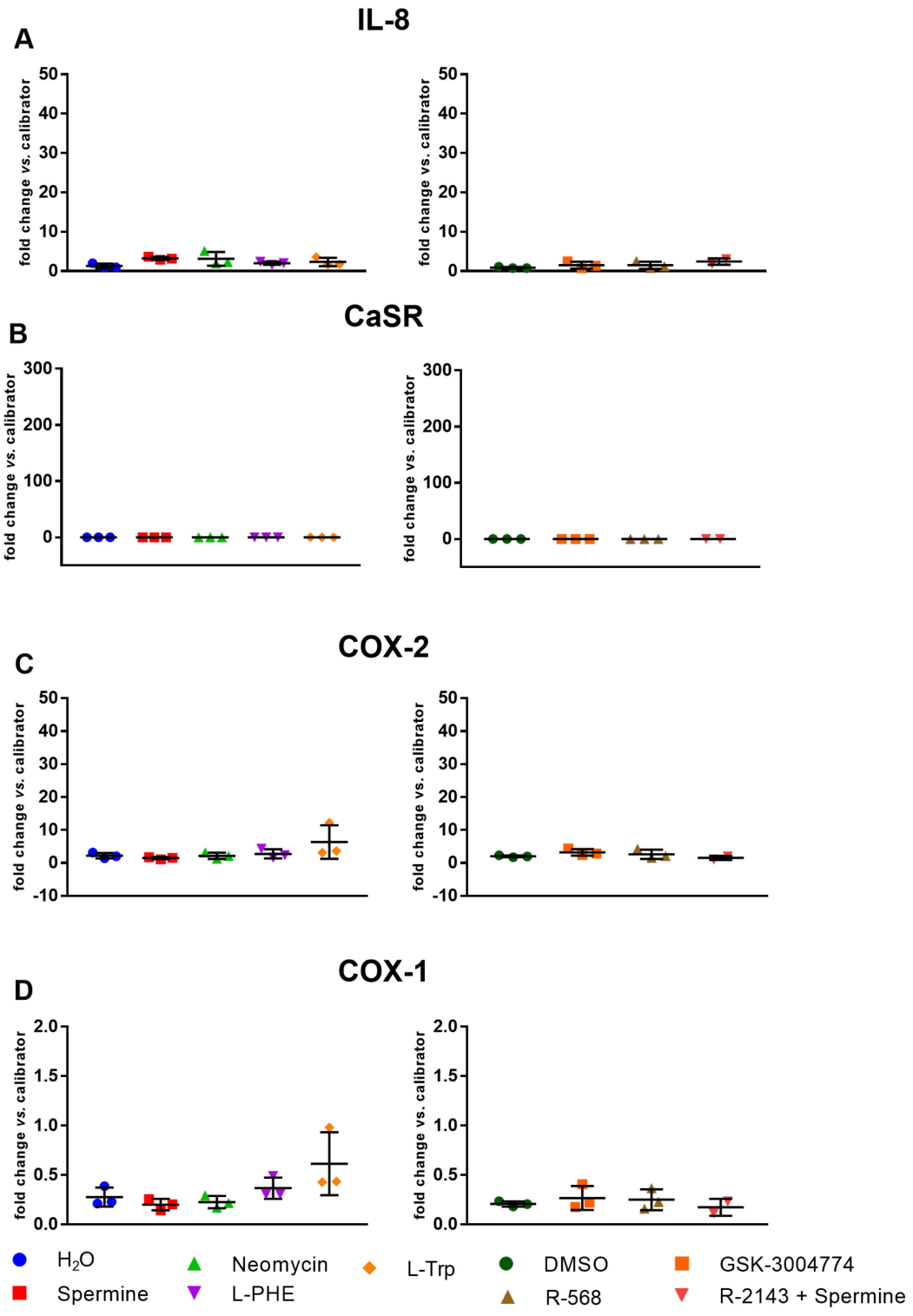

Figure 34: Relative gene expression results of treated HT29^{GFP} cells.

RT-qPCR results for the gene targets IL-8 (A), CaSR (B), COX-2 (C), and COX-1 (D). For the treatments 2 µl H_2O, 5 mM spermine, 300 µM neomycin, 1 mM L-phenylalanine and 1 mM L-tryptophan were used. Control treatment was 1 µM NPS R-568. Data are represented as a mean ± SD, N=2-5. Statistical analysis was performed using ordinary one-way ANOVA with multiple comparison to DMSO or H_2O with Dunnett post-test (Spermine + NPS R-2143 was not included in the analysis, as only two replicates were performed).

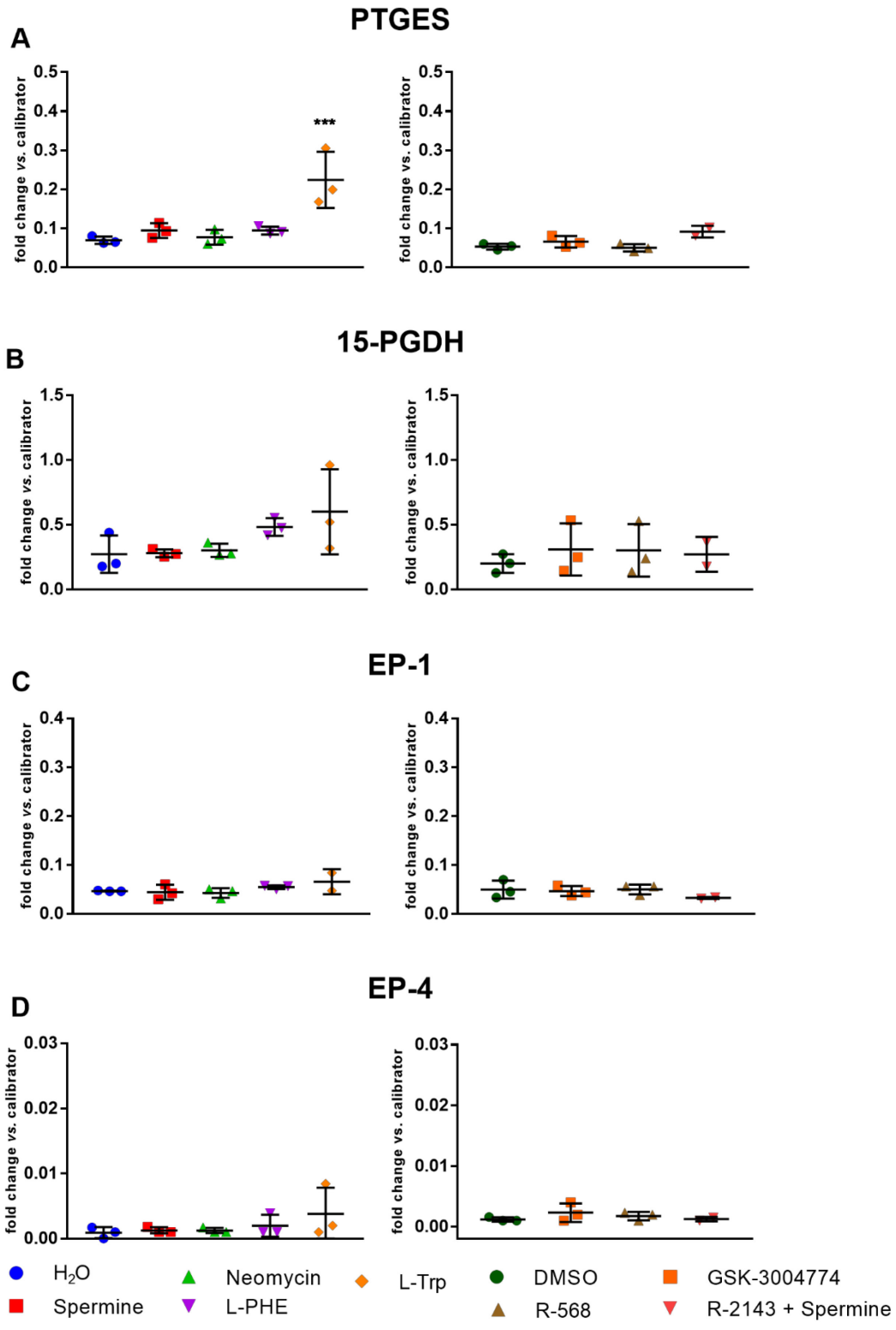

Figure 35: Relative gene expression results of treated HT29^{GFP} cells.

RT-qPCR results for the gene targets PTGES (A), 15-PGDH (B), EP-1 (C), and EP-4 (D). For the treatments 2 µl H_2O, 5 mM spermine, 300 µM neomycin, 1 mM L-phenylalanine and 1 mM L-tryptophan were used. Control treatment was 1 µM NPS R-568. Data are represented as a mean ± SD, N=2-5. Statistical analysis was performed using ordinary one-way ANOVA with multiple comparison to DMSO or H_2O with Dunnett post-test (Spermine + NPS R-2143 was not included in the analysis, as only two replicates were performed).

3.4 Establishment of lipofectamine transfection of CaSR-mutants in HT29 cells

I established the transfection of HT29 cells with CaSR mutant plasmids. To this end, I transformed chemically competent *E. Coli* with the CaSR-plasmids vectors. I extracted the multiplied plasmids from the bacteria by performing a MiniPrep. A small aliquot of the plasmids was digested *via* the restriction enzyme Sal1 to assure that the extracted plasmid contained the right product (CaSR). The vector plasmid pcDNA3.1 with the inserted CaSR gene (3.234 bp) has 8.662 bp (**Figure 36**). As Sal1 cuts at 3.241 bp and 5.426 bp, I am expecting after the restriction digest two fragments of the size 2.185 bp and 6.477 bp.

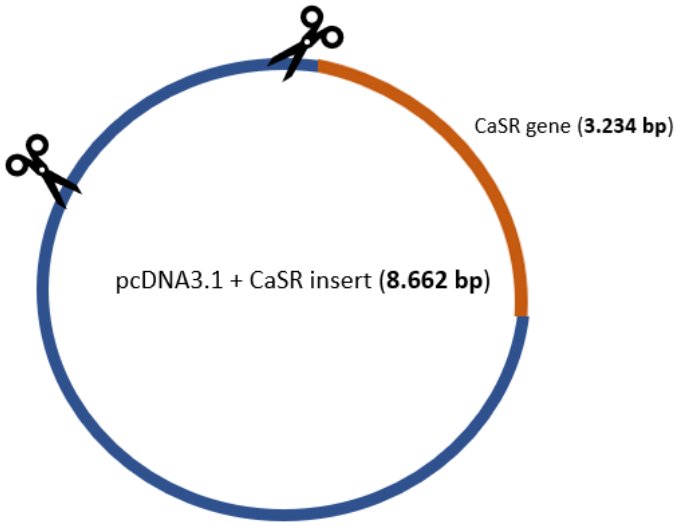

Figure 36: Scheme of the pcDNA3.1 vector with the inserted CaSR gene.
The CaSR gene (3.234 bp) was inserted into the pcDNA3.1 vector with a total of 8.662 bp. The scissors indicate where the restriction enzyme Sal1 is cutting the plasmid into two fragments.

After performing the restriction digestion, the two plasmid-bands with the expected sizes of around 6.500 bp and 2.200 bp were visible (**Figure 37**).

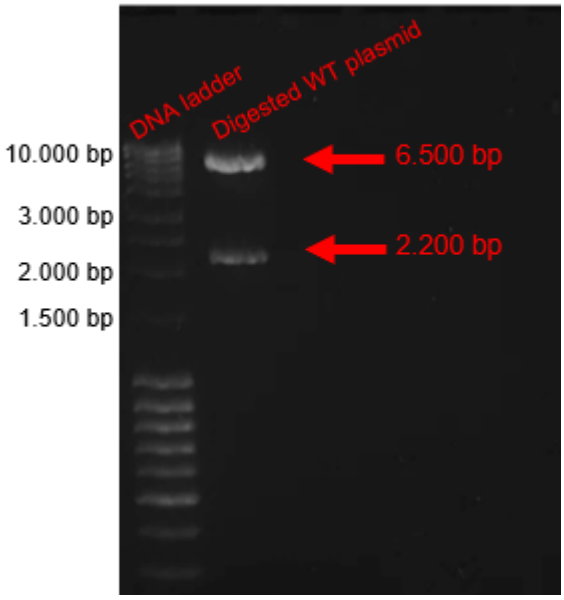

Figure 37: Picture of gel electrophoresis with the digested WT plasmid.
The plasmid was digested with the restriction enzyme SalI, which cuts the plasmid into two fragments of the size 7000 bp and 2200 bp.

To optimize the transfection conditions, I seeded different numbers of cells in a 24-well plate. After seeding $2x10^5$ cells, the cells were 70-80% confluent the next day as it was proposed by the manufacture's protocol (**Figure 38**).

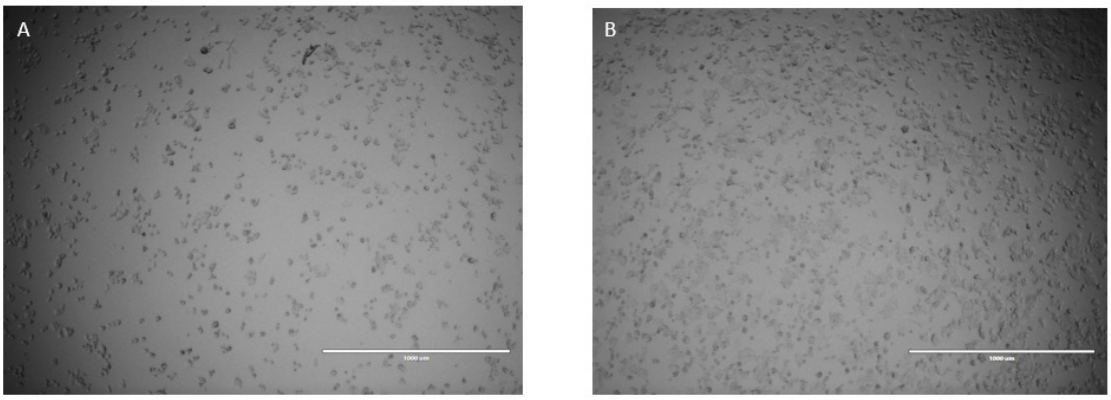

Figure 38: Microscopic picture of HT29 cells.
Different amounts of HT29 cells were seeded in 24-well plates to compare confluency the next day. On the left side (A), 1x 10^5 cells were seeded, cells were barely confluent the next day. On the right side (B), 2x 10^5 cells were seeded reached confluency of 70-80% after 24 hours.

For the transfection, I varied the amount of lipofectamine and plasmid DNA (**Table 13**). The best results were obtained by using 2 µl lipofectamine and 5 ng plasmid DNA. This was evaluated by transfecting an empty vector labelled with green fluorescence protein (GFP) and with the subsequent evaluation of cellular fluorescence with a fluorescence microscope. Representative pictures of the cells after transfection are shown in **Figure 39**.

Table 13: Overview for the transfection conditions.
To establish the best transfection conditions, the right amount of cells was evaluated to reach a confluency of 70-80% the next day. Further, different lipofectamine and plasmid DNA amounts were tested.

Cells seeded	Lipofectamine [µl]	Plasmid DNA [µg]
$0.5x10^5$	2	3
$1x\ 10^5$	3	5
$1.4x\ 10^5$	4	7
$2x\ 10^5$	5	

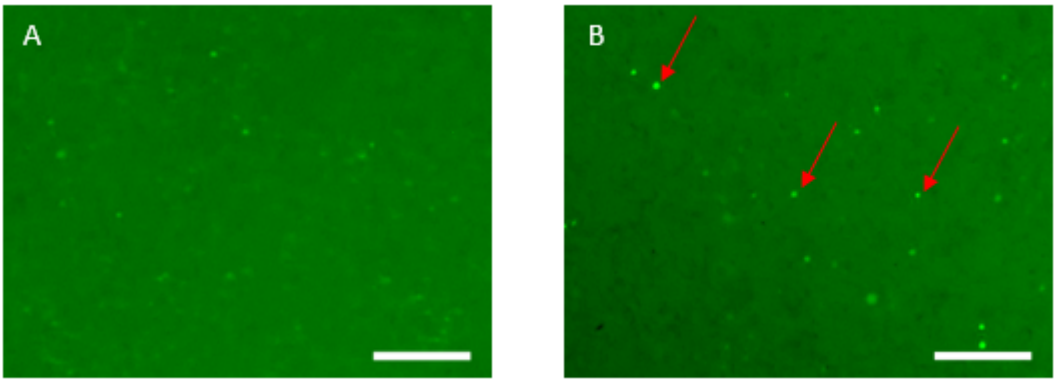

Figure 39: Fluorescence picture of transfected HT29 cells.
HT29 cells were transfected with an empty vector labelled with GFP. (A): I seeded $0.5x10^5$ cells and used 2 µl Lipofectamine + 3 µg plasmid DNA. (B): I seeded $2x10^5$ cells and used 2 µl Lipofectamine + 5 µg plasmid DNA. The red arrows indicate specific fluorescent cells. The picture was cropped and contrast was nonlinearly adjusted for the purpose of visualization. Scale bar: 100 µm.

Two days after transfection, I isolated the RNA and measured CaSR mRNA expression. If the plasmids were transfected efficiently, there should be CaSR gene expression in the samples. I performed two controls, for the first control I added only the CaSR WT plasmid, the lipofectamine plus reagent and the OPTIMEM medium but no lipofectamine. I expected no CaSR gene expression in those cells, as the "vehicle" is missing to transport the plasmids into the cells. For the second control, I only added OPTIMEM medium but none of the other components. CaSR expression was observed for all plasmid constructs (**Figure 40**). The most efficient transfection was seen for the WT construct and the A986S construct. The Q1011E construct was not transfected efficiently. No CaSR gene expression was measured in the two controls.

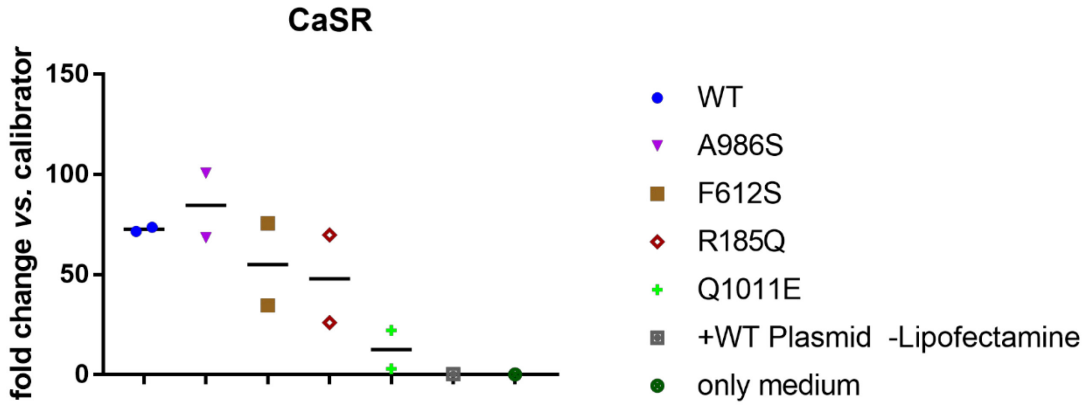

Figure 40: Relative gene expression results of transfected HT29 cells.
RT-qPCR results for the transfected HT29 cells with the different CaSR-mutant plasmids. Target gene is CaSR, and the gene expression is given in fold change vs calibrator. Cells treated with the WT plasmid but without Lipofectamine and cells treated only with OPTIMEM medium are used as a control.

4 Discussion

In the course of my work, I was able to answer the questions of my master thesis:

1) The inflammatory response observed after treatment of $HT29^{GFP\text{-}CaSR}$ cells with NPS R-568 and Ca^{2+} was indeed mediated *via* the CaSR; this was proven using enantioselective modulators of the CaSR. $HT29^{GFP\text{-}CaSR}$ cells show a strong IL-1β dose-dependent increase in IL-8 expression.

2) This pro-inflammatory effect of the CaSR is ligand dependent. Of the tested agonists, only 5 mM spermine had an effect on the inflammatory response in $HT29^{GFP\text{-}CaSR}$ cells.

3) I have successfully established the transfection of CaSR mutant plasmids in HT29 cells. Due to time constraints, I could not test whether these transfected mutants had an effect on general gene expression or the inflammatory gene response. This will be the task for further investigations.

These *in vitro* findings substantiate our knowledge about the pro-inflammatory role of the CaSR in colorectal cancer cells and the pro-inflammatory role of the CaSR in the intestine in general.

4.1 **Calcium-Sensing Receptor-mediated inflammatory response is ligand dependent**

In my experiments, I have proven that the previously observed induction of inflammatory gene expression (by calcimimetics) in $HT29^{GFP\text{-}CaSR}$ cells [95] is indeed mediated by the CaSR and that this effect is ligand-dependent. The activation of the CaSR by NPS R-568 and spermine increased the expression of the inflammatory markers IL-8 and CCL-20, as well as of certain members of the PGE2 pathway (discussed below). This effect was not seen for the unspecific-binding enantiomer NPS S-568. Neither NPS R-2143 nor NPS S-2143 had an effect on inflammatory gene expression. On the protein / product level I observed the same effect, as only NPS R-568 increased the expression of IL-8 and the level of PGE2. The treatment combinations NPS R-568 + NPS R-2143 inhibited

the expression of the inflammatory genes compared to the treatment with NPS R-568 + NPS S-2143, which gives evidence that the inhibition of the CaSR can counteract the inflammatory effect. These findings support the results of a previous work in our group [95], where an increase of inflammatory gene expression was observed after treatment with NPS R-568. They further showed by gene ontology enrichment analysis that the treatment with NPS R-568 upregulated genes belonging to pathways of the immune response [95]. To investigate the role of the CaSR in the expression of inflammatory markers *in vivo*, mice were injected with $HT29^{GFP\text{-}CaSR}$ cells to generate xenograft tumors. The mice were orally treated with cinacalcet to assess the effect of CaSR modulation on tumor growth. Contrary to the *in vitro* results, two previous students of our group, Katharina Gall and Michael Schwarzkopf, found that the calcimimetic cinacalcet did not lead to an increase of inflammatory markers or inflammatory cells in CaSR overexpressing xenograft tumors from $H29^{CaSR\text{-}GFP}$ cells [148, 149].

A possible explanation could lie in the different setting of the *in vivo* and *in vitro* situation. If the immune system is responsible for mediated inflammatory effects *via* the CaSR *in vivo,* as suggested by the observation of increased immune cell infiltration of cinacalcet treated mice with chemically induced colitis [94], the lack of an immune system in my *in vitro* experiment could explain this discrepancies. However, the exact reason for this discrepancy cannot be determined at this time and will require further investigation, *e.g.* using mouse models of different tumors or studies with intact human tissue.

In a previous study of our group a mouse-colitis model was used to examine the effect of the calcimimetics cinacalcet and GSK-3004774 in an inflammatory environment [94]. Colitis was induced *via* DSS, and the mice were treated orally with NPS R-2143, cinacalcet or GSK-3004774. The treatment with cinacalcet but not with GSK-3004774 had a pro-inflammatory effect [94]. The pro-inflammatory effect of cinacalcet was most prominently shown by a reduction in mucin levels and in an increase in pro-inflammatory cytokines in the plasma. Treating the mice with NPS R-2143 improved the clinical symptoms of colitis, leading to a lower clinical score and reduced infiltration of immune cells [94]. The latter finding is

especially interesting as two of my investigated target genes for CaSR-induced inflammation were CCL-20 (see below) and IL-8, chemokines related to attract and activate immune cells [150]. IL-8 is known to be strongly upregulated in the intestinal mucosa and immune system in patients with IBD [151]. This could indicate that one of the main modalities through which the CaSR influences inflammation *in vivo* could be immune cell activation and attraction.

Michael Schwarzkopf compared the inflammatory gene expression in the colons of these mice [148]. He found that cinacalcet increased both PGE2 pathway member genes PGES and EP3, while the treatment with GSK-3004774 increased PGES in inflamed colons, while NPS R-2143 had no effect on the expression of any of the investigated genes. Of note, no combination of NPS R-568 and NPS R-2143 was administered. Treatment with high doses of CaSR modulators also did not affect PGE2 pathway genes in healthy mice. These findings suggested a pro-inflammatory effect of the allosteric CaSR-modulation *only* in an inflamed environment *in vivo*, which is in line with my findings *in vitro*.

The effects of GSK-3004774 are rather inconsistent. While the gut-restricted compound had no effect on the inflammatory gene expression in my experiments, or on the clinical score of the induced colitis [94], it did increase PGES expression in the colons of inflamed mice. It might be argued that GSK-3004774 is not very active at all – however, the batch of the compound I (and the previous study) used had indeed shown to be biologically active in enhancing CaSR sensitivity to extracellular Ca^{2+} in HEK-293 cells stably transfected with the human CaSR (Martin Schepelmann, personal communication and [94]). GSK-3004774 was first described in a paper from 2017 [44]. Even though it was a promising approach to develop a non-absorbable calcimimetic to treat hyperparathyroidism no further studies were published since the first publication in 2017. This could be due to the lack of *in vivo* effects and highlights the importance of publishing so called “negative” results.

In addition, I found that the activation of the CaSR by NPS R-568 and spermine increased the expression of the *CaSR* gene itself. This can be explained by the unique feature of the CaSR, ADIS, which ensures that changes in Ca^{2+} levels will be rapidly sensed by newly maturated and inserted receptors [17] which

apparently also influences gene expression and thus probably induction of *de novo* receptor transcription.

Not only activation, but already the presence of the CaSR seems to potentiate the inflammatory response. The basal expression of all inflammatory markers was higher in $HT29^{GFP\text{-}CaSR}$ cells than in $HT29^{GFP}$ cells. This effect was also seen by Iamartino *et al*, where the over-expression of the CaSR in HT29 cells alone already changed the expression of several genes involved in inflammatory pathways, compared to the control cells. This effect was further enhanced by the activation of the CaSR through NPS R-568 [95]. These results show a pro-inflammatory effect of the expression and even more of the activation of the CaSR in colon cancer cells. This would suggest that drugs, such as calcimimetics, which are used to treat diseases like hyperparathyroidism could hold the risk of an inflammatory effect in certain tissues. For the calcimimetic cinacalcet an FDA warning was published in 2017 [152], where patients with risk factors for upper GI bleeding were mentioned to be at increased risk. Pro-inflammatory effects of the CaSR were also shown in other tissues such as in adipose tissue [90] and in the lung [23], which fits with our results There, calcimimetics could possibly also lead to inflammatory responses and serious side effects, but to my knowledge, no such effects have been reported yet. As calcimimetics are only used in small collective of patients with putatively many comorbidities (chronic kidney disease), it is unclear whether such effects would be attributed to the drug or would be masked by the underlying disease.

As the CaSR itself is upregulated with increased presence of ligands (ADIS), it suggests a positive feedback loop, *i.e*. a vicious circle, in which the CaSR is increasingly expressed upon activation and potentiates the inflammatory gene response even more. If the abundance of the CaSR correlates with the severity of inflammation, the CaSR could possibly be a potential diagnostic marker for the severity of inflammatory processes in the intestine. Studies on human samples from patients suffering from IBD will be needed to confirm this hypothesis.

Treatments with different concentrations of IL-1β affected IL-8 expression in a strong dose-dependent manner, while the cells lacking the CaSR, $HT29^{GFP}$, did (almost) not respond to IL-1β treatment. IL-1β is an inflammatory cytokine, known

to induce acute and chronic inflammation [153] and to be key mediator of carcinogenesis [154, 155]. IL-1β levels were correlated with the severity of inflammation in patients suffering of IBD [156-158]. In addition, IL-1β in the tumor microenvironment accelerates production of DNA damaging molecules, leading to mutations in the colon epithelium and thus to promotion of cancer development [159]. *In vivo* studies also showed evidence for a link between inflammatory cytokines and the CaSR, as intraperitoneal injection of IL-1β and IL-6 reduced $1,25(OH)_2D_3$ and PTH levels, which led to a decreased serum Ca^{2+} [160, 161]. Taken together with my results, the activation of the CaSR thus seems to increase the inflammatory response and further potentiate the inflammatory effect of IL1-β. This suggests an amplification loop in which IL-1β and the CaSR potentiate each other's inflammatory response, as already discussed above. Whether this result is limited to inflammation induced by IL-1β or holds true for other pro-inflammatory cytokines like TNFα is unclear and will need to be investigated further.

I have demonstrated that CaSR activation itself leads to heightened inflammatory responses, among them the PGE2 pathway and IL-8 as well as CCL20 production, indicating a wide variety of CaSR mediated inflammatory target genes, which was also seen in the RNASeq experiments performed by our group [95]. Furthermore, as the exogenously induced inflammation through IL-1β was that much stronger in CaSR expressing cells, it would now be highly relevant to investigate whether this exogenously and apparently CaSR-potentiated inflammatory response could be suppressed by inhibiting the CaSR itself and experiments to this effect will be performed in the near future.

The activation of the CaSR through NPS R-568 affected certain genes of the PGE2 pathway, an effect which I did not observe for the unspecific-binding enantiomers. This provides evidence that the PGE2 pathway is involved in the inflammatory response mediated *via* the CaSR. The treatment with NPS R-568 significantly increased the expression of COX-2, the key enzyme of the PGE2 pathway. This effect on the inflammatory gene response was also seen for the treatment with spermine but for none of the other ligands, which is probably due to the ligand biased signaling of the CaSR. Spermine increased the expression

of IL-8 and of the PGE2 pathway member genes COX-2, PTGES and EP1. The other PGE2 pathway genes I tested, COX-1, PTGES, 15-PGDH, EP-1, and EP-4, were affected in a similar fashion, but did not reach statistical significance. The pre-treatment with NPS R-2143 inhibited the inflammatory effect of spermine and gives evidence that NPS R-2143, binding allosterically to the receptor, decreased the receptor's sensitivity for the orthosterically-binding spermine. Spermine is released by damaged or dead cells and reduces inflammation by suppressing macrophage cytokine synthesis and preventing excessive macrophage-mediated tissue damage [162]. It is interesting that my results suggest a pro-inflammatory role of spermine by the activation of the CaSR. The effect of spermine should be tested in other cell types expressing the CaSR to see whether the same effect is observed.

Michael Schwarzkopf already showed an impact of CaSR-modulation on the PGE2 pathway *in vivo,* which is now supported by my *in vitro* results. However, in contrast to my findings with the genetically modified colon cancer cells, he observed an upregulation of PGES2 and EP3 in the colons of cinacalcet treated colitis mice while COX2 and EP-1 were not affected. This may be due to species differences or the more artificial situation of my *in vitro* experiments. Interestingly, the same upregulations were not detected in $HT29^{CaSR\text{-}GFP}$ xenograft tumors in immuno-deficient mice [148, 149], as indeed the tumors were not affected by CaSR directed treatments in any way. Whether this is due to the drugs not reaching the tumors or the malignant microenvironment prevent an effect of the drugs is unknown.

The members of the PGE2 pathway are known to be involved in tumorigenesis. COX-2 is known to be upregulated in malignant colorectal tissue [109]. Its pro-tumorigenic effect is linked to its role in producing PGE2 [163, 164]. Increased levels of PGE2 have been reported in human colorectal adenomas and carcinomas, promoting cell proliferation and survival [165]. PTGES is responsible for the conversion of PGH2 to PGE2 and was shown to be highly upregulated in inflammatory tissues and tumors [166]. Specifically, PGE2 is markedly increased in colon, lung, and breast cancer [167-169]. Studies in hepatocellular carcinoma cells revealed that PGE2 regulates through the EP1 receptor the expression of

the anti-apoptotic protein survivin [170]. Interestingly, in the experiment where I tested the effect of different CaSR ligands, NPS R-568 increased EP1 expression (**Figure 32**). This was not seen in the experiment for the enantio-selective activation of the CaSR (**Figure 18**). These results currently cannot be explained, however, a small, albeit non-significant increase from baseline can be seen (p=0.24 for NPS R-568 *vs.* DMSO), so it is possible that the lack of a statistically significant effect is due to low statistical power. It thus needs further confirmation whether EP1 is indeed influenced by CaSR-activation.

The amino acids I tested, L-phenylalanine and L-tryptophan, as well as the antibiotic neomycin had no effect on the inflammatory gene expression. Mine *et al* showed a CaSR-mediated anti-inflammatory effect of L-amino acids in colon cells [144] and also in an *in vivo* mouse-model [91]. In their study, 5 mM L-tryptophan highly reduced IL-8 expression in HT29 and Caco-2. This strong anti-inflammatory effect cannot be seen in my data. This could be due to the lower concentration of L-phenylalanine and L-tryptophan (1 mM) I used for my experiments. In further studies a higher concentration of the amino acids could be used to assess whether the cells respond differently. However, their results are surprising as especially HT29 cells do not express the CaSR in any meaningful quantity (see results) which is why I used the CaSR transfected cells. It is possible that the amino acid elicited its effect through other receptors rather than the CaSR in their study. This is even more plausible as the authors of that study observed an anti-inflammatory effect through L-tryptophan, which would indicate a complete reversal of the CaSR's role based on the ligand. While CaSR signaling is ligand biased, this opposite effect seems unlikely, especially as both an orthosteric (Ca^{2+}) and allosteric (NPS R-568) modulator, which already signal differently through the CaSR both increased the inflammatory response of the cells.

This was the first study which systemically tested the enantiomers of NPS-568 and NPS 2143. In pharmacology research it is generally of great importance to determine stereospecificity of a compound and thus that the effects of both enantiomers are tested. Even though NPS S-568 and NPS S-2143 had no effect on the inflammatory gene response, the CaSR-unspecific calcilytics are not

biologically inert molecules. For example, the S (CaSR-unspecific forms) of amino alcohol calcilytics have a much higher affinity for β-adrenergic receptors [70] than the R-forms. Whether other cellular functions are influenced by the CaSR-unspecific enantiomers remains to be investigated, but the pro-inflammatory responses are clearly not affected. These experiments are of course limited by the fact that the transfected cell line $HT29^{GFP\text{-}CaSR}$ is a genetically modified cell line, which was established to study the effect of the CaSR *in vitro.* Colorectal cancer cells lose their expression of the CaSR due to their dedifferentiation [150], which makes the use of this rather artificial surrogate necessary. Furthermore, in the course of my project, I only tested the effect of the different enantiomers on one colon cancer cell line. In a next step, it would be important to test the same treatment on another cell cline (*e.g.* the also established $Caco\text{-}2^{CaSR\text{-}GFP}$ cell line [95]). Of course, an *in vitro* study cannot answer questions about the situations in whole organisms. My results point out the necessity of further *in vivo* studies, to investigate the role of the CaSR in the intestine.

As already mentioned above, I only used one concentration from each ligand for the treatments. For the concentrations, I referred to the current literature, using concentrations from the high-end of standard concentrations normally used in CaSR related experiments (see methods) but nevertheless also other concentrations of the different ligands may have to be tested. In addition, the genes of other inflammatory pathways should be examined. I showed in my results that NPS R-568 increased the expression of CCL-20, a chemokine that binds to the chemokine receptor 6 (CCR6). Both, CCL-20 and CCR6 are upregulated in CRC [171-173] and lead to the activation of extracellular signal-regulated (ER)-mitogen-activated protein (MAP) kinase and Akt pathways [174]. It would be of interest if CaSR-modulation in colon cancer cells also upregulates CCR6 or members of ERK-MAP kinase and Akt pathways.

The fact that only the R-form of the calcilytic was able to suppress the NPS R-568 induced inflammatory response and that neither R- nor S-form of the calcilytic, nor the unspecific NPS S-568 induced any inflammatory response themselves, strongly indicates a strong specificity of the elicited inflammation

response to CaSR modulation**.** The pro-inflammatory influence of the CaSR in HT29 cells seems to be ligand dependent and affects the PGE2 pathway. These findings give further evidence for the crucial role of the CaSR in intestinal inflammation and may help to understand the molecular mechanisms of intestinal inflammation. The accumulating evidence for the pro-inflammatory effect of the CaSR in the intestine strongly suggest the CaSR as a therapeutic target for intestinal inflammation in the clinic.

5 Summary and conclusion

Within this project, I confirmed the pro-inflammatory role of CaSR, which was previously reported in CaSR-modulated $HT29^{GFP\text{-}CaSR}$ cells [95]. I showed that the inflammatory response in $HT29^{GFP\text{-}CaSR}$ cells is ligand-dependent and that the activation of the CaSR by allosteric modulators and spermine influences the pro-inflammatory PGE2 pathway. Furthermore, I established the transfection of CaSR-mutants into HT29 cells. This *in vitro* model gives the opportunity to study the effect of CaSR mutants on the inflammatory gene response in the near future.

My findings give further evidence for the role of the CaSR in intestinal inflammation and may help to understand the molecular mechanisms of intestinal inflammation. The accumulating evidence for the pro-inflammatory effect of the CaSR in the intestine suggest the CaSR as a potential therapeutic target for intestinal inflammation in the clinic.

6 Outlook

For further experiments, it is necessary to compare my results to different colorectal cancer cell lines, such as the already established $Caco2^{GFP\text{-}CaSR}$ and $Caco2^{GFP}$ cell lines and with cells expressing the CaSR endogenously. Also other genes of the PGE2 pathway should be tested, *e.g.* other prostaglandin synthase enzymes or prostaglandin transporters. Furthermore, it may be useful to test different concentrations of the L-amino acids to see whether higher concentrations would lead to an alteration of the inflammatory response.

The results of my master thesis give rise to a variety of further questions. Most importantly, it remains unclear, why cinacalcet had different effects in *in vitro* [95] [results of my thesis] and *in vivo* [148, 149] studies. Here, further studies are necessary. In general, the roles of other inflammatory pathways and mechanisms such as *e.g.* NF-κB signaling and cell attraction need to be investigated.

7 References

1. Li, K., Wang, X.F., Li, D.Y., Chen, Y.C., Zhao, L.J., Liu, X.G., Guo, Y.F., Shen, J., Lin, X., Deng, J., et al. (2018). The good, the bad, and the ugly of calcium supplementation: a review of calcium intake on human health. Clin Interv Aging *13*, 2443-2452.

2. Baird, G.S. (2011). Ionized calcium. Clin Chim Acta *412*, 696-701.

3. Minisola, S., Pepe, J., Piemonte, S., and Cipriani, C. (2015). The diagnosis and management of hypercalcaemia. BMJ *350*, h2723.

4. Chernow, B., Zaloga, G., McFadden, E., Clapper, M., Kotler, M., Barton, M., and Rainey, T.G. (1982). Hypocalcemia in critically ill patients. Crit Care Med *10*, 848-851.

5. Brown, E.M., Gamba, G., Riccardi, D., Lombardi, M., Butters, R., Kifor, O., Sun, A., Hediger, M.A., Lytton, J., and Hebert, S.C. (1993). Cloning and characterization of an extracellular Ca(2+)-sensing receptor from bovine parathyroid. Nature *366*, 575-580.

6. Pin, J.P., Kniazeff, J., Goudet, C., Bessis, A.S., Liu, J., Galvez, T., Acher, F., Rondard, P., and Prezeau, L. (2004). The activation mechanism of class-C G-protein coupled receptors. Biol Cell *96*, 335-342.

7. Chou, Y.H., Brown, E.M., Levi, T., Crowe, G., Atkinson, A.B., Arnqvist, H.J., Toss, G., Fuleihan, G.E., Seidman, J.G., and Seidman, C.E. (1992). The gene responsible for familial hypocalciuric hypercalcemia maps to chromosome 3q in four unrelated families. Nat Genet *1*, 295-300.

8. Hendy, G.N., Canaff, L., and Cole, D.E. (2013). The CASR gene: alternative splicing and transcriptional control, and calcium-sensing receptor (CaSR) protein: structure and ligand binding sites. Best Pract Res Clin Endocrinol Metab *27*, 285-301.

9. Brauner-Osborne, H., Jensen, A.A., Sheppard, P.O., O'Hara, P., and Krogsgaard-Larsen, P. (1999). The agonist-binding domain of the calcium-sensing receptor is located at the amino-terminal domain. J Biol Chem *274*, 18382-18386.

10. Geng, Y., Mosyak, L., Kurinov, I., Zuo, H., Sturchler, E., Cheng, T.C., Subramanyam, P., Brown, A.P., Brennan, S.C., Mun, H.C., et al. (2016). Structural mechanism of ligand activation in human calcium-sensing receptor. Elife *5*.

11. Khan, M.A., and Conigrave, A.D. (2010). Mechanisms of multimodal sensing by extracellular Ca(2+)-sensing receptors: a domain-based survey of requirements for binding and signalling. Br J Pharmacol *159*, 1039-1050.

12. Fan, G., Goldsmith, P.K., Collins, R., Dunn, C.K., Krapcho, K.J., Rogers, K.V., and Spiegel, A.M. (1997). N-linked glycosylation of the human Ca2+ receptor is essential for its expression at the cell surface. Endocrinology *138*, 1916-1922.

13. Pidasheva, S., Grant, M., Canaff, L., Ercan, O., Kumar, U., and Hendy, G.N. (2006). Calcium-sensing receptor dimerizes in the endoplasmic reticulum: biochemical and biophysical characterization of CASR mutants retained intracellularly. Hum Mol Genet *15*, 2200-2209.

14. Cavanaugh, A., Huang, Y., and Breitwieser, G.E. (2012). Behind the curtain: cellular mechanisms for allosteric modulation of calcium-sensing receptors. Br J Pharmacol *165*, 1670-1677.

15. Brown, E.M. (2013). Role of the calcium-sensing receptor in extracellular calcium homeostasis. Best Pract Res Clin Endocrinol Metab *27*, 333-343.

16. Charlton, S.J. (2009). Agonist efficacy and receptor desensitization: from partial truths to a fuller picture. Br J Pharmacol *158*, 165-168.

17. Grant, M.P., Stepanchick, A., Cavanaugh, A., and Breitwieser, G.E. (2011). Agonist-driven maturation and plasma membrane insertion of calcium-sensing receptors dynamically control signal amplitude. Sci Signal *4*, ra78.

18. Riccardi, D., and Kemp, P.J. (2012). The calcium-sensing receptor beyond extracellular calcium homeostasis: conception, development, adult physiology, and disease. Annu Rev Physiol *74*, 271-297.

19. Molostvov, G., James, S., Fletcher, S., Bennett, J., Lehnert, H., Bland, R., and Zehnder, D. (2007). Extracellular calcium-sensing receptor is functionally expressed in human artery. Am J Physiol Renal Physiol *293*, F946-955.

20. Schreckenberg, R., and Schluter, K.D. (2018). Calcium sensing receptor expression and signalling in cardiovascular physiology and disease. Vascul Pharmacol.

21. Molostvov, G., Fletcher, S., Bland, R., and Zehnder, D. (2008). Extracellular calcium-sensing receptor mediated signalling is involved in human vascular smooth muscle cell proliferation and apoptosis. Cell Physiol Biochem *22*, 413-422.

22. Schepelmann, M., Yarova, P.L., Lopez-Fernandez, I., Davies, T.S., Brennan, S.C., Edwards, P.J., Aggarwal, A., Graca, J., Rietdorf, K., Matchkov, V., et al. (2016). The vascular Ca2+-sensing receptor regulates blood vessel tone and blood pressure. Am J Physiol Cell Physiol *310*, C193-204.

23. Yarova, P.L., Stewart, A.L., Sathish, V., Britt, R.D., Jr., Thompson, M.A., AP, P.L., Freeman, M., Aravamudan, B., Kita, H., Brennan, S.C., et al. (2015). Calcium-sensing receptor antagonists abrogate airway hyperresponsiveness and inflammation in allergic asthma. Sci Transl Med *7*, 284ra260.

24. Tu, C.L., and Bikle, D.D. (2013). Role of the calcium-sensing receptor in calcium regulation of epidermal differentiation and function. Best Pract Res Clin Endocrinol Metab *27*, 415-427.

25. Bikle, D.D., Ratnam, A., Mauro, T., Harris, J., and Pillai, S. (1996). Changes in calcium responsiveness and handling during keratinocyte differentiation. Potential role of the calcium receptor. J Clin Invest *97*, 1085-1093.

26. Bikle, D.D., Jiang, Y., Nguyen, T., Oda, Y., and Tu, C.L. (2016). Disruption of Vitamin D and Calcium Signaling in Keratinocytes Predisposes to Skin Cancer. Front Physiol *7*, 296.

27. Kleeman, C.R., Massry, S.G., and Coburn, J.W. (1971). The clinical physiology of calcium homeostasis, parathyroid hormone an, and calcitonin. I. Calif Med *114*, 16-43.

28. Song, L. (2017). Calcium and Bone Metabolism Indices. Adv Clin Chem *82*, 1-46.

29. Borba, V.Z., and Manas, N.C. (2010). The use of PTH in the treatment of osteoporosis. Arq Bras Endocrinol Metabol *54*, 213-219.

30. Magno, A.L., Ward, B.K., and Ratajczak, T. (2011). The calcium-sensing receptor: a molecular perspective. Endocr Rev *32*, 3-30.

31. Tennakoon, S., Aggarwal, A., and Kallay, E. (2016). The calcium-sensing receptor and the hallmarks of cancer. Biochim Biophys Acta *1863*, 1398-1407.

32. Riccardi, D., Park, J., Lee, W.S., Gamba, G., Brown, E.M., and Hebert, S.C. (1995). Cloning and functional expression of a rat kidney extracellular calcium/polyvalent cation-sensing receptor. Proc Natl Acad Sci U S A *92*, 131-135.

33. Pegg, A.E. (2014). The function of spermine. IUBMB Life *66*, 8-18.

34. Morgan, D.M. (1998). Polyamines. An introduction. Methods Mol Biol *79*, 3-30.

35. Byrd, W.J., Jacobs, D.M., and Amoss, M.S. (1977). Synthetic polyamines added to cultures containing bovine sera reversibly inhibit in vitro parameters of immunity. Nature *267*, 621-623.

36. Zhang, M., Caragine, T., Wang, H., Cohen, P.S., Botchkina, G., Soda, K., Bianchi, M., Ulrich, P., Cerami, A., Sherry, B., et al. (1997). Spermine inhibits proinflammatory cytokine synthesis in human mononuclear cells: a counterregulatory mechanism that restrains the immune response. J Exp Med *185*, 1759-1768.

37. Conigrave, A.D., Mun, H.C., and Lok, H.C. (2007). Aromatic L-amino acids activate the calcium-sensing receptor. J Nutr *137*, 1524S-1527S; discussion 1548S.

38. Nemeth, E.F. (2002). Pharmacological regulation of parathyroid hormone secretion. Curr Pharm Des *8*, 2077-2087.

39. Nemeth, E.F., and Goodman, W.G. (2016). Calcimimetic and Calcilytic Drugs: Feats, Flops, and Futures. Calcif Tissue Int *98*, 341-358.

40. Hannan, F.M., Olesen, M.K., and Thakker, R.V. (2018). Calcimimetic and calcilytic therapies for inherited disorders of the calcium-sensing receptor signalling pathway. Br J Pharmacol *175*, 4083-4094.

41. Nemeth, E.F. (2006). Misconceptions about calcimimetics. Ann N Y Acad Sci *1068*, 471-476.

42. Goodman, W.G., Frazao, J.M., Goodkin, D.A., Turner, S.A., Liu, W., and Coburn, J.W. (2000). A calcimimetic agent lowers plasma parathyroid hormone levels in patients with secondary hyperparathyroidism. Kidney Int *58*, 436-445.

43. Martin, K.J., Bell, G., Pickthorn, K., Huang, S., Vick, A., Hodsman, P., and Peacock, M. (2014). Velcalcetide (AMG 416), a novel peptide agonist of the calcium-sensing receptor, reduces serum parathyroid hormone and FGF23 levels in healthy male subjects. Nephrol Dial Transplant *29*, 385-392.

44. Sparks, S.M., Spearing, P.K., Diaz, C.J., Cowan, D.J., Jayawickreme, C., Chen, G., Rimele, T.J., Generaux, C., Harston, L.T., and Roller, S.G. (2017). Identification of potent, nonabsorbable agonists of the calcium-sensing receptor for GI-specific administration. Bioorg Med Chem Lett *27*, 4673-4677.

45. Davies, S.L., Ozawa, A., McCormick, W.D., Dvorak, M.M., and Ward, D.T. (2007). Protein kinase C-mediated phosphorylation of the calcium-sensing receptor is stimulated by receptor activation and attenuated by calyculin-sensitive phosphatase activity. J Biol Chem *282*, 15048-15056.

46. Nemeth, E.F., Delmar, E.G., Heaton, W.L., Miller, M.A., Lambert, L.D., Conklin, R.L., Gowen, M., Gleason, J.G., Bhatnagar, P.K., and Fox, J. (2001). Calcilytic compounds: potent and selective Ca2+ receptor antagonists that stimulate secretion of parathyroid hormone. J Pharmacol Exp Ther *299*, 323-331.

47. Gowen, M., Stroup, G.B., Dodds, R.A., James, I.E., Votta, B.J., Smith, B.R., Bhatnagar, P.K., Lago, A.M., Callahan, J.F., DelMar, E.G., et al. (2000). Antagonizing the parathyroid calcium receptor stimulates parathyroid hormone secretion and bone formation in osteopenic rats. J Clin Invest *105*, 1595-1604.

48. Nemeth, E.F., Van Wagenen, B.C., and Balandrin, M.F. (2018). Discovery and Development of Calcimimetic and Calcilytic Compounds. Prog Med Chem *57*, 1-86.

49. Fitzpatrick, L.A., Dabrowski, C.E., Cicconetti, G., Gordon, D.N., Papapoulos, S., Bone, H.G., 3rd, and Bilezikian, J.P. (2011). The effects of ronacaleret, a calcium-sensing receptor antagonist, on bone mineral density and biochemical markers of bone turnover in postmenopausal women with low bone mineral density. J Clin Endocrinol Metab *96*, 2441-2449.

50. Halse, J., Greenspan, S., Cosman, F., Ellis, G., Santora, A., Leung, A., Heyden, N., Samanta, S., Doleckyj, S., Rosenberg, E., et al. (2014). A

phase 2, randomized, placebo-controlled, dose-ranging study of the calcium-sensing receptor antagonist MK-5442 in the treatment of postmenopausal women with osteoporosis. J Clin Endocrinol Metab *99*, E2207-2215.

51. Berridge, M.J., Bootman, M.D., and Roderick, H.L. (2003). Calcium signalling: dynamics, homeostasis and remodelling. Nat Rev Mol Cell Biol *4*, 517-529.

52. Gao, Y., Robertson, M.J., Rahman, S.N., Seven, A.B., Zhang, C., Meyerowitz, J.G., Panova, O., Hannan, F.M., Thakker, R.V., Brauner-Osborne, H., et al. (2021). Asymmetric activation of the calcium-sensing receptor homodimer. Nature *595*, 455-459.

53. Kifor, O., MacLeod, R.J., Diaz, R., Bai, M., Yamaguchi, T., Yao, T., Kifor, I., and Brown, E.M. (2001). Regulation of MAP kinase by calcium-sensing receptor in bovine parathyroid and CaR-transfected HEK293 cells. Am J Physiol Renal Physiol *280*, F291-302.

54. Gorvin, C.M. (2018). Insights into calcium-sensing receptor trafficking and biased signalling by studies of calcium homeostasis. J Mol Endocrinol *61*, R1-R12.

55. Putney, J.W., and Tomita, T. (2012). Phospholipase C signaling and calcium influx. Adv Biol Regul *52*, 152-164.

56. Cook, D.R., Rossman, K.L., and Der, C.J. (2014). Rho guanine nucleotide exchange factors: regulators of Rho GTPase activity in development and disease. Oncogene *33*, 4021-4035.

57. Somlyo, A.P., and Somlyo, A.V. (2003). Ca2+ sensitivity of smooth muscle and nonmuscle myosin II: modulated by G proteins, kinases, and myosin phosphatase. Physiol Rev *83*, 1325-1358.

58. Wheeler, A.P., and Ridley, A.J. (2004). Why three Rho proteins? RhoA, RhoB, RhoC, and cell motility. Exp Cell Res *301*, 43-49.

59. Strutt, D.I., Weber, U., and Mlodzik, M. (1997). The role of RhoA in tissue polarity and Frizzled signalling. Nature *387*, 292-295.

60. McBeath, R., Pirone, D.M., Nelson, C.M., Bhadriraju, K., and Chen, C.S. (2004). Cell shape, cytoskeletal tension, and RhoA regulate stem cell lineage commitment. Dev Cell *6*, 483-495.

61. Hill, C.S., Wynne, J., and Treisman, R. (1995). The Rho family GTPases RhoA, Rac1, and CDC42Hs regulate transcriptional activation by SRF. Cell *81*, 1159-1170.

62. Smith, K.A., Ayon, R.J., Tang, H., Makino, A., and Yuan, J.X. (2016). Calcium-Sensing Receptor Regulates Cytosolic [Ca (2+)] and Plays a Major Role in the Development of Pulmonary Hypertension. Front Physiol *7*, 517.

63. Smith, J.S., Lefkowitz, R.J., and Rajagopal, S. (2018). Biased signalling: from simple switches to allosteric microprocessors. Nat Rev Drug Discov *17*, 243-260.

64. Davey, A.E., Leach, K., Valant, C., Conigrave, A.D., Sexton, P.M., and Christopoulos, A. (2012). Positive and negative allosteric modulators promote biased signaling at the calcium-sensing receptor. Endocrinology *153*, 1232-1241.

65. IUPAC (2014). IUPAC - absolute configuration (A00020). Volume 2021.

66. Miller, M.T. (1991). Thalidomide embryopathy: a model for the study of congenital incomitant horizontal strabismus. Trans Am Ophthalmol Soc *89*, 623-674.

67. Eriksson, T., Bjorkman, S., Roth, B., and Hoglund, P. (2000). Intravenous formulations of the enantiomers of thalidomide: pharmacokinetic and initial pharmacodynamic characterization in man. J Pharm Pharmacol *52*, 807-817.

68. Teo, S.K., Colburn, W.A., Tracewell, W.G., Kook, K.A., Stirling, D.I., Jaworsky, M.S., Scheffler, M.A., Thomas, S.D., and Laskin, O.L. (2004). Clinical pharmacokinetics of thalidomide. Clin Pharmacokinet *43*, 311-327.

69. Nemeth, E.F., Steffey, M.E., Hammerland, L.G., Hung, B.C., Van Wagenen, B.C., DelMar, E.G., and Balandrin, M.F. (1998). Calcimimetics with potent and selective activity on the parathyroid calcium receptor. Proc Natl Acad Sci U S A *95*, 4040-4045.

70. Nemeth, E.F. (2002). The search for calcium receptor antagonists (calcilytics). J Mol Endocrinol *29*, 15-21.

71. Vahe, C., Benomar, K., Espiard, S., Coppin, L., Jannin, A., Odou, M.F., and Vantyghem, M.C. (2017). Diseases associated with calcium-sensing receptor. Orphanet J Rare Dis *12*, 19.

72. L.L. Cavalli-Sforza, W.F.B. (1999). The Genetics of Human Populations.

73. Heath, H., 3rd, Odelberg, S., Jackson, C.E., Teh, B.T., Hayward, N., Larsson, C., Buist, N.R., Krapcho, K.J., Hung, B.C., Capuano, I.V., et al. (1996). Clustered inactivating mutations and benign polymorphisms of the calcium receptor gene in familial benign hypocalciuric hypercalcemia suggest receptor functional domains. J Clin Endocrinol Metab *81*, 1312-1317.

74. Miedlich, S., Lamesch, P., Mueller, A., and Paschke, R. (2001). Frequency of the calcium-sensing receptor variant A986S in patients with primary hyperparathyroidism. Eur J Endocrinol *145*, 421-427.

75. Cole, D.E., Peltekova, V.D., Rubin, L.A., Hawker, G.A., Vieth, R., Liew, C.C., Hwang, D.M., Evrovski, J., and Hendy, G.N. (1999). A986S polymorphism of the calcium-sensing receptor and circulating calcium concentrations. Lancet *353*, 112-115.

76. Cole, D.E., Vieth, R., Trang, H.M., Wong, B.Y., Hendy, G.N., and Rubin, L.A. (2001). Association between total serum calcium and the A986S polymorphism of the calcium-sensing receptor gene. Mol Genet Metab *72*, 168-174.

77. Cetani, F., Borsari, S., Vignali, E., Pardi, E., Picone, A., Cianferotti, L., Rossi, G., Miccoli, P., Pinchera, A., and Marcocci, C. (2002). Calcium-sensing receptor gene polymorphisms in primary hyperparathyroidism. J Endocrinol Invest *25*, 614-619.

78. Pollak, M.R., Brown, E.M., Chou, Y.H., Hebert, S.C., Marx, S.J., Steinmann, B., Levi, T., Seidman, C.E., and Seidman, J.G. (1993). Mutations in the human Ca(2+)-sensing receptor gene cause familial hypocalciuric hypercalcemia and neonatal severe hyperparathyroidism. Cell *75*, 1297-1303.

79. Bai, M., Pearce, S.H., Kifor, O., Trivedi, S., Stauffer, U.G., Thakker, R.V., Brown, E.M., and Steinmann, B. (1997). In vivo and in vitro characterization of neonatal hyperparathyroidism resulting from a de novo, heterozygous mutation in the Ca2+-sensing receptor gene: normal maternal calcium homeostasis as a cause of secondary hyperparathyroidism in familial benign hypocalciuric hypercalcemia. J Clin Invest *99*, 88-96.

80. Huang, Y., Zhou, Y., Castiblanco, A., Yang, W., Brown, E.M., and Yang, J.J. (2009). Multiple Ca(2+)-binding sites in the extracellular domain of the Ca(2+)-sensing receptor corresponding to cooperative Ca(2+) response. Biochemistry *48*, 388-398.

81. Bai, M., Quinn, S., Trivedi, S., Kifor, O., Pearce, S.H., Pollak, M.R., Krapcho, K., Hebert, S.C., and Brown, E.M. (1996). Expression and characterization of inactivating and activating mutations in the human Ca2+o-sensing receptor. J Biol Chem *271*, 19537-19545.

82. Mancilla, E.E., De Luca, F., Ray, K., Winer, K.K., Fan, G.F., and Baron, J. (1997). A Ca(2+)-sensing receptor mutation causes hypoparathyroidism by increasing receptor sensitivity to Ca2+ and maximal signal transduction. Pediatr Res *42*, 443-447.

83. Hendy, G.N., and Canaff, L. (2016). Calcium-sensing receptor, proinflammatory cytokines and calcium homeostasis. Semin Cell Dev Biol *49*, 37-43.

84. Kowal-Vern, A., Walenga, J.M., Hoppensteadt, D., Sharp-Pucci, M., and Gamelli, R.L. (1994). Interleukin-2 and interleukin-6 in relation to burn wound size in the acute phase of thermal injury. J Am Coll Surg *178*, 357-362.

85. Caldwell, F.T., Jr., Graves, D.B., and Wallace, B.H. (1997). Pathogenesis of fever in a rat burn model: the role of cytokines and lipopolysaccharide. J Burn Care Rehabil *18*, 525-530.

86. Kelly, A., and Levine, M.A. (2013). Hypocalcemia in the critically ill patient. J Intensive Care Med *28*, 166-177.

87. Nielsen, P.K., Rasmussen, A.K., Butters, R., Feldt-Rasmussen, U., Bendtzen, K., Diaz, R., Brown, E.M., and Olgaard, K. (1997). Inhibition of PTH secretion by interleukin-1 beta in bovine parathyroid glands in vitro is associated with an up-regulation of the calcium-sensing receptor mRNA. Biochem Biophys Res Commun *238*, 880-885.

88. Meurs, H., Maarsingh, H., and Zaagsma, J. (2003). Arginase and asthma: novel insights into nitric oxide homeostasis and airway hyperresponsiveness. Trends Pharmacol Sci *24*, 450-455.

89. Yarova, P.L., Huang, P., Schepelmann, M.W., Bruce, R., Ecker, R., Nica, R., Telezhkin, V., Traini, D., Gomes Dos Reis, L., Kidd, E.J., et al. (2021). Characterization of Negative Allosteric Modulators of the Calcium-Sensing Receptor for Repurposing as a Treatment of Asthma. J Pharmacol Exp Ther *376*, 51-63.

90. Cifuentes, M., Fuentes, C., Tobar, N., Acevedo, I., Villalobos, E., Hugo, E., Ben-Jonathan, N., and Reyes, M. (2012). Calcium sensing receptor activation elevates proinflammatory factor expression in human adipose cells and adipose tissue. Mol Cell Endocrinol *361*, 24-30.

91. Mine, Y., and Zhang, H. (2015). Anti-inflammatory Effects of Poly-L-lysine in Intestinal Mucosal System Mediated by Calcium-Sensing Receptor Activation. J Agric Food Chem *63*, 10437-10447.

92. Zhang, H., Kovacs-Nolan, J., Kodera, T., Eto, Y., and Mine, Y. (2015). gamma-Glutamyl cysteine and gamma-glutamyl valine inhibit TNF-alpha signaling in intestinal epithelial cells and reduce inflammation in a mouse model of colitis via allosteric activation of the calcium-sensing receptor. Biochim Biophys Acta *1852*, 792-804.

93. Cheng, S.X., Lightfoot, Y.L., Yang, T., Zadeh, M., Tang, L., Sahay, B., Wang, G.P., Owen, J.L., and Mohamadzadeh, M. (2014). Epithelial CaSR deficiency alters intestinal integrity and promotes proinflammatory immune responses. FEBS Lett *588*, 4158-4166.

94. Elajnaf, T., Iamartino, L., Mesteri, I., Muller, C., Bassetto, M., Manhardt, T., Baumgartner-Parzer, S., Kallay, E., and Schepelmann, M. (2019). Nutritional and Pharmacological Targeting of the Calcium-Sensing Receptor Influences Chemically Induced Colitis in Mice. Nutrients *11*.

95. Iamartino, L., Elajnaf, T., Gall, K., David, J., Manhardt, T., Heffeter, P., Grusch, M., Derdak, S., Baumgartner-Parzer, S., Schepelmann, M., et al. (2020). Effects of pharmacological calcimimetics on colorectal cancer cells over-expressing the human calcium-sensing receptor. Biochim Biophys Acta Mol Cell Res *1867*, 118836.

96. Marks, D.J., and Segal, A.W. (2008). Innate immunity in inflammatory bowel disease: a disease hypothesis. J Pathol *214*, 260-266.

97. Abraham, C., and Cho, J.H. (2009). Inflammatory bowel disease. N Engl J Med *361*, 2066-2078.

98. Orholm, M., Munkholm, P., Langholz, E., Nielsen, O.H., Sorensen, T.I., and Binder, V. (1991). Familial occurrence of inflammatory bowel disease. N Engl J Med *324*, 84-88.

99. Cho, J.H., and Weaver, C.T. (2007). The genetics of inflammatory bowel disease. Gastroenterology *133*, 1327-1339.

100. Ricciotti, E., and FitzGerald, G.A. (2011). Prostaglandins and inflammation. Arterioscler Thromb Vasc Biol *31*, 986-1000.

101. Weinberg, J.B., Fermor, B., and Guilak, F. (2007). Nitric oxide synthase and cyclooxygenase interactions in cartilage and meniscus: relationships to joint physiology, arthritis, and tissue repair. Subcell Biochem *42*, 31-62.

102. Greenhough, A., Smartt, H.J., Moore, A.E., Roberts, H.R., Williams, A.C., Paraskeva, C., and Kaidi, A. (2009). The COX-2/PGE2 pathway: key roles in the hallmarks of cancer and adaptation to the tumour microenvironment. Carcinogenesis *30*, 377-386.

103. Nasrallah, R., Hassouneh, R., and Hebert, R.L. (2016). PGE2, Kidney Disease, and Cardiovascular Risk: Beyond Hypertension and Diabetes. J Am Soc Nephrol *27*, 666-676.

104. Narumiya, S. (1994). Prostanoid receptors. Structure, function, and distribution. Ann N Y Acad Sci *744*, 126-138.

105. Ensor, C.M., and Tai, H.H. (1995). 15-Hydroxyprostaglandin dehydrogenase. J Lipid Mediat Cell Signal *12*, 313-319.

106. Smith, W.L., Garavito, R.M., and DeWitt, D.L. (1996). Prostaglandin endoperoxide H synthases (cyclooxygenases)-1 and -2. J Biol Chem *271*, 33157-33160.

107. Laine, L., Takeuchi, K., and Tarnawski, A. (2008). Gastric mucosal defense and cytoprotection: bench to bedside. Gastroenterology *135*, 41-60.

108. Sinicrope, F.A., and Gill, S. (2004). Role of cyclooxygenase-2 in colorectal cancer. Cancer Metastasis Rev *23*, 63-75.

109. Elder, D.J., and Paraskeva, C. (1998). COX-2 inhibitors for colorectal cancer. Nat Med *4*, 392-393.

110. Jacoby, R.F., Seibert, K., Cole, C.E., Kelloff, G., and Lubet, R.A. (2000). The cyclooxygenase-2 inhibitor celecoxib is a potent preventive and therapeutic agent in the min mouse model of adenomatous polyposis. Cancer Res *60*, 5040-5044.

111. Eberhart, C.E., Coffey, R.J., Radhika, A., Giardiello, F.M., Ferrenbach, S., and DuBois, R.N. (1994). Up-regulation of cyclooxygenase 2 gene expression in human colorectal adenomas and adenocarcinomas. Gastroenterology *107*, 1183-1188.

112. Kargman, S.L., O'Neill, G.P., Vickers, P.J., Evans, J.F., Mancini, J.A., and Jothy, S. (1995). Expression of prostaglandin G/H synthase-1 and -2 protein in human colon cancer. Cancer Res *55*, 2556-2559.

113. Kutchera, W., Jones, D.A., Matsunami, N., Groden, J., McIntyre, T.M., Zimmerman, G.A., White, R.L., and Prescott, S.M. (1996). Prostaglandin H synthase 2 is expressed abnormally in human colon cancer: evidence for a transcriptional effect. Proc Natl Acad Sci U S A *93*, 4816-4820.

114. Sano, H., Kawahito, Y., Wilder, R.L., Hashiramoto, A., Mukai, S., Asai, K., Kimura, S., Kato, H., Kondo, M., and Hla, T. (1995). Expression of cyclooxygenase-1 and -2 in human colorectal cancer. Cancer Res *55*, 3785-3789.

115. Karpisheh, V., Nikkhoo, A., Hojjat-Farsangi, M., Namdar, A., Azizi, G., Ghalamfarsa, G., Sabz, G., Yousefi, M., Yousefi, B., and Jadidi-Niaragh, F. (2019). Prostaglandin E2 as a potent therapeutic target for treatment of colon cancer. Prostaglandins Other Lipid Mediat *144*, 106338.

116. Ahrenstedt, O., Hallgren, R., and Knutson, L. (1994). Jejunal release of prostaglandin E2 in Crohn's disease: relation to disease activity and first-degree relatives. J Gastroenterol Hepatol *9*, 539-543.

117. Dey, I., Lejeune, M., and Chadee, K. (2006). Prostaglandin E2 receptor distribution and function in the gastrointestinal tract. Br J Pharmacol *149*, 611-623.

118. Kudo, T., Narisawa, T., and Abo, S. (1980). Antitumor activity of indomethacin on methylazoxymethanol-induced large bowel tumors in rats. Gan *71*, 260-264.

119. Pollard, M., and Luckert, P.H. (1981). Effect of indomethacin on intestinal tumors induced in rats by the acetate derivative of dimethylnitrosamine. Science *214*, 558-559.

120. Thun, M.J., Namboodiri, M.M., Calle, E.E., Flanders, W.D., and Heath, C.W., Jr. (1993). Aspirin use and risk of fatal cancer. Cancer Res *53*, 1322-1327.

121. Thun, M.J., Namboodiri, M.M., and Heath, C.W., Jr. (1991). Aspirin use and reduced risk of fatal colon cancer. N Engl J Med *325*, 1593-1596.

122. Fund, W.C.R. Colorectal cancer statistics | World Cancer Research Fund International. Volume 2021.

123. Europe, W. (2008). WHO/Europe | Colorectal cancer. Volume 2021.

124. Theodoratou, E., Timofeeva, M., Li, X., Meng, X., and Ioannidis, J.P.A. (2017). Nature, Nurture, and Cancer Risks: Genetic and Nutritional Contributions to Cancer. Annu Rev Nutr *37*, 293-320.

125. Hampel, H., Frankel, W.L., Martin, E., Arnold, M., Khanduja, K., Kuebler, P., Clendenning, M., Sotamaa, K., Prior, T., Westman, J.A., et al. (2008). Feasibility of screening for Lynch syndrome among patients with colorectal cancer. J Clin Oncol *26*, 5783-5788.

126. Juhn, E., and Khachemoune, A. (2010). Gardner syndrome: skin manifestations, differential diagnosis and management. Am J Clin Dermatol *11*, 117-122.

127. Grady, W.M., and Markowitz, S.D. (2015). The molecular pathogenesis of colorectal cancer and its potential application to colorectal cancer screening. Dig Dis Sci *60*, 762-772.

128. Bernstein, C.N., Blanchard, J.F., Kliewer, E., and Wajda, A. (2001). Cancer risk in patients with inflammatory bowel disease: a population-based study. Cancer *91*, 854-862.

129. Ullman, T.A., and Itzkowitz, S.H. (2011). Intestinal inflammation and cancer. Gastroenterology *140*, 1807-1816.

130. Feagins, L.A., Souza, R.F., and Spechler, S.J. (2009). Carcinogenesis in IBD: potential targets for the prevention of colorectal cancer. Nat Rev Gastroenterol Hepatol *6*, 297-305.

131. Canavan, C., Abrams, K.R., and Mayberry, J. (2006). Meta-analysis: colorectal and small bowel cancer risk in patients with Crohn's disease. Aliment Pharmacol Ther *23*, 1097-1104.

132. Itzkowitz, S.H., and Yio, X. (2004). Inflammation and cancer IV. Colorectal cancer in inflammatory bowel disease: the role of inflammation. Am J Physiol Gastrointest Liver Physiol *287*, G7-17.

133. Shigaki, K., Mitomi, H., Fujimori, T., Ichikawa, K., Tomita, S., Imura, J., Fujii, S., Itabashi, M., Kameoka, S., Sahara, R., et al. (2013). Immunohistochemical analysis of chromogranin A and p53 expressions in ulcerative colitis-associated neoplasia: neuroendocrine differentiation as an early event in the colitis-neoplasia sequence. Hum Pathol *44*, 2393-2399.

134. Burmer, G.C., Rabinovitch, P.S., Haggitt, R.C., Crispin, D.A., Brentnall, T.A., Kolli, V.R., Stevens, A.C., and Rubin, C.E. (1992). Neoplastic progression in ulcerative colitis: histology, DNA content, and loss of a p53 allele. Gastroenterology *103*, 1602-1610.

135. Yashiro, M. (2014). Ulcerative colitis-associated colorectal cancer. World J Gastroenterol *20*, 16389-16397.

136. Brown, E.M., and MacLeod, R.J. (2001). Extracellular calcium sensing and extracellular calcium signaling. Physiol Rev *81*, 239-297.

137. Brennan, S.C., Thiem, U., Roth, S., Aggarwal, A., Fetahu, I., Tennakoon, S., Gomes, A.R., Brandi, M.L., Bruggeman, F., Mentaverri, R., et al. (2013). Calcium sensing receptor signalling in physiology and cancer. Biochim Biophys Acta *1833*, 1732-1744.

138. Fetahu, I.S., Hobaus, J., Aggarwal, A., Hummel, D.M., Tennakoon, S., Mesteri, I., Baumgartner-Parzer, S., and Kallay, E. (2014). Calcium-sensing receptor silencing in colorectal cancer is associated with promoter hypermethylation and loss of acetylation on histone 3. Int J Cancer *135*, 2014-2023.

139. Aggarwal, A., Prinz-Wohlgenannt, M., Tennakoon, S., Hobaus, J., Boudot, C., Mentaverri, R., Brown, E.M., Baumgartner-Parzer, S., and Kallay, E.

(2015). The calcium-sensing receptor: A promising target for prevention of colorectal cancer. Biochim Biophys Acta *1853*, 2158-2167.

140. MacLeod, R.J. (2013). Extracellular calcium-sensing receptor/PTH knockout mice colons have increased Wnt/beta-catenin signaling, reduced non-canonical Wnt signaling, and increased susceptibility to azoxymethane-induced aberrant crypt foci. Lab Invest *93*, 520-527.

141. Rey, O., Chang, W., Bikle, D., Rozengurt, N., Young, S.H., and Rozengurt, E. (2012). Negative cross-talk between calcium-sensing receptor and beta-catenin signaling systems in colonic epithelium. J Biol Chem *287*, 1158-1167.

142. Quinn, S.J., Ye, C.P., Diaz, R., Kifor, O., Bai, M., Vassilev, P., and Brown, E. (1997). The Ca2+-sensing receptor: a target for polyamines. Am J Physiol *273*, C1315-1323.

143. Ziegelstein, R.C., Xiong, Y., He, C., and Hu, Q. (2006). Expression of a functional extracellular calcium-sensing receptor in human aortic endothelial cells. Biochem Biophys Res Commun *342*, 153-163.

144. Mine, Y., and Zhang, H. (2015). Calcium-sensing receptor (CaSR)-mediated anti-inflammatory effects of L-amino acids in intestinal epithelial cells. J Agric Food Chem *63*, 9987-9995.

145. Brian Matlock, T.F.S. Assessment of Nucleic Acid Purity Volume 2021.

146. technologies, I. Real-Time PCR handbook. Volume 2021.

147. Mifflin, R.C., Saada, J.I., Di Mari, J.F., Adegboyega, P.A., Valentich, J.D., and Powell, D.W. (2002). Regulation of COX-2 expression in human intestinal myofibroblasts: mechanisms of IL-1-mediated induction. Am J Physiol Cell Physiol *282*, C824-834.

148. Schwarzkopf, M. (2021). Influence of Calcium-Sensing Receptor (CaSR) modulation on inflammation marker expression in the colon. (University of Applied Science, FH Campus Wien).

149. Gall, K. (2021). The role of the Calcium-Sensing Receptor in xenograft tumours from colorectal cancer cells. (University of Vienna).

150. Williams, I.R. (2006). CCR6 and CCL20: partners in intestinal immunity and lymphorganogenesis. Ann N Y Acad Sci *1072*, 52-61.

151. Hanai, H. (2006). Positions of selective leukocytapheresis in the medical therapy of ulcerative colitis. World J Gastroenterol *12*, 7568-7577.

152. Administration, F.a.D. (2017). FDA warning and precautions. Volume 2021.

153. Bird, S., Zou, J., Wang, T., Munday, B., Cunningham, C., and Secombes, C.J. (2002). Evolution of interleukin-1beta. Cytokine Growth Factor Rev *13*, 483-502.

154. Saijo, Y., Tanaka, M., Miki, M., Usui, K., Suzuki, T., Maemondo, M., Hong, X., Tazawa, R., Kikuchi, T., Matsushima, K., et al. (2002).

Proinflammatory cytokine IL-1 beta promotes tumor growth of Lewis lung carcinoma by induction of angiogenic factors: in vivo analysis of tumor-stromal interaction. J Immunol *169*, 469-475.

155. Song, X., Voronov, E., Dvorkin, T., Fima, E., Cagnano, E., Benharroch, D., Shendler, Y., Bjorkdahl, O., Segal, S., Dinarello, C.A., et al. (2003). Differential effects of IL-1 alpha and IL-1 beta on tumorigenicity patterns and invasiveness. J Immunol *171*, 6448-6456.

156. Mahida, Y.R., Wu, K., and Jewell, D.P. (1989). Enhanced production of interleukin 1-beta by mononuclear cells isolated from mucosa with active ulcerative colitis of Crohn's disease. Gut *30*, 835-838.

157. Klampfer, L. (2011). Cytokines, inflammation and colon cancer. Curr Cancer Drug Targets *11*, 451-464.

158. Kaler, P., Augenlicht, L., and Klampfer, L. (2009). Macrophage-derived IL-1beta stimulates Wnt signaling and growth of colon cancer cells: a crosstalk interrupted by vitamin D3. Oncogene *28*, 3892-3902.

159. Westbrook, A.M., Wei, B., Braun, J., and Schiestl, R.H. (2009). Intestinal mucosal inflammation leads to systemic genotoxicity in mice. Cancer Res *69*, 4827-4834.

160. Canaff, L., and Hendy, G.N. (2005). Calcium-sensing receptor gene transcription is up-regulated by the proinflammatory cytokine, interleukin-1beta. Role of the NF-kappaB PATHWAY and kappaB elements. J Biol Chem *280*, 14177-14188.

161. Canaff, L., Zhou, X., and Hendy, G.N. (2008). The proinflammatory cytokine, interleukin-6, up-regulates calcium-sensing receptor gene transcription via Stat1/3 and Sp1/3. J Biol Chem *283*, 13586-13600.

162. Zhang, M., Wang, H., and Tracey, K.J. (2000). Regulation of macrophage activation and inflammation by spermine: a new chapter in an old story. Crit Care Med *28*, N60-66.

163. Pugh, S., and Thomas, G.A. (1994). Patients with adenomatous polyps and carcinomas have increased colonic mucosal prostaglandin E2. Gut *35*, 675-678.

164. Rigas, B., Goldman, I.S., and Levine, L. (1993). Altered eicosanoid levels in human colon cancer. J Lab Clin Med *122*, 518-523.

165. Kawamori, T., Uchiya, N., Sugimura, T., and Wakabayashi, K. (2003). Enhancement of colon carcinogenesis by prostaglandin E2 administration. Carcinogenesis *24*, 985-990.

166. Isono, M., Suzuki, T., Hosono, K., Hayashi, I., Sakagami, H., Uematsu, S., Akira, S., DeClerck, Y.A., Okamoto, H., and Majima, M. (2011). Microsomal prostaglandin E synthase-1 enhances bone cancer growth and bone cancer-related pain behaviors in mice. Life Sci *88*, 693-700.

167. Schumacher, Y., Aparicio, T., Ourabah, S., Baraille, F., Martin, A., Wind, P., Dentin, R., Postic, C., and Guilmeau, S. (2016). Dysregulated CRTC1

activity is a novel component of PGE2 signaling that contributes to colon cancer growth. Oncogene *35*, 2602-2614.

168. Nandi, P., Girish, G.V., Majumder, M., Xin, X., Tutunea-Fatan, E., and Lala, P.K. (2017). PGE2 promotes breast cancer-associated lymphangiogenesis by activation of EP4 receptor on lymphatic endothelial cells. BMC Cancer *17*, 11.

169. Wang, T., Jing, B., Xu, D., Liao, Y., Song, H., Sun, B., Guo, W., Xu, J., Li, K., Hu, M., et al. (2020). PTGES/PGE2 signaling links immunosuppression and lung metastasis in Gprc5a-knockout mouse model. Oncogene *39*, 3179-3194.

170. Bai, X.M., Jiang, H., Ding, J.X., Peng, T., Ma, J., Wang, Y.H., Zhang, L., Zhang, H., and Leng, J. (2010). Prostaglandin E2 upregulates survivin expression via the EP1 receptor in hepatocellular carcinoma cells. Life Sci *86*, 214-223.

171. Nandi, B., Pai, C., Huang, Q., Prabhala, R.H., Munshi, N.C., and Gold, J.S. (2014). CCR6, the sole receptor for the chemokine CCL20, promotes spontaneous intestinal tumorigenesis. PLoS One *9*, e97566.

172. Frick, V.O., Rubie, C., Kolsch, K., Wagner, M., Ghadjar, P., Graeber, S., and Glanemann, M. (2013). CCR6/CCL20 chemokine expression profile in distinct colorectal malignancies. Scand J Immunol *78*, 298-305.

173. Vicinus, B., Rubie, C., Stegmaier, N., Frick, V.O., Kolsch, K., Kauffels, A., Ghadjar, P., Wagner, M., and Glanemann, M. (2013). miR-21 and its target gene CCL20 are both highly overexpressed in the microenvironment of colorectal tumors: significance of their regulation. Oncol Rep *30*, 1285-1292.

174. Brand, S., Olszak, T., Beigel, F., Diebold, J., Otte, J.M., Eichhorst, S.T., Goke, B., and Dambacher, J. (2006). Cell differentiation dependent expressed CCR6 mediates ERK-1/2, SAPK/JNK, and Akt signaling resulting in proliferation and migration of colorectal cancer cells. J Cell Biochem *97*, 709-723.